Experimental volcanic lightning under early Earth conditions: Implications for prebiotic synthesis and the origin of life

Christina Springsklee

München 2023

Experimental volcanic lightning under early Earth conditions: Implications for prebiotic synthesis and the origin of life

Christina Springsklee

Dissertation zur Erlangung des Doktorgrades
an der Fakultät für Geowissenschaften
der Ludwig-Maximilians-Universität München

Vorgelegt von
Christina Springsklee
Aus Lüdinghausen, Deutschland
München, den 25.01.2023

Antrag auf Promotion: Taufkirchen, den 25.03.2020

Erstgutachterin: Prof. Dr. Bettina Scheu

Zweitgutachter: Prof. Dr. Donald B. Dingwell

Tag des Antrags auf Promotion: 25.03.2020

Tag der Einreichung der Promotion: 25.01.2023

Tag der mündlichen Prüfung: 04.07.2023

‘If you wish to make an apple pie from scratch, you must first invent the universe.’
— Carl Sagan

Table of Contents

List of figures

List of tables

Preamble

Chapter 3 of this dissertation is published in a peer-reviewed journal (Journal of Geophysical Research: Solid Earth). **Chapter 4** of this dissertation is published in a peer-reviewed journal (Geophysical Research Letter). **Chapter 2** is in preparation as a standalone publication and submitted to Volcanica. The content of these publications has not been altered for this dissertation, but the format was changed, matching this thesis's overall format. The full references are listed below. Additionally, my scientific contribution to two individual studies is further listed below. The full references of the papers are the following:

Springsklee, C., Scheu, B., Manga, M., Cigala, V., Cimarelli, C., & Dingwell, D.B. (2022). The Influence of Grain Size Distribution on Laboratory-Generated Volcanic Lightning. Journal of Geophysical Research: Solid Earth 127(10), e2022JB024390. https://doi.org/10.1029/2022JB024390

Springsklee, C., Scheu, B., Manga, M., Cigala, V., Cimarelli, C., & Dingwell, D.B. (2022). Experimental dataset for the influence of grain size distribution on experimental volcanic lightning. GFZ Data Services. https://doi.org/10.5880/fidgeo.2022.009

Springsklee, C., Manga, M., Scheu, B., Cimarelli, C., & Dingwell, D.B. (2022). Electric discharge in erupting mud. Geophysical Research Letters 49(23), e2022GL100852. https://doi.org/10.1029/2022GL100852

Springsklee, C., Manga, M., Scheu, B., Cimarelli, C., & Dingwell, D.B. (2022). Experimental insights on electric discharges as a potential mechanism for self-ignition of mud volcanoes. GFZ Data Services. https://doi.org/10.5880/fidgeo.2022.026

Springsklee, C. Scheu, B., Seifert, C., Manga, M., Cimarelli, C., Gaudin, D., Dingwell, D.B. & Trapp, O. (2022). A gas-tight shock tube apparatus for experimental volcanic lightning under varying atmospheric conditions. Submitted to Volcanica.

The additional outcome of this thesis is listed below:

Matreux, T., Le Vay, K., Schmid, A., Aikkila, P., Belohlavek, L., Çalışkanoğlu, A.Z., Salibi, E., Kühnlein, A., **Springsklee, C.,** Scheu, B., Dingwell, D.B., Braun, D., Mutschler, H. & Mast, C.B. (2021). Heat flows in rock cracks naturally optimize salt compositions for ribozymes. Nature Chemistry, 13(11), 1038-1045. https://doi.org/10.1038/s41557-021-00772-5

Günther, A., Lohringer, H., Müller, D., Schmidbauer, E., & **Springsklee, C.** (2022). Electrical and dielectric properties of polycrystalline VO_2 discriminating between bulk and grain boundary conduction. Journal of Physics and Chemistry of Solids, 170, 110897. https://doi.org/10.1016/j.jpcs.2022.110897

Author contributions

Chapter 2: B.S. and C.S. designed the study and the experimental setup. B.S. provided supervision. D.G., B.S. and C.C. provided the methodology. D.G. and C.C. designed the processing code to analyze the raw signal. C.S., B.S. and M.M. performed the experiments, analyzed, and visualized the results, prepared the samples, sampled the solid sample and gas mixtures, and wrote the original draft. C.SE. and O.T. analyzed the gas samples. All authors contributed to the discussion and revised the manuscript. B.S. and D.B.D. acquired funding.

Chapter 3: B.S. and C.S. designed the experimental setup and the study. B.S. and M.M. provided supervision. B.S. and C.C. provided the methodology. C.S. prepared the sample and performed the grain size analysis, density measurements and further investigations to characterize the sample material. C.S. performed the experiments and obtained high-speed recordings. C.S. analyzed and visualized the results and wrote the original draft. M.M. and C.S. scaled the results to nature. All authors contributed to the discussion and revised the manuscript. B.S. and D.B.D. acquired funding.

Chapter 4: M.M., B.S., C.C. and C.S. designed the experimental setup and designed the study. M.M. provided the samples. C.S., B.S. and C.C. prepared and analyzed the samples. C.S. performed the experiments, analyzed, and visualized the results. M.M. wrote the original draft. All authors contributed to the discussion and revised the manuscript. B.S., M.M. and D.B.D. acquired funding.

Summary

The emergence of life is one of the most enigmatic and substantial questions in human existence. Although science has advanced progressively unraveling many potential reaction mechanisms and discovering many puzzle pieces to explain the emergence of life, it is still not fully understood nor reproducible under laboratory conditions. The emergence of life remains a mystery.

The search for the emergence of life includes the search for a geologically plausible environmental setting. A plausible environmental setting must provide all necessary prerequisites like a source of energy to initiate chemical reactions, a sufficient concentration of the abiotic building blocks for life, liquid water, temperature conditions enhancing chemical reactions but not destroying organic molecules, and disequilibrium conditions. The search for plausible environmental settings for the emergence of life is a challenging task as Earth's system has changed significantly since its origin. The atmosphere has changed significantly from an an-oxic state to its current oxic conditions. Oxygen is a waste product of today's metabolism, so free oxygen was almost nonexistent before the emergence of life. The ocean composition and oxidation state have also changed significantly since the Earth's origin. Unfortunately, no geological rock record survived from the time most plausible for the emergence of life and the exact geological conditions of early Earth are not known today.

Many plausible environmental settings have been proposed in the research concerning the emergence of life. Here, the focus is on active volcanic settings. Volcanoes were active on early Earth and represented a highly diverse environment. Surrounded by the early Earth's ocean, volcanic eruptions were the leading source of volatiles in the primary atmosphere. In addition to the heat emitted by magma, volcanic lightning also accompanies these explosive erruptions; both of which are important energy sources for prebiotic reactions. Recent explosive volcanism is accompanied by volcanic lightning: electrical discharges in and/or from the eruption column. The electrical activity within a volcanic plume can be characterized into three categories, whereby the boundaries overlap. Close to the vent, smaller discharges, vent-discharges, and near-vent lightning are observable. Further up in the plume, a large and impressive plume lightning takes place. Various charging and discharging mechanisms contribute in different amounts to each of those three discharge categories. This thesis focuses on near-vent lightning, which is dominantly generated by triboelectrification. Triboelectrification describes the process of frictional, non-disruptive interaction between the expelled ash particles. A grain size-dependent charging is observed during this process: smaller particles tend to charge negatively, whereas larger particles obtain a positive charge due to their frictional interaction with the smaller particles. The separation of the charged particles results in discharges. As discharges are regarded as one potential prebiotic synthesis mechanism for creating the first organics, the aim of this thesis is to determine the impact of

environmental conditions as the atmospheric composition on the discharge behavior in experimentally generated volcanic lightning.

An experimental setup to recreate different atmospheric compositions relevant to early Earth and extra-terrestrial bodies was built, as the atmospheric composition and pressure changed during the evolution of the Earth. This setup makes it possible to explore the influencing parameters of volcanic lightning and test if volcanic lightning might have been equally efficient under those conditions as it had been in current volcanic eruptions (**Chapter 2**). The experimental setup needs a gas-tight and secure supply of various gases. For this thesis, the impact of CO_2 and CO as components of the enveloping atmosphere was tested on volcanic lightning, and equally vigorous generation of near-vent discharges compared to experiments conducted in an atmosphere containing current air was observed. To test the impact of the transporting gas phase, two transporting gas phases (argon and nitrogen) were used in the experiments. The change in transporting gas phase significantly changes the magnitude and number of detected near-vent discharges. Those results imply that the exsolved gas phase in the volcanic plume significantly impacts near-vent discharges. The recovered ash was analyzed for organic compounds by GC/MS, but no newly formed organic compounds were detected in the samples.

Also, the overall magma composition of volcanic eruptions has changed over time. Therefore, the ability of two different volcanic materials, a phonolitic pumice and a recent tholeiitic basalt, to create discharges was compared against an analog material made of synthetic soda-lime glass beads (**Chapter 3**). The experimental generation of discharges allowed us to apply similar eruption conditions (10 MPa). The results demonstrate that all three materials can produce discharges during an eruption. To further evaluate the parameters governing the intensity and number of discharges, experiments to investigate the influence of grain size distribution on the bimodally distributed grain size compositions were performed. Each material's coarse and fine grain size fraction was mixed and used in the decompression experiments. The results demonstrated that for the synthetic soda-lime glass beads and the tholeiitic basalt, the abundance of a very fine grain size fraction (< 10 µm) was necessary to produce discharges. The more porous phonolitic pumice needed a broader grain size distribution to generate detectable discharges. Nonetheless, the abundance of fines was crucial to generate discharges for the pumice. The analysis of the high-speed recordings of the decompressed jets suggested that the coupling of the particles to the transporting gas-phase is the main governing factor controlling the generation of charge and discharge between particles.

Additionally, as clay minerals in mud are a widely used material in the prebiotic context, experiments investigating discharges in mud eruptions as a potential ignition mechanism were performed (**Chapter 4**). Modern mud volcanism represents a source of methane emission, a highly reactive reducing gas. Today, very explosive, destructive mud eruptions are often accompanied by spectacular flames that can sustain for centuries. As the previous experiments suggest discharges between particles as a potential energy source for reactions in reducing gas phases, it was

tested if potential discharges might occur, which could potentially ignite the methane-gas emitted in those eruptions. The mud samples analyzed in this study originate from the Davis-Schrimpf location (California, USA). Careful sample preparation caused only slight changes in the grain size distribution of the sampled mud. For safety reasons, the transporting gas phase was not methane but argon. The dried samples showed intense discharges during decompression. To test the influence of grain size distribution and humidity, a fraction of the dry samples was mixed with coarser sand grains, and another fraction was exposed to controlled humid conditions. Increasing the humidity and coarse grain size fraction decreases the number and magnitude of discharges. The results demonstrate that dry natural mud samples can cause discharges, representing a potential ignition mechanism in natural mud eruptions.

The experimentally obtained results emphasize the probability of volcanic lightning as a potential prebiotic synthesis mechanism on early Earth as in the experiments with an enveloping atmosphere containing CO_2, N_2 and CO discharges were successfully detected. The environmental conditions so far tested in the experiments permit near-vent discharges, which can react with the transporting gas phase of the plume, in the experimental case, the jet. The results obtained so far strongly encourage further investigation of active volcanic settings as a potential environment for the emergence of life.

Kurzfassung

Die Entstehung des Lebens ist eine der rätselhaftesten und wichtigsten Fragen der Menschheitsgeschichte. Obwohl die Wissenschaft auch in dieser Frage bereits weit fortgeschritten ist, also viele potenzielle Reaktionsmechanismen entschlüsselt und viele Puzzlestücke entdeckt hat, ist die Frage nach der Entstehung des Lebens noch immer nicht vollständig beantwortet. Noch immer kann die Entstehung des Lebens nicht in seiner Gänze unter Laborbedingungen reproduziert werden, sie ist und bleibt ein Rätsel.

Die Suche nach der Entstehung von Leben umfasst die Suche nach einer geologisch plausiblen Umwelt und den dazugehörigen plausiblen Umweltbedingungen. Eine plausible Umwelt muss alle notwendigen Voraussetzungen bieten, wie z.B. eine Energiequelle zur Initiierung von chemischen Reaktionen, eine ausreichende Konzentration der abiotischen Bausteine des Lebens, flüssiges Wasser, Temperaturbedingungen, welche die chemischen Reaktionen begünstigen, aber organische Moleküle nicht zerstören, sowie Ungleichgewichtsbedingungen. Die Suche nach plausiblen Umweltbedingungen für die Entstehung von Leben ist noch immer eine schwierige Aufgabe, da sich das System Erde seit seiner Entstehung in seiner Gesamtheit erheblich verändert hat. Die Atmosphäre hat sich von einem anoxischen Zustand zu den heutigen oxischen Bedingungen erheblich verändert. Heutzutage ist Sauerstoff ein Abfallprodukt der biologischen Stoffwechselprozesse, wohingegen freier Sauerstoff vor der Entstehung des Lebens kaum in der Atmosphäre vorhanden war. Auch die Zusammensetzung und der Oxidationszustand der Ozeane haben sich seit der Entstehung der Erde signifikant verändert. Leider gibt es heute kaum geologische Indizien, also keine Gesteinsablagerungen aus jener Zeit, die für die Entstehung des Lebens am plausibelsten ist, um die damaligen Umweltbedingungen zu rekonstruieren. Die genauen geologischen Bedingungen der frühen Erde sind also heute bisher nicht bekannt.

In der Forschung über die Entstehung des Lebens sind viele plausible Umweltbedingungen vorgeschlagen worden. In dieser Arbeit liegt der Fokus auf Umgebungen mit aktivem Vulkanismus. Vulkane waren in der frühen Erdzeit aktiv und stellten eine äußerst vielfältige Umwelt dar. Umgeben vom frühen Erdozean waren mafische Vulkanausbrüche die wichtigste Quelle für Volatile in der Uratmosphäre. Nicht nur die vom Magma abgegebene Wärme stellt eine potentielle Energiequelle für präbiotische Reaktionen dar, auch vulkanische Blitze, die explosive Eruptionen begleiten, sind eine bedeutende Energiequelle. Heutiger explosive Vulkanismus wird von vulkanischen Blitzen, Entladungen in der Eruptionssäule, begleitet. Die elektrische Aktivität innerhalb einer Eruptionssäule kann in drei Kategorien eingeteilt werden, wobei sich die Grenzen überschneiden. In der Nähe des Schlots sind kleinere Entladungen, Schlotentladungen und schlotnahe Blitze zu beobachten. Weiter oben in der Eruptionswolke sind große und beeindruckende Blitze zu sehen. Es wurden verschiedene Auf- und Entladungsmechanismen

identifiziert, die in unterschiedlichem Maße zu jeder dieser drei Entladungskategorien beitragen. In dieser Dissertation liegt der Fokus auf elektrischen Entladungen in der Nähe der Schlotöffnung, die hauptsächlich durch Triboelektrifikation erzeugt werden. Triboelektrifizierung beschreibt den Prozess der reibungsbedingten, nicht-disruptiven Interaktion zwischen den ausgestoßenen Aschepartikeln. Bei diesem Prozess wird eine von der Korngröße abhängige Aufladung beobachtet: kleinere Partikel laden sich eher negativ auf, während größere Partikel aufgrund ihrer Reibungswechselwirkung mit den kleineren Partikeln eine positive Ladung erhalten. Die Trennung der geladenen Teilchen führt zu elektrischen Entladungen, also einem Blitz. Da elektrische Entladungen als ein möglicher präbiotischer Synthesemechanismus für die Entstehung des ersten organischen Materials angesehen werden, wird in dieser Arbeit der Einfluss der Umweltbedingungen wie z.B. der atmosphärischen Zusammensetzung auf das Entladungsverhalten in experimentell erzeugten vulkanischen Blitzen untersucht.

Da sich die atmosphärische Zusammensetzung und der atmosphärische Druck während der Entwicklung der Erde verändert haben, wurde ein Versuchsaufbau entwickelt, mit dem verschiedene atmosphärische Zusammensetzungen, die für die frühe Erde und andere Planeten relevant sind, experimentell nachgebildet werden können. Mit diesem Versuchsaufbau können die Einflussparameter vulkanischer Blitze untersucht und überprüft werden, ob vulkanische Blitze unter diesen Bedingungen ebenso intensiv waren wie bei rezenten Vulkanausbrüchen (**Kapitel 2**). Der Versuchsaufbau benötigt eine gasdichte und sichere Versorgung mit verschiedenen Gasen. Der Einfluss von CO_2 und CO als Komponenten der Uratmosphäre auf vulkanische Blitze wurde untersucht und es konnte gezeigt werden, dass in dieser Zusammensetzung elektrischen Entladungen in der Nähe des Schlotes genauso effizient entstehen wie bei Experimenten in einer Atmosphäre mit rezenter Luft. Um den Einfluss der Transportgasphase zu testen, wurden zwei Transportgasphasen (Argon und Stickstoff) in den Experimenten verwendet. Der Wechsel der Transportgasphase verändert signifikant die Intensität und Anzahl der gemessenen elektrischen Entladungen in der Nähe der experimentellen Schlotöffnung. Diese Ergebnisse deuten darauf hin, dass die transportierende Gasphase in der Eruptionssäule die schlotnahen Entladungen erheblich beeinflusst. Die zurückgewonnene Asche wurde mittels GC/MS auf organische Verbindungen untersucht, jedoch wurden in den Proben keine neu gebildeten organischen Verbindungen nachgewiesen.

Außerdem hat sich die allgemeine Magmazusammensetzung von Vulkanausbrüchen im Laufe der Zeit verändert. Daher wurden zwei verschiedene vulkanische Materialien, ein rezenter phonolitischer Bimsstein und ein rezenter tholeiitischer Basalt, hinsichtlich ihrer Fähigkeit zur Erzeugung von Entladungen mit synthetischen Kalk-Natron-Glasperlen verglichen (**Kapitel 3**). Die experimentelle Erzeugung von elektrischen Entladungen ermöglichte es, die Proben unter ähnlichen Eruptionsbedingungen zu vergleichen. Die Ergebnisse zeigen, dass alle drei Materialien während einer Eruption elektrische Entladungen erzeugen können. Zur

weiteren Bewertung der Parameter, die die Intensität und Anzahl der Entladungen bestimmen, haben wir den Einfluss der Korngrößenverteilung in bimodal verteilten Korngrößenzusammensetzungen untersucht. Eine grobkörnige und eine feinkörnige Korngrößenfraktion jedes Materials wurde gemischt und eruptiert. Die Ergebnisse zeigten, dass für die synthetischen Kalk-Natron-Glasperlen und dem tholeiitischen Basalt eine sehr feine Korngrößenfraktion (< 10 µm) erforderlich war, um Entladungen zu erzeugen. Der porösere phonolitische Bimsstein benötigte eine breitere Korngrößenverteilung, um nachweisbare Entladungen zu erzeugen. Nichtsdestotrotz war der Anteil an Feinkorn entscheidend für die Erzeugung von Entladungen im Bimsstein. Die Analyse der Aufnahmen einer Hochgeschwindigkeitskamera des dekomprimierten Jets deutet darauf hin, dass die Kopplung der Partikel an die transportierende Gasphase der wichtigste Faktor für die Erzeugung von Ladung und Entladung zwischen den Partikeln ist.

Da Tonminerale in Schlamm ein reaktives und bereits häufig getestetes Material in präbiotischen Syntheseexperimenten sind, wurden außerdem Experimente durchgeführt, um Entladungen in Schlammeruptionen als möglichen Zündmechanismus zu untersuchen (**Kapitel 4**). Moderner Schlammvulkanismus stellt heute eine wichtige Quelle für Methan-emissionen, also für die Emission eines hochreaktiven reduzierenden Gases, dar. Starke und sehr explosive Eruptionen von Schlammvulkanen werden oft von spektakulären Flammen begleitet, die Jahrhunderte lang brennen können. Da elektrische Entladungen zwischen Partikeln als potenzielle Energiequelle für Reaktionen in reduzierenden Gasphasen vermutet werden, wurde in dieser Arbeit getestet, ob elektrische Entladungen entstehen, die das bei diesen Eruptionen emittierte Methangas innerhalb der Eruptionswolke möglicherweise entzünden könnten. Die Schlammproben wurden in der Umgebung der „Salten Sea“ (Davis-Schrimpf, Kalifornien, USA) genommen. Durch eine sorgfältige Probenvorbereitung wurde die Korngrößenverteilung der Schlammproben beim Trocknen nur geringfügig verändert. Aus Sicherheitsgründen wurde als Transportgasphase nicht Methan, sondern Argon verwendet. Die getrockneten Proben zeigten bei der Dekompression starke elektrische Entladungen. Um den Einfluss der Korngrößenverteilung und der Materialfeuchtigkeit zu testen, wurde eine Fraktion der trockenen Proben mit gröberen Sandkörnern gemischt und eine andere Fraktion wurde unter kontrollierten feuchten Bedingungen getestet. Je höher die Feuchtigkeit und der Anteil an groben Körnern, desto geringer sind Anzahl und Intensität der elektrischen Entladungen. Die Ergebnisse zeigen, dass die trockenen Schlammproben elektrische Entladungen verursachen können, die einen potenziellen Zündmechanismus bei natürlichen Schlammeruptionen darstellen können.

Die experimentell gewonnenen Ergebnisse unterstreichen die Wahrscheinlichkeit vulkanischer Blitze als möglicher präbiotischer Synthesemechanismus in der frühen Erdgeschichte, da wir in Experimenten mit einer CO_2-, N_2- und CO-haltigen Atmosphäre erfolgreich elektrische Entladungen nachweisen konnten. Die bisher in unseren Experimenten getesteten Umgebungsbedingungen erlauben elektrische

Entladungen in der Nähe des Schlots, die mit der transportierenden Gasphase der Eruptionswolke, in unserem experimentellen Fall dem Jet, reagieren können. Die bisher erzielten Ergebnisse unterstreichen die Bedeutung von vulkanischen Blitzen als präbiotischer Synthesemechanismus in der frühen Erdgeschichte und betonen die Wichtigkeit weiterer Untersuchungen von Regionen mit aktivem Vulkanismus als potenzielle Umgebung für die Entstehung von Leben.

Chapter 1 – Introduction

1.1 Scope and motivation

Motivation

The origin of life is one of the oldest and most elusive enigma in human history. It describes our nascence and the transition from abiotic to biotic nature. The origin of life dates back to a time which is not accessible and elusive to us as humans. What were the physical and chemical conditions necessary for this transitional step? Is there an exact line between biotic and abiotic nature? For as long as humanity has existed, philosophy, religion, and science have tried to tackle these questions. So far, there exists no entirely satisfactory answer.

The emergence of life needs disequilibrium conditions: Geological setting of active volcanoes

One crucial aspect for investigating the emergence of life are the potential environments that provide all necessary prerequisites for this transition from abiotic to biotic matter to enhance the process of abiogenesis. A diverse variety of potential environmental settings has been proposed so far to represent the potential cradle of life (e.g., Bada & Korenaga, 2018; Basiuk & Navarro-González, 1996; Deamer et al., 2006; Haldane, 1929; Martin & Russell, 2007; Oparin, 1957; Russell et al., 2010). All plausible environments have the following in common: liquid water is accessible, a source of energy to drive chemical reactions is abundant and chemical elements, the so-called building blocks for life, are present in a sufficient concentration (as summarized by e.g., Hazen, 2012). Volcanically active environments represent such a diverse and highly dynamic environment and therefore are the scope of this thesis (e.g., Basiuk & Navarro-González, 1996; Johnson et al., 2008). The focus is on volcanic lightning (VL) as a potential energy source to drive prebiotic synthesis reactions, as discharges have been efficiently tested in laboratory prebiotic synthesis experiments.

Discharges as a potential prebiotic synthesis mechanism

An experimental investigation on volcanic activity relevant to early Earth-related conditions helps to determine the importance of VL for the origin of life. Discharges had been proposed and tested as a potential prebiotic synthesis mechanism (e.g., Basiuk & Navarro-González, 1996; Lavrentiev et al., 1984; Miller, 1953; Plankensteiner et al., 2004). The famous prebiotic synthesis experiments by Miller (1953) demonstrated the synthesis of amino acids by discharges in a highly reducing atmosphere. Today, the early atmosphere is assumed to have been only weakly reducing (Catling & Zahnle, 2020), so volcanic lightning in a more neutral to weakly reducing atmosphere needs to be tested. Although, of course, the most favourable result of this thesis is to perform prebiotic synthesis of organic molecules experimentally, the physical conditions relevant to volcanic processes are the focus of this thesis.

A setup to recreate early Earth conditions in the lab

As the environmental conditions on modern Earth's surface differ significantly from the ancient Earth conditions relevant to the emergence of life, this thesis aimed to build a setup capable of performing decompression experiments to mimic volcanic eruptions under varying atmospheric conditions. Environmental conditions like atmospheric composition, plume composition and atmospheric pressure were investigated in this thesis to compare how effective VL might have been on early Earth or extra-terrestrial systems as a potential synthesis mechanism.

Investigation of parameters controlling recent VL

Nonetheless, not only parameters which refer to our ancient Earth or extra-terrestrial systems were investigated. Many aspects of current VL demand further investigation to evaluate their influence. For example, the effect of the sample material erupting during an explosive volcanic eruption is still not thoroughly evaluated. How and if the magmatic composition influences the intensity of VL needs to be investigated in further detail. For this purpose, we performed experiments with varying sample materials and investigated the importance of grain size distribution (GSD) within the sample. We investigate materials like tholeiitic basalt, especially relevant for early Earth and potential Martian volcanism, against a comparison of phonolitic pumice and synthetic soda-lime glass beads. Another highly interesting material in the prebiotic context is mud. In experiments, clay minerals were found to potentially play a role as a catalyst in prebiotic synthesis reactions (Kloprogge & Hartman, 2022). As structures on Mars also resemble mud volcanism (Skinner Jr & Mazzini, 2009), this material also became part of the thesis.

The unique properties of ash particles

As previously mentioned, volcanic settings represent a highly diverse environment where several mechanisms depend on each other forming complex interactive systems. Not only are discharges within a plume a potential energy source for synthesis reactions, worth further studies, but so are the erupted materials, the ash particles and their interaction. Glass is a highly reactive material, which alters in geological timescales relatively fast and therefore represents a suitable source of potential nutrient release. The charging and discharging of particles within the plume not only evoke the charging of the particles and consequently of discharges but also may lead to agglomeration processes and hence may represent a way to accumulate the particles and locally increase the concentration locally of chemicals. Further, the ash particles react with the surrounding plume (e.g., Casas et al., 2019), so the hot gas phase enveloping the particles during an eruption. All those reactions are noteworthy in a potential environmental setting for the emergence of life but beyond the scope of this thesis.

1.2 Overview of dissertation

The first chapter of this thesis (**Chapter 1**) summarizes its motivation. Further, **Chapter 1** presents a short summary of the relevant theories of the emergence of life and relevant geological background information about the proposed environmental conditions for early Earth. Furthermore, a short comprehension of VL is given, to introduce the reader to the basic concepts of VL.

Chapter 2 presents a modification of the shock tube apparatus developed to experimentally investigate VL under varying atmospheric conditions. This chapter presents the first results of experimental VL in different atmospheric conditions and transporting gas phases.

For this thesis, additional experiments to the presented experiments in **Chapter 2** were performed. The additional results are presented in the Appendix A. Experiments with tholeiitic basalt were performed, and the sample and the filter from the exhaust air pipe were recovered. The filters which collect the very fine ash fraction were analyzed to investigate them for potential organic compounds synthesized during the experiments. Furthermore, gas sampling bottles were attached to the exhaust air pipe of the setup and the gas within the particle collector tank was purged through distilled H_2O. The water was analyzed for NO_2 and NO_3 to identify potential nitrogen fixation during the experimental runs.

Chapter 3 presents the results of a study on the influence of grain size distribution and sample composition on experimental VL. This chapter introduces an approach to scale the experiments to nature. The supplementary figures are provided in the Appendix B. Additionally, an image subtraction algorithm was applied to the high-speed video recordings to enhance the visibility of the particle movement within the jet. Examples of the image subtraction are given as well in the Appendix B.

Mud represents another highly interesting geomaterial in the research about the emergence of life. In **Chapter 4** we investigated VL as a potential ignition mechanism in recent mud volcanism, and whether VL is plausible for mud volcanoes. Further, the impact of humidity of the mud samples on VL was experimentally tested as well as the grains size distribution. The supplementary figures are provided in the Appendix C.

Chapter 5 discusses the results of this thesis in the context of the emergence of life and concludes on the impact of this thesis. This chapter also addresses the limitations of this thesis.

Chapter 6 presents an outlook on further studies which can be conducted based on the results of this thesis.

1.3 Environments for the emergence of life

1.3.1 The origin of life

In this work, experimental VL was created under environmental conditions relevant to the origin of life. The parameters that influence charging mechanisms and discharge mechanisms in volcanic plumes pertinent to conditions on early Earth were investigated as volcanically active environments are considered possible environments for the origin of life. Discharges are a potential energy source to promote prebiotic synthesis reactions (e.g., Basiuk & Navarro-González, 1996; Lavrentiev et al., 1984; Miller, 1953; Navarro-González & Segura, 2004; Plankensteiner et al., 2004). Therefore, how VL might have emerged on early Earth was investigated in this thesis. The question of how VL might have differed from present-day electrical charging mechanisms in a volcanic plume implies the question of the environmental conditions under which early life might have formed and evolved. Since our planet Earth is an ever-evolving system, environmental conditions have changed significantly since its beginning. The question of environments for the origin of life first requires a definition of life. So, what are we talking about when we ask about the origin of life?

The definition of life

The search for the origin of life has constantly been challenged by what we define as 'life'. Beginning with the search for the origin of life on Earth, this question is still up-to-date when we explore the universe and search for traces of life on other extra-terrestrial planetary bodies, like Mars.

Despite the ongoing search for the origin of life and extra-terrestrial life, several definitions exist for life. An overwhelming amount of attempts to define life or to evaluate the definition of life is proposed in the literature (Chyba & McDonald, 1995; Cleland & Chyba, 2002, 2007; Dupré & O'Malley, 2009; Fleischaker, 1990; Joyce, 1995; Kamminga, 1988; Koshland Jr, 2002; Macklem & Seely, 2010; Ruiz-Mirazo et al., 2010; Sagan, 2010; Tsokolov, 2009). Tsokolov (2009) observed that over one hundred different scientific definitions have been proposed within the last century but concluded that all of them suffer from a principal inconsistency.

For example, definitions based on terrestrial life were confronted with the question: metabolism or genes first? The statement 'genes first' connects the definition of life to the first evolutionary steps of life. If evolution is a prerequisite for identifying life, the successor of the discovered life form must also be identified to match the definition of life itself. If an organism can evolve but has not done so far, which period is needed to investigate its ability to evolve? A kind of 'chemical Darwinian definition' of life was chosen by Joyce (1995), which says that life is a self-sustained chemical system capable of undergoing Darwinian evolution. By this definition, the origin of life is the same as the beginning of evolution. This definition might conflict with ideas of early life forms, which are supposed to be protein-based creatures capable of metabolism but predating nucleic acid-based replication. If such organisms were discovered, we

would not hesitate to call them a life form, although they would not match the 'Darwinian definition' (Cleland & Chyba, 2002).

Another short and easy definition for life was given e.g., by Koshland Jr (2002). Koshland Jr (2002) wrote that if he was forced to give a definition, he would offer

> *'a living organism is an organized unit, which can carry out metabolic reactions, defend itself against injury, respond to stimuli, and has the capacity to be at least a partner in reproduction.' (Koshland Jr, 2002, p. 2215)*

It becomes evident that the definition of 'life' is explicit or implicit for projects searching for life in the universe (Cleland & Chyba, 2002). Therefore, the search for extra-terrestrial life requires a non-Earth-centric definition (Conrad & Nealson, 2001) not to overlook biosignatures which are not within the scope of the definition of life. An Earth-centric definition of life might not apply to the search for extra-terrestrial life, e.g. for the exploration of Europa (Chyba & Phillips, 2001).

To overcome the hurdle of an Earth-centric definition, Conrad and Nealson (2001) emphasized six characteristics of life as a base for a definition:

(1) Structure: life is a machine to convert energy into a biologically valuable form, and some 'hardware' is needed to do so.

(2) Unique chemistry: the structure is combined with an unique chemistry. The nature of its chemistry is evaluated as less important than its uniqueness.

(3) High-fidelity replication: life needs to replicate and proceeds from few to many copies of complex molecules.

(4) Evolution: during the replication, errors will occur. This ensures that some variability exits within the system.

(5) Energy consumption and metabolic production: some fraction of energy within a living system will be converted into a biologically helpful form or synthesized into complex chemical structures. Energy will become consumed, and metabolic products will be produced.

(6) Deliberate movement: life must have obtained some mobility to escape its metabolic end products and/or approach fresh nutrients. Deliberate movements are suggested by Conrad and Nealson (2001) as the first innovation for early life.

Despite the variability in the definition of life, the search for early life and extra-terrestrial life requires a definition with characteristics that can be measured and quantified to some degree (Conrad & Nealson, 2001). Fleischaker (1990) concluded that

> *'(…) the fact remains that we must be able to* conceptualize *the object of our search before we can* recognize *it: only with rigorous criteria to identify the living will we ever find life in outer space or demonstrate the origin of its operations in our laboratory'. (Fleischaker, 1990, p.136)*

However, although all human beings consider themselves living organisms, a general acknowledged definition of life remains a challenge. As Benner (2014) concluded

> *'A substantial amount of ink has been consumed by efforts to define life, without consensus' (Benner, 2014, p. 339).*

Challenged by all those controversies, Cleland and Chyba (2002) pointed out that it is characteristic for most definitions to have vague boundaries and natural categories are delimited by nature rather than by human interests.

Abiogenesis and prebiotic synthesis

At some point in Earth's history, non-living matter (e.g., carbon, hydrogen, oxygen, nitrogen, sulfur and phosphorous) must have transformed into organic molecules. The first step in the emergence of life was probably the synthesis and accumulation of abundant carbon-based biomolecules (Hazen, 2012). Abiogenesis describes the transformation of abiotic molecules to first organic molecules, which can be regarded as the prerequisites of life. Benner (2014) described it as we are now in an era of prebiotic chemistry in which tens of thousands of papers attempted to define processes by which 'molecules that look like biology' originated from 'molecules that do not look like biology'.

This thesis focuses on environmental conditions favouring the possibility of forming the first organic molecules. Three key resources are considered essential for the emergence of life: liquid water, a source of energy (e.g. radiant energy from the sun, lightning etc.) and chemical elements which form combined essential biomolecules (Hazen, 2012). It is typically assumed that those compounds originate from an abiotic synthesis process, accumulated, condensed into polymers, interacted and eventually evolved into self-sustaining systems through natural/geological processes on early Earth (Kitadai & Maruyama, 2018) (**Figure 1-1**). At some point in Earth's history, the abiotic synthesis of life's building blocks (amino acids, ribose, nucleobases, fatty acids and nucleotides) occurred. Those building blocks must have faced polymerization to bio-macromolecules (peptides and oligonucleotides), and biological functions like replication and compartmentalization emerged (Kitadai & Maruyama, 2018).

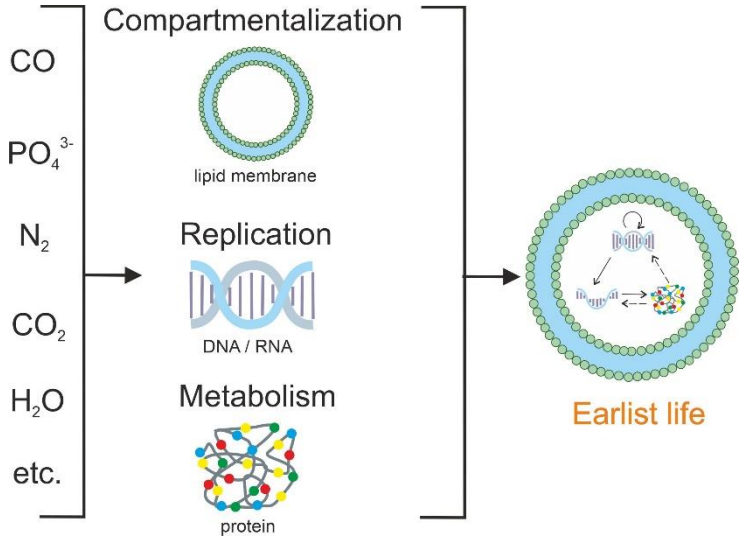

Figure 1-1. Schematic representation of how abiotic building blocks are transformed into bio-macromolecules operating three fundamental functions of life: compartmentalization, replication, and metabolism. The illustration was modified after Kitadai and Maruyama (2018).

However, the geochemical setting that could drive all critical stages of chemical evolution remains unclear. For instance, Kitadai and Maruyama (2018) concluded that at least eight reaction conditions are required to obtain the necessary diversity for the stages in the chemical evolution:

(1) a reductive gas phase,

(2) an alkaline pH,

(3) freezing temperature,

(4) fresh water,

(5) dry/dry-wet cycles,

(6) coupling with high-energy reactions,

(7) heating-cooling cycles in water and

(8) extra-terrestrial input of life's building blocks and reactive nutrients.

This variety in prerequisites indicates that life might not have originated in one setting, but rather, diverse and dynamic environments are required.

As expressed by Iris Fry's article about the controversies in the research about the emergence of life, '(…) the study of the origin of life is characterized by its high degree of controversy' (Fry, 1995). As there is no geological rock evidence about the conditions on early Earth when life began, several settings and environmental conditions are considered as a potential habitat for the emergence of life and therefore, several different theories were proposed, which might enable the evolution of abiogenetic matter to first organic molecules which developed further.

Various environments are proposed so far as plausible sites for the emergence of life:

- Primordial/ primaeval soup (e.g., Haldane, 1929; Miller, 1953; Oparin, 1957), possibly the primaeval ocean.
- Lakes or ponds (Bada & Korenaga, 2018), in addition with seasonal wet-dry cycles, molecules with increased complexity might have formed.
- Submarine hydrothermal systems, e.g. black smokers or alkaline vents (Corliss et al., 1981; Martin et al., 2008; Martin & Russell, 2007; Russell et al., 1994; Russell et al., 2005; Russell et al., 2010; Shock & Schulte, 1998; Villafañe-Barajas & Colín-García, 2021; Wächtershäuser, 1988).
- Geothermal systems and geysers (e.g., Damer & Deamer, 2015; Deamer & Georgiou, 2015; Mulkidjanian et al., 2012a; Mulkidjanian et al., 2012b). Deamer et al. (2006) added mixtures of representative solutes to natural geothermal settings to investigate their relevance for the emergence of life.
- Extra-terrestrial origin (Panspermia hypothesis) or extra-terrestrial material as a potential source for precursors relevant to prebiotic synthesis (e.g., Anders, 1989; Chyba et al., 1990; Clark, 1988; Oró, 1961; Oró et al., 2006; Oró et al., 1991). Some authors suggested Mars as an interesting birthplace for the origin of life (Kirschvink & Weiss, 2002), and whether there is or was life on Mars was discussed (Schulze-Makuch et al., 2008). Other environments than Mars have been proposed as well to possibly shelter life. Such an environment might be represented, for example, on Enceladus (e.g. Barge & White, 2017; Deamer & Damer, 2017; Kahana et al., 2019).
- Floating pumice rafts (Brasier et al., 2013; Brasier et al., 2011). The ability to float on water exposes the pumice to the air-water interface and exposes the pumice to a wide range of conditions.
- Sedimentary-hosted geothermal systems (Westall et al., 2018) provide rapid alteration of mafic and ultra-mafic rocks and are therefore characterized by temperature and pH disequilibria accompanied by the formation of silica gels.
- Active volcanoes, whereas different settings are addressed. The volcanic plume (Basiuk & Navarro-González, 1996; Johnson et al., 2008) and volcanic-hosted splash pools (Fox & Strasdeit, 2013) were proposed plausible environments for the origin of life.

The settings are not clearly separatable from each other and overlap. For example, lagoons are part of the primordial oceans, and ponds are a compartment of geothermal fields. Also, mineral surfaces (e.g., Bernal, 1949; Cleaves II et al., 2012; Hazen, 2012; Hazen et al., 2001; Hazen & Sverjensky, 2010; Lambert, 2008; Orgel, 1998; Schoonen et al., 2004), and in particular Fe-Mg clay minerals (e.g., Kloprogge & Hartman, 2022), are considered to provide catalytic characteristics to mineral surface-organic interactions.

All settings have in common that they need to be far from equilibrium but with a source of energy that must have been present to drive synthetic reactions. One

potential environment proposed by, for example, Basiuk and Navarro-González (1996) are volcanic ash-clouds, which is the focus of this work. A combination of active hot-spot volcanism with volcanic lightning and warm or cold little ponds as a relevant geological setting for the emergence of life is suggested by Bada and Korenaga (2018).

Chemical and physical diversity are prerequisites for life, requiring a complex interaction among the diverse geochemical processes (Kitadai & Maruyama, 2018). This idea was suggested, e.g. by Stüeken et al. (2013). Following this hypothesis, Dohm and Maruyama (2015) proposed a new concept of a habitable environment. This habitable environment involves atmosphere, water and landmass with continuous material circulation between the three driven by the Sun.

The proposed features for possible geological settings where synthesis reactions might have occurred are characteristics of volcanically active environments. The geological setting of an active volcano on early Earth matches this geochemical diversity proposed (e.g., Dohm & Maruyama, 2015; Stüeken et al., 2013), only that the driving energy which initiates the material circulation is not the sun but the ongoing volcanic activity.

1.3.2 The Early Earth

What is a reasonable estimate of the age of life? Can we narrow the period of time for the potential emergence of life on Earth? Based on the assumption that early life may have originated on Earth, we must clarify the prevailing environmental conditions when life evolved appropriately.

Earth's early history

Exact ages, e.g., for the origin of the Earth or the universe, are still subjected to changes due to always new and more precise measurements. In general, it can be said that our universe formed around 13.8 Ga ago (Planck Collaboration et al., 2020, p.15, Table 2). The variety in approaches to determining certain ages in geological history becomes especially obvious for determining the age of the Earth (Dalrymple, 2001). The age of the Earth is nowadays determined as ~ 4.6 Ga. Earth's beginning is called the Precambrian (~ 4.6 Ga – 538.8 ±0.2 Ma (Cohen et al., 2013; updated)). The Precambrian is subdivided into three Eons: the Hadean (~ 4.6 – 4.0 Ga), the Archean (4.0 – 2.5 Ga) and the Proterozoic (2.5 Ga – 538.8 ±0.2 Ma). **Figure 1-2** shows significant events since the universe's formation.

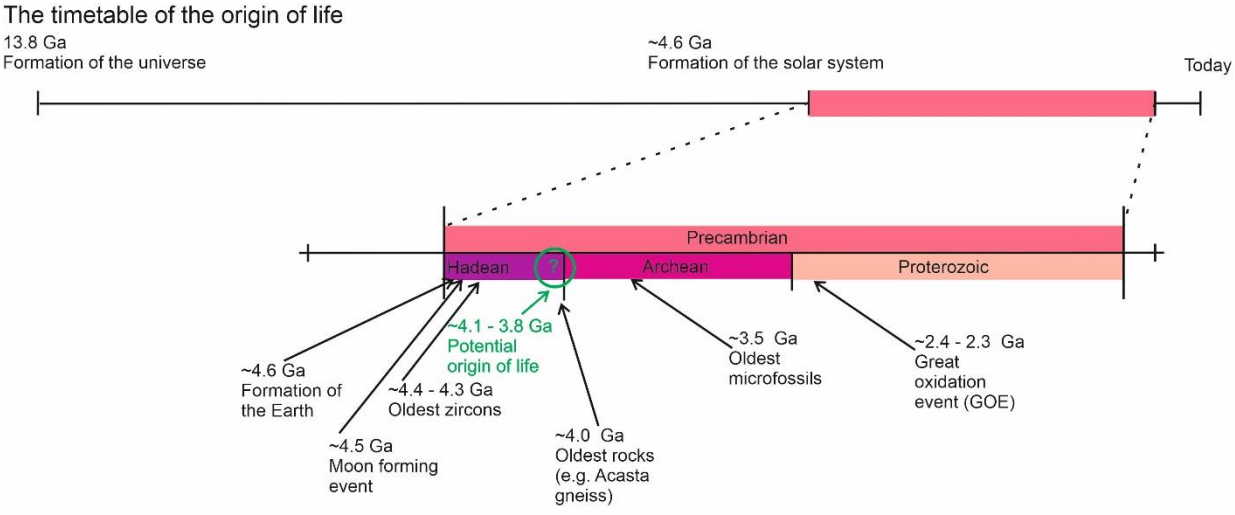

Figure 1-2. The timetable of the origin of life. Formal subdivision of the Precambrian annotated with important events relevant to the emergence of life. The illustration was modified after Cohen et al. (2013; updated); Gradstein et al. (2004); Joyce (2002); Knoll and Nowak (2017).

The Hadean proceeds the Archean. Termed after the Greek mythological underworld Hades, it can be understood as the period in Earth's history for which almost no preserved rock record exists (e.g., Cloud, 1972; Gradstein et al., 2004). Although a discrete 'late heavy bombardment phase' is still debated, the Hadean Earth was subjected to intense bombardment. A significant and important event in Earth's history during the Hadean was the Moon-forming event when a Mars-sized planetary object collided with the early proto-Earth resulting in the formation of today's Moon (e.g., Canup, 2004; Canup & Asphaug, 2001). The deposition of an enormous amount of kinetic energy of this impact resulted in the formation of a deep magma ocean (Tonks & Melosh, 1993). The vigorously convective magma ocean cooled afterwards.

Zahnle et al. (2007) pictured the Hadean Earth as follows:

> *'Today the Hadean is widely and enduringly pictured as a world of exuberant volcanism, exploding meteors, huge craters, infernal heat, and billowing sulfurous steams; that is, a world of fire and brimstone punctuated with blows to the head. In the background a red Moon looms gigantic in the sky.' (Zahnle et al., 2007, p.37)*

After the Moon-forming event, another precondition for the potential origin of life became abundant: liquid water (see **Chapter 1.3.3**). First hints for liquid water are given by oxygen-isotope evidence from zircons, which are around 4.3 Ga (Mojzsis et al., 2001). Zahnle et al. (2007) argue that it is even possible that Earth became potentially habitable 10 - 20 Myrs after the Moon-forming impact and other researchers as well regard the end of the Hadean as the potential time range for the emergence of life (e.g., Battistuzzi et al., 2004; Kitadai & Maruyama, 2018). The Hadean is referred to as the time period without a rock record. The oldest rocks remnants on Earth date back to ~ 4.0 Ga (Acasta Gneiss (Bowring & Williams,

1999)) whereas the oldest minerals, zircons, date back ~ 4.4 - 4.3 Ga (Harrison et al., 2008; Mojzsis et al., 2001; Wilde et al., 2001).

The Archean was initially conceived as the period from after the origin of life to the advent of free oxygen in the atmosphere (Catling & Zahnle, 2020; Cloud, 1972). Early microbial evidence for life stems from findings ~ 3.5 Ga old (Hickman-Lewis et al., 2018; Westall et al., 2006). The first traces of life are, e.g., the $\delta^{13}C$ depleted microparticles (Rosing, 1999) from 3.7 Ga, which also points to the conclusion that life must have emerged substantially earlier than 3.7 Ga. The Archean is also the Eon with a significant change in the Earth's atmosphere as the atmosphere became oxygenated due to microbial activity. The rise in oxygen concentration is termed the 'Great Oxidation Event' (GOE) and was ~ 2.5 - 2.3 Ga (Lyons et al., 2014). Those disequilibrium conditions in a planet's atmosphere are regarded to be an indicator of life itself (e.g., Krissansen-Totton, Olson, et al., 2018) and should be considered in the search for extra-terrestrial life.

The small summary of Earth's history points strongly to the end of the Hadean and the very beginning of the Archean as the potential origin of life. Therefore, experiments considering Earth as the birthplace of life should focus on environmental conditions prevalent at this time in the Earth's history, which is not an easy task as almost no rock record is preserved from this time. We want to focus further on three governing parameters regarding the environmental conditions of the late Hadean/early Archean: Exposed land areas, ocean formation and the atmosphere.

1.3.3 The early hydrosphere

The emergence of the first oceans

During the final accretionary phase of the early Earth and especially during the time following the Moon-forming event, the Earth's surface was probably not yet solidified and more likely covered by a liquid rock/magma ocean and water would be in a state of steam rather than forming oceans on the early Earth's surface (Sleep et al., 2001). Based on the assumption that the early water content of Earth was steaming hot, Bada (2004) concluded that Earth was likely devoid of any organic carbon reservoir during this time period. The water present on Earth is supposed to have originated from degassing of hydrated minerals initially present in the mantle (e.g. Pahlevan et al., 2019) and from asteroids and comets (e.g. Dauphas et al., 2000).

Although no rock record is preserved from the Hadean, some zircons ($ZrSiO_4$) are possible hints for early Earth conditions and might reveal the existence of an early hydrosphere. For example, Wilde et al. (2001) investigated zircons with an age of ~ 4.4 Ga, which show the signature to have undergone a low-temperature interaction with a liquid hydrosphere and which is interpreted by the authors as the earliest evidence for continental crust and oceans on Earth. The same conclusion was drawn from zircons with an age of ~ 4.3 Ga by Mojzsis et al. (2001). The oxygen isotope signal $\delta^{18}O$ indicates that the zircon was formed from a magma containing amounts

of reworked continental crust that formed in the presence of water near the Earth's surface (Mojzsis et al., 2001). Other investigations on Hadean zircons back up those results (Cavosie et al., 2005). These results lead to the image of a rather 'cool' early Earth (Valley et al., 2002), and there was liquid water ~ 4.4 – 4.3 Gyr ago (Cavosie et al., 2005; Mojzsis et al., 2001; Valley et al., 2002; Wilde et al., 2001). Nonetheless, the zircons remain silent on whether the early hydrosphere was 273 K or 500 K hot (Zahnle et al., 2007).

The temperature of the early ocean

The temperature of the early ocean is another ambiguous topic. Morse and Mackenzie (1998) remain vague about precise estimations of the temperature of the early oceans on Earth. They conclude that at some point in the Hadean, the ocean temperature was close to boiling (Morse & Mackenzie, 1998). For the modelling of their Hadean (4.3 – 3.8 Ga) seawater composition, they set their temperature limit from 100 °C (close to boiling) to 70°C, what they expect to be the start of the Precambrian Eon (Morse & Mackenzie, 1998). The analysis of the oxygen isotope signal in cherts of the 3.5 – 3.2 Ga Swaziland Supergroup (Baberton greenstone belt, South Afrika) indicates high ocean temperatures of 55 - 85 °C (Knauth & Lowe, 2003). Sleep (2010) proposed the idea that early Earth started in a hot state, and the pressure of CO_2 of the early atmosphere was causing the water to become liquid. He compared it to a pressure cooker (Sleep, 2010). Silicon isotope analysis in cherts implies that seawater temperature changed from ~ 70 °C at 3.5 Ga to ~ 20 °C at 0.8 Ga, as discussed by Robert and Chaussidon (2006).

Composition of the early ocean

As the Earth's hydrosphere and atmosphere are interconnected systems, the oxidation state of the early ocean cannot be addressed without addressing the oxidation state of the atmosphere. The history of the oxygenation of the atmosphere and the ocean is highly disputed, but in general, it is acknowledged that at the beginning of Earth's history, the atmosphere and the oceans were essentially free of oxygen (e.g., Farquhar et al., 2000; Holland, 2006; Kasting, 2001; Kasting & Siefert, 2002). The isotopic signature from sulfides and sulfates in Precambrian rocks leads to the conclusion that free oxygen in the atmosphere first increased significantly between 2090 and 2450 Ma and before, at which time the partial pressure of oxygen was quite low (Farquhar et al., 2000). Though the contrary model for an oxygenated atmosphere early in Earth's history can explain the sulfur isotope signal (Ohmoto et al., 2006) by another interpretation of the data, the prevalent accepted theory is that the early atmosphere and the early ocean were scarce in oxygen.

In general, the early ocean is believed to have been anoxic, and with time it became more oxygenated. Based on the theory that the ancient oceans were hotter than today (55 - 85 °C), Knauth (2005) points out that O_2 solubility decreases strongly with increasing temperature and salinity, and therefore, the Archean ocean was anoxic. Even for a scenario where the archean atmosphere would contain only 30 % less

oxygen than the modern value, the oceans would have been anaerobic due to lack of oxygen per Knauth (2005).

Today, the exchange of elements between the hot oceanic crust and the seawater plays a significant role in the composition of ocean chemistry. It is plausible that those exchange processes between the basaltic/komatiitic crust and water were also the main mechanisms controlling the Hadean – early Archean seawater chemistry (Nisbet, 1985), as well as the exchange with the atmosphere. The input by the runoff by erosion of continental crust as it is today might have been less important due to the lack of long-lived continental cratons.

Information about ocean chemistry can be derived from marine evaporites for the last 3.5 Ga (Holland, 1972). However, as H.D. Holland already stated in his paper in 1972, the rock record of evaporites does not extend further back in time than the late Precambrian. One hypothesis about early Earth's ocean chemistry is the Soda Ocean Hypothesis (SOH) (e.g. Kempe & Degens, 1985; Kempe & Kazmierczak, 1994). The Soda Ocean Hypothesis states that the Precambrian Ocean had very high alkalinity, similar to those of modern soda lakes. The high alkalinity is supposed to result from the weathering of the komatiitic crust in the presence of water and carbonic acid (Kempe & Kazmierczak, 1994). Contrary to this theory, the early ocean is believed to have been a halite-dominated solution early on (e.g., Holland, 1984; Morse & Mackenzie, 1998). A comprehension of the possible significant constituents of the Archean ocean was given by Catling and Zahnle (2020); see **Table 1-1**.

Table 1-1. Possible composition of Archean seawater after Catling and Zahnle (2020) and references therein.

Parameter or species	Published constraint	Age (year before present)	Basis of constraint
pH	6.4 - 7.4	At 4 Ga	95% confidence ranges from a carbon cycle model with 10^4-ppm Archean CH_4 (Krissansen-Totton, Arney, et al., 2018)
	6.75 - 7.8	At 2.5 Ga	
SO_4^{2-} (aq) (bulk sea)	< 2.5 µM	> 2.4 Ga	Lack of mass-dependent sulfur isotope fractionation (Crowe et al., 2014)
NO_3^- (aq) (bulk sea)	~ 0	> 2.4 Ga	By analogy to the deep, anoxic Black Sea
NH_4^+ (aq)	0.03-10.3 mM (probably porewater rather than seawater)	~ 3.8 Ga	From the N content of biotites (originally clays), derived from adsorption of dissolved NH_4^+ (aq) (Stüeken, 2016)
Fe^{2+} (aq) (deep sea)	40 - 120 µM (2-7 ppm by weight)	> 2.4 Ga	Based on solubility constraints of Fe^{2+} (Holland, 1984)
Salinity (g/kg)	~ 20-50 at 40°-0°C versus modern of 35	3.5 - 3.0 Ga	From seawater fluid inclusions in quartz (Marty et al., 2018)
Potassium	Cl/K ~ 50 versus modern 29	3.5 - 3.0 Ga	From seawater fluid inclusions in quartz (Marty et al., 2018)

The salinity is particularly interesting as it has a major influence on potential reactions in the salty brines on early Earth. Peptide formation reactions are influenced by salt concentration, e.g. salt-induced peptide formation reaction in connection with adsorption processes on clay minerals (Rode, 1999; Rode et al., 1999) or that a hypersaline environment is favorable for the preservation of specific biological macromolecular structures, for example transfer RNA (Tehei et al., 2002).

Nonetheless, the salinity of the early ocean is another highly debated topic: De Ronde et al. (1997) and Channer et al. (1997) investigated fluid inclusions from the Ironstone Pod deposits (Baberton greenstone belt, South Africa) to achieve insights about ancient hydrothermal water compositions and by taking the mixing with ambient seawater into account, calculating a possible seawater composition. However, Lowe and Byerly (2003) reinterpreted the deposits as Cenozoic spring deposits.

Hay et al. (2001) estimated the salinity to be around 50 ‰ during the Paleozoic and declined during the Mesozoic and Cenozoic to finally reach its modern value (Hay et al., 2001). Although this is no precise statement about the salinity in Hadean times, their estimation concludes that the salinity must have been significantly higher in the

Hadean or Archean than it is today. Knauth (2005) estimated, based on the sedimentation on continents (Knauth, 1998), a possible salinity up to values of 1.5 – 2x the modern value (Knauth, 2005). Also, Morse and Mackenzie (1998) saw in the lack of evidence of bedded evaporites an indication for taking the sodium concentration twice of modern seawater (salinity of 35 g/kg), and the amount of Cl^- remains similar to Na^+ to balance the charge. Also, Sleep (2010) favours a dense NaCl brine from the moment the temperature drops to 500 °C, if not before (Sleep, 2010).

Marty et al. (2018) analyzed fluids trapped in hydrothermal quartz crystals by the extended argon-argon method by stepwise crushing the samples from the North Pole (NW Australia) and the Baberton greenstone belt (South Africa), 3.5 – 3.0 Ga-old (Marty et al., 2018). They pointed out that besides evaporation as a sink for NaCl, subduction to the mantle must be considered. Their data suggests that the Archean salinity is similar to modern oceans. The ratio between Cl/K was lower than today (Archean ~ 50 compared to today 29). Catling and Zahnle (2020) summarized that the results indicate a salinity of ~ 20 – 50 g/kg at a surface temperature of 0 – 40 °C based on Figure 2 by Marty et al. (2018) (see **Table 1-1**).

1.3.4 The early atmosphere

Primary vs secondary atmosphere

Today's Earth's atmosphere is often described as a secondary atmosphere, which implies a history in the evolution of Earth's atmospheric history which is again not fully unraveled today. Holland (1962) described a three-stage model in which the Earth's atmosphere started in a highly reducing state prior to core formation. The second stage was a weakly reducing atmosphere, similar to what was proposed by Rubey (1955), mainly composed of CO_2 and N_2. The third stage describes approximately today's modern O_2-rich atmosphere (see **Figure 1-3**).

At the beginning of Earth's accretion, the primordial atmosphere was supposedly composed mainly of hydrogen and helium (e.g., Hayashi et al., 1979; Ikoma & Genda, 2006; Mizuno et al., 1980; Owen et al., 2020) and was hot enough to melt the surface, but it got lost over time to space.

Origin of the atmosphere

Before the emergence of life and photosynthesis, a primary source of modern O_2 in today's atmospheric air, the atmosphere's composition was driven by abiotic processes. The atmosphere was composed mainly of outgassing products of the interior of the Earth, either from the magma ocean or later in Earth's history by volcanism (Ortenzi et al., 2020). Degassing from volcanism can be subdivided into originating from deeper magmatic emplacements (passive degassing) and extrusive volcanism. The mantle redox state is central to the atmosphere's chemical composition (Ortenzi et al., 2020). Today, the Earth's upper mantle is oxidized, and

although the time of transition is still debated, the geological evidence suggests that during its earliest evolution, it already transformed from a reduced upper mantle (fO_2 of ~4.5 log units below fayalite-magnetite-quartz (FMQ) buffer) to an oxidized one (approximately MFQ) (Frost et al., 2008; Frost & McCammon, 2008; Nicklas et al., 2018; Trail et al., 2011). Today's mantle has an oxidation state near the fayalite-magnetite-quartz buffer, and the loss of the primordial hydrogen would explain the quite oxidized state (Sharp et al., 2013). Another possible explanation would be the disproportionation of mantle FeO and Fe loss to the mantle (Frost & McCammon, 2008). An early core formation concurrently with Earth's formation itself implies that stage one in the atmospheric evolution of Holland (1962) would only describe the period of the primary accretion, and a later formed atmosphere (formed by volcanic outgassing) would be more neutral or weakly reducing (stage two) (Catling & Kasting, 2017, Chapter 7).

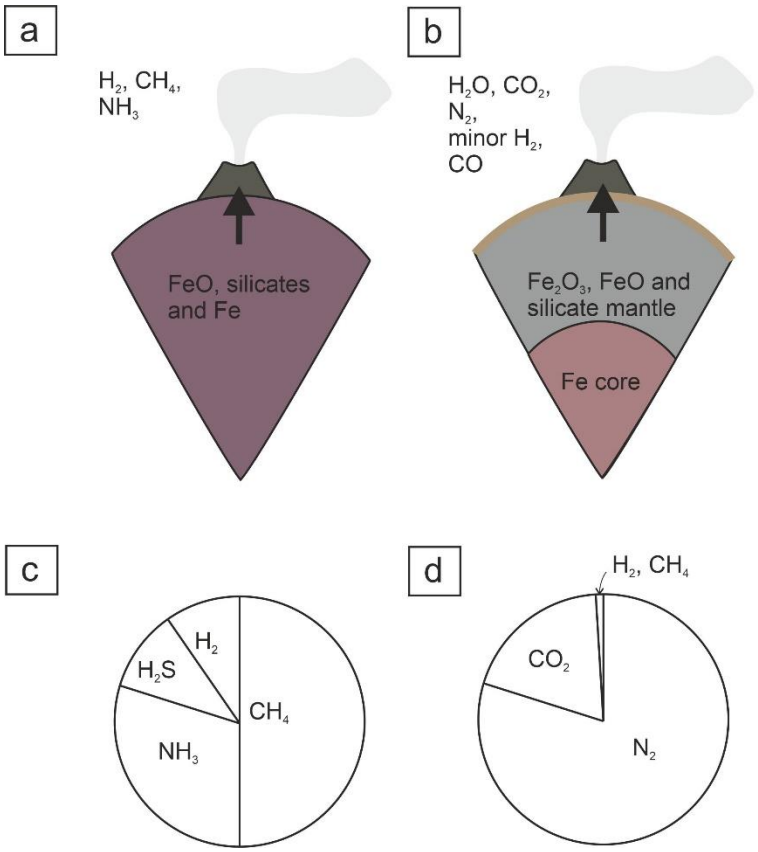

Figure 1-3. Two concepts of the early Earth's atmosphere: the reducing atmosphere and the weakly reducing/neutral atmosphere. a) Before core formation, reducing gases (e.g., H_2, CO, CH_4 and HN_3) outgas and influence the atmosphere. b) After core formation, the mantle's oxygen fugacity has changed and weakly reducing gases (e.g., H_2O, CO_2 and N_2) outgas into the atmosphere. Illustrations a) and b) are modified after Catling and Claire (2005). c) presents a potential reducing atmospheric composition, whereas d) represents a weakly reducing atmospheric composition. The illustrations c) and d) are modified after Catling and Kasting (2017), p. 199.

Composition of the atmosphere

Cyanobacterial ancestors most probably produced by oxygenic photosynthesis O_2 as a waste product. In general, the Hadean and Archean are supposed to be a period

devoid of free oxygen in the atmosphere until the Great Oxidation Event (GOE) (Catling & Claire, 2005; Catling & Zahnle, 2020; Farquhar et al., 2000), although contradicting opinions do exist on this topic as well (e.g., Ohmoto et al., 2006). The rise in oxygen concentration was rapid, between 2.4 and 2.3 Ga (Catling & Claire, 2005; Catling & Zahnle, 2020). One indicator for the GOE is the disappearance of mass-independent fractionation (MIF) of sulfur isotopes. This change in sulfur isotopes marks the transition within the rock record from an oxygen-poor to an oxygen-rich atmosphere (Farquhar et al., 2000; Luo et al., 2016). This hypothesis is corroborated by MIF of sulfur isotopes and other geochemical proxies (Johnson et al., 2014; Rasmussen & Buick, 1999; Rye & Holland, 1998). However, local oxygen 'whiffs' are possible before the GOE.

Today, many geoscientists doubt that the primitive atmosphere was as highly/strongly reducing as, e.g. the composition used by Miller (1953) in his famous prebiotic synthesis experiments had been (Bada, 2004). It is believed that the early atmosphere was more nearly neutral or mildly/weakly reducing (Rubey, 1955) than highly reducing and mainly composed of the volatiles CO_2, H_2O, and N_2 (Catling & Zahnle, 2020), whereas 'weakly reducing' means that minor levels of components like CO, H_2 and CH_4 might have been abundant. Nonetheless, e.g. Bada (2004) proposes that other gaseous compositions might have occurred due to gas emission by active volcanism and that a locally more reduced gas release which was immediately exposed to volcanic lightning might have existed (Bada, 2004).

CO_2

Following the hypothesized weakly reducing/neutral atmosphere, the most likely outgassed specification of carbon is CO_2, which is Earth's most important non-condensable greenhouse gas (Catling & Zahnle, 2020). The other most likely outgassed carbon volatiles next to CO_2 are CH_4 and CO, and the final outgassing redox state depends on the oxidation state of the mantle. Presumably, the oxidation state of the mantle was early in Earth's history quite oxidizing (Frost et al., 2008; Nicklas et al., 2018; Trail et al., 2011), the redox state of the outgassing carbon is presumably like today: CO_2. The early Earth's atmosphere probably had much higher concentrations of CO_2 than today based on estimates from paleosols (Driese et al., 2011; Hessler et al., 2004; Sheldon, 2006), and declined over time to today's CO_2 levels. Some scientists suggest that the range of values for pCO_2 asks for an additional greenhouse gas in the atmosphere to overcome the 'Faint Young Sun (FYS)' paradox (e.g. Sagan & Mullen, 1972; Sheldon, 2006). The theory predicts that the sun's luminosity was about 70% of today's luminosity (Gough, 1981). To overcome the FYS, the atmospheric composition is proposed as one mechanism balancing against the faint young sun, as liquid water requires moderate temperatures on the surface of Earth. Methane, for example, is suggested to be an additional greenhouse gas (Driese et al., 2011; Hessler et al., 2004; Sheldon, 2006) and NH_3 (Sagan & Chyba, 1997; Sagan & Mullen, 1972). However, direct evidence for the Archean CO_2 content of the atmosphere remains scanty (Catling & Zahnle, 2020).

N_2

Today, volcanic gas emissions contain N_2 as a nitrogen specification. It is difficult to measure the N_2 concentrations as N_2 is the bulk gas in the air and easily contaminates the sampling procedure (Catling & Kasting, 2017, Chapter 7). In addition to volcanic emissions of nitrogen, oxygenic weathering of organic material is a nitrogen source, and it is released as either N_2O or N_2 (Catling & Kasting, 2017, Chapter 7). For a weakly reducing atmosphere scenario, N_2 is the primary nitrogen species in the atmosphere. Although N_2 was one of the bulk atmospheric gases, its Hadean level remains unclear (Catling & Zahnle, 2020). Either in the Hadean, the pN_2 started high and then decreased (Goldblatt et al., 2009) by processes of the geological nitrogen cycle or was controlled by partitioning into the magma ocean (Wordsworth, 2016). For the Archean, different lines of evidence were used to estimate the N_2 concentration. For example, fossil raindrop imprints (Som et al., 2012), analysis of nitrogen and argon isotopes in fluid inclusions trapped in 3.0-3.5 Ga hydrothermal quartz (Marty et al., 2013), atmospheric gases trapped in fluid inclusions contained in minerals (Avice et al., 2018) and the size distribution of gas bubbles in basaltic lava flows (Som et al., 2016) give first constraints about Archean pN_2.

Catling and Zahnle (2020) reviewed what is so far known about the Archean atmosphere and gave an overview of the post-Archean atmospheric evolution (**Figure 1-4**). Catling and Zahnle (2020) conclude that the Archean atmosphere was devoid of oxygen but enriched in greenhouse gases like CO_2 and CH_4 to counter the Faint Young Sun. The concentration of N_2 in the Archean atmosphere was similar to today's concentrations. The abundance of N_2 highly depends on the Archean nitrogen cycle which needs further understanding how it operated under oxygen-free conditions.

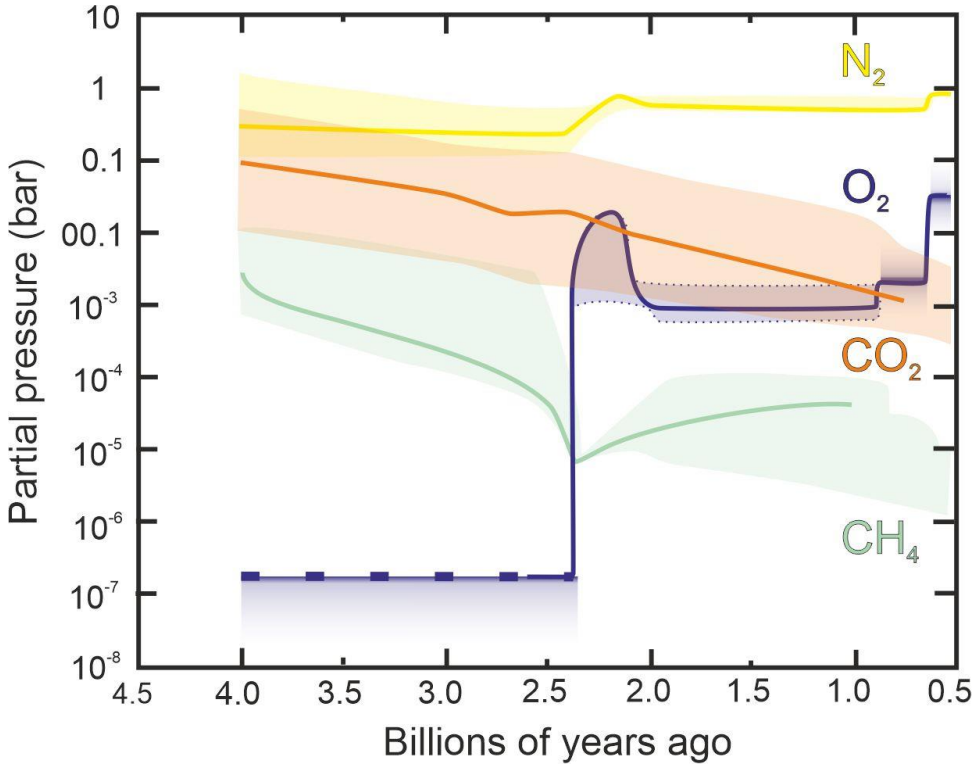

Figure 1-4. Overview of post-Archean atmospheric evolution, modified after Catling and Zahnle (2020) and references therein. The uncertainties on gas concentrations are a factor of a few or more, as detailed in Catling and Zahnle (2020) Table 1, text and the other figures.

1.3.5 Early exposed land areas

Several emergence of life scenarios, e.g. the Darwinian 'warm little pond' theory, require exposed land areas. Therefore, an essential environmental key parameter of early Earth is if there was exposed land area and, in case there was, the amount and type of exposed area above sea level (Bada & Korenaga, 2018).

O'Neil et al. (2008) described a locality near Hudson Bay as the oldest rock record found. Their methodology used a short-lived radioactive isotopic system where isotope ^{146}Sm decayed to the stable isotope ^{142}Nd, and they obtained an isochron age of ~ 4.28 Ga for the investigated 'faux-amphibolite'. Sleep (2010) evaluated their results that their data points to an early formation and persistence of crust at a minimum.

However, as we focus on the very early stage of Earth, the availability of rock records becomes more scarce the deeper we go in time. As no substantial rock record is available on Earth from the Hadean, we have to rely on the information given by the oldest remnants we have on Earth: zircons ($ZrSiO_4$). The lack of a geological rock record of Hadean rocks does not necessarily imply that there was no exposed land. Another obstacle is that definitions relevant to modern Earth, like the distinction between continental and oceanic crust, cannot be applied that easily to early Earth (Cawood et al., 2022) and continental-type crust may have been more mafic than today, so for example possibly basaltic in composition. The exposed land area on

early Earth does not necessarily imply or define continental crust as we understand it today. Modern plate tectonics is a mechanism to recycle surface material back to the interior of Earth by subduction (Condie, 2013) and, by doing so, is continually refreshing the Earth's surface. Even if expansive land existed before 3 Ga, it could have been easily recycled by plate tectonics (Korenaga, 2021).

Based on the comparison of initial Pb-isotope signatures of several early Archean lithologies and minerals Kamber et al. (2003) proposed the existence of substantial heterogeneity in the early Archean mantle. They developed a model in which the precursors for ≥ 3.8 Ga tonalites and monzodiorite gneisses are not mantle-derived but formed by remelting or differentiation of an ancient basaltic crust. They propose that a stable basaltic proto-crust might have existed during the Hadean. This model explicitly refutes processes such as sediment recycling or melting in subduction zones (Kamber et al., 2003). Based on the importance of mafic rock during the Hadean (Cawood et al., 2018), especially basalts (Kamber, 2015; Kamber et al., 2003), tholeiitic basalt was employed as an analogue sample material in this thesis.

Information from zircons

Although no continental crust is preserved from the Hadean period, the resisting minerals point by their geochemically signature to an early onset of continental crust formation. The geochemically signature of the oldest zircons with an age of around 4.4 Ga was interpreted as the zircons first crystallising in a magma derived from melting existing continental crust (Wilde et al., 2001). The amount and rate of continental crust formation still stay elusive. Korenaga (2021) points out that the extent of exposed land differs from that of continents, as the former refers to only the part of continents above sea level with contributions from oceanic islands.

Earth is so far the only known planet with what we define as modern plate tectonics (Stern et al., 2018). The onset of modern plate tectonics, possible precursor modes and the growth rate of continental crust is another highly debated topic of Earth's earliest history (e.g. reviewed by Cawood et al., 2022). The proposed hypotheses so far range from stagnant lid convection (e.g. Cawood et al., 2018; Debaille et al., 2013; O'Neill & Debaille, 2014; Piper, 2013) to rapid plate tectonics/ rapid crustal growth (e.g. Guo & Korenaga, 2020; Rosas & Korenaga, 2018; Sleep et al., 2014). Hawkesworth et al. (2017) emphasize the variation in crustal growth models (**Figure 1-5**) by comprehending published models for the growth of the continental crust.

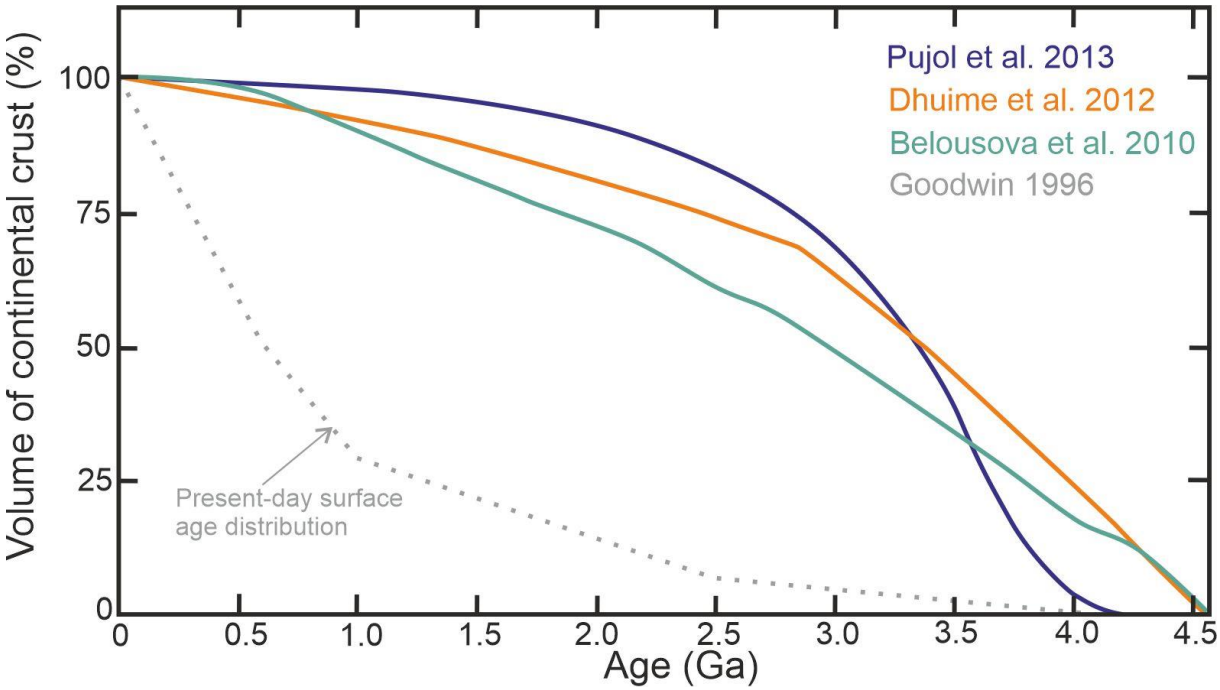

Figure 1-5. Mean curves from the continental growth models comprehended by Hawkesworth et al. (2017) and references given therein (blue line: Pujol et al. (2013), orange line: Dhuime et al. (2012) and green line: Belousova et al. (2010)). The grey dashed line reflects the proportion of juvenile crust of different ages preserved today (Goodwin, 1996). Modified after Hawkesworth et al. (2017).

A critical consideration of the onset of plate tectonics, implying the formation of continental crust, is the abundance of liquid water. Campbell and Taylor (1983) summarized it 1983 as easy as 'no water, no granites – no oceans, no continents': The formation of stable continental crust requires a mechanism to form sufficient felsic rock to offset the high density of the basaltic, ultra-mafic component and prevent the subduction of the felsic material. The formation of an oceanic crust and its subduction seems inescapable as a heat loss mechanism, but this process does not necessarily imply an Archean continental drift or modern-style linear subduction zones. So, primitive Archean felsic magma might have formed by the starting point as the subduction of hydrated basaltic or ultra-mafic crust back into the mantle (Campbell & Taylor, 1983). Given the geochemical indications for an early ocean (Cavosie et al., 2005; Mojzsis et al., 2001; Wilde et al., 2001), the presence of some kind of plate tectonic is not utterly unthinkable in the Hadean (Korenaga, 2021). Condie and Kröner (2008) hypothesize that it is unlikely that plate tectonics began on Earth as a single global event at a specific time in the early Archean. They propose that it is more probable that a few mantle 'returns' became cool enough that some kind of steep subduction locally became possible. As those slabs could descend at steep angles more common, a 'steep mode' subduction developed similar to modern subduction styles (Condie & Kröner, 2008). Cawood et al. (2022) propose to separate Earth's evolution into seven phases:

1) Proto-Earth: the initiation and formation of Earth (4.57–4.45 Ga).

2) Primordial Earth: the formation of mafic and initial felsic crust (ca. 4.45–3.80 Ga).

3) Primitive Earth: Large-scale craton formation (ca. 3.8–3.2 Ga).

4) Juvenile Earth: The stabilization of the cratons (ca. 3.2–2.5 Ga).

5) Youthful Earth: The dispersal of the cratons and initial continental assembly (at 2.5–1.8 Ga).

6) Middle Earth: An apparent global stability of much of the Earth system established during Earth's middle age (at ca. 1.8–0.8 Ga).

7) Contemporary Earth: The establishment of the current Earth system (since 0.8 Ga until today).

The seven phases by Cawood et al. (2022) are dominated by different tectonic styles or represent a transitional phase in Earth's history. The Proto-Earth underwent the initial accretion and the impact events. The Earth was largely molten, and the core formed. During the period of the primordial Earth, an early proto-crust formed from the solidified magma-ocean, which was mafic (e.g., basaltic) to ultra-mafic in composition. Hadean zircons and outcrops of the Acasta Gneiss complex provide pieces of evidence for the formation of felsic melts. The tectonic style during this stage was a stagnant lid/ squishy lid. The primitive Earth marks the beginning of the preservation of significant rock record, and squishy lid tectonics dominated. For the juvenile Earth, Cawood et al. (2022) propose a transitional tectonic style to an early mode of plate tectonics present during the stage of the youthful and the middle Earth. Lastly, for the contemporary Earth, modern plate tectonics operate (Cawood et al., 2022).

Hot spot volcanism causing exposed land area

The onset of plate tectonics, the emergence of the first continental crust and its growth rate are today still highly debated. However, as volcanism was supposed to be very active during the early stage of Earth (Basiuk & Navarro-González, 1996), hot spot volcanism and its accompanying hot spot volcanic islands comparable to modern Hawaii are supposed to be potentially exposed land areas on early Earth (Bada & Korenaga, 2018). For both model end members, either the stagnant lid or the early continental growth theory, hot spot volcanism is a process that might have taken place on early Earth and poses a potential source for exposed land area. Nonetheless, Korenaga (2021) points out that an estimate of the amount of exposed land area on early Earth requires a deep understanding of the entire Earth system and that such an estimate is highly speculative.

1.3.6 Early volcanism

Remnants of volcanism

Again, as in the previous chapters about the environmental condition of early Earth, an insurmountable obstacle is the lack of rock records from the Hadean. The first profound rock record starts with Archean rocks.

The abundance of volcanism

The primary driving mechanism of volcanisms for early and modern Earth should remain the same but was there a change in eruption style?

Basiuk and Navarro-González (1996) assume that volcanic eruptions should have been much more abundant and violent in the Archean. As previously discussed, the early Earth's interior was sweltering immediately after formation, resulting in a vigorously operating mantle convection causing rapid cooling. The vigorously operating mantle convection is assumed to have lasted at least for several 100 Myrs and might have caused intense volcanisms on early Earth. Also, as early Earth was exposed to intense bombardment in its very beginning, the colliding impacts were likely to destroy the first incipient crust and trigger volcanism. Therefore, it seems likely that volcanism (e.g., plume volcanism, subaqueous explosions) was a dominant process taking place on early Earth (e.g. Abbott & Isley, 2002; Basiuk & Navarro-González, 1996; Richter, 1985).

As volcanisms had been an essential and vivid process on early Earth, responsible for potentially exposed surface area, and atmospheric composition and relevant as a potential energy source, what might volcanism on early Earth have been like? As not much is known with certainty about the early Earth, it is possible that modern and primordial volcanoes could differ in general parameters from each other. Such general parameters include the composition of volcanic gases and the surrounding atmosphere, ash composition, temperature, pressure and the properties of the electric discharges within the plume (Basiuk & Navarro-González, 1996).

Eruption types and typical lithologies

Komatiites are an almost entirely Precambrian rock which is no longer generated by modern processes. The ultra-mafic rock was first and in detail described in 1969 by Morris and Richard Viljoen (M. J. Viljoen & R. P. Viljoen, 1969; Viljoen & Viljoen, 2019; R. P. Viljoen & M. J. Viljoen, 1969). Komatiites are ultra-mafic volcanic rocks with a MgO content higher than 18 wt% (Arndt & Lesher, 2004; Le Bas, 2000). Komatiitic magma erupted at temperatures of ~ 1600 °C (Arndt & Lesher, 2004; Green et al., 1975; Nisbet et al., 1993) with a very low viscosity. A komatiitic flow shows internal zoning, which can be subdivided into an A-zone and a B-zone (Pyke et al., 1973), where the A-zone with spinifex structures reflects a cooling history and the B-zone, with accumulated and settled olivine or pyroxene phenocrysts displays the crystallization history (Renner et al., 1994). Although komatiites are intensely investigated, some parameters remain debated, e.g. the explosivity of komatiites (Eriksson et al., 2004).

Low viscosity and high-temperature do not favor explosive fragmentation, but pyroclastic komatiite deposits (Saverikko, 1985) and vesicular komatiite forming pyroclastic deposits (Schaefer & Morton, 1991) are described. Eriksson et al. (2004) interpret those fragmentation processes as probably autoclastic but do not exclude those volatile-rich komatiites interacting with seawater in a shallow-water setting may

produce Surtseyan-type eruptions producing small-volume pyroclastic deposits. Komatiites are also regarded as a robust indicator of global plume activity which is characteristic of superplumes by Abbott and Isley (2002) and therefore indicate high volcanic activity.

Komatiites have long been regarded as an essential component of greenstone belts, which are Archean to Proterozoic terranes. Though de Wit and Ashwal (1995) conclude that the volume of komatiites in greenstone belts has probably been overestimated and overemphasized, komatiites constitute less than 5 % of the total volcanic rocks in most greenstone belts.

To give a precise definition of what determines a greenstone belt is not uncomplex and, as pointed out by de Wit and Ashwal (1995), became increasingly cumbersome. Condie (1981) addresses the issue of whether greenstone belts are only restricted to the Archean depending on its definition. A somewhat generalized definition in which greenstone belts are described as a supracrustal succession in which mafic volcanics dominate is not restricting greenstone belts to the Archean. In a more restricted definition that includes the presence of relatively large amounts of ultra-mafic and komatiite volcanics, post-Archean examples become rare or even absent (Condie, 1981).

Condie (1981) gives general features for greenstone belts that greenstone belt terranes are composed in large part of granitic and gneissic rocks (80 – 90 %), which surround and, in part, intrude greenstone belts. Condie (1981) describes the greenstone succession as composed chiefly of pillowed, mafic rocks. The calc-alkaline volcanic rocks increase in abundance with stratigraphic height in some successions, and some may contain an abundance of ultra-mafic to komatiitic lavas in their lower parts. Sediments comprise a minor but essential part of greenstone belts, generally most abundant in upper stratigraphic levels (Condie, 1981). They are linear to irregular-shaped, synformal supracrustal successions ranging in width from 5 to 250 km and in length up to several hundred kilometers. Greenstone belts are usually metamorphosed to the greenschist or amphibolite facies, and metamorphic grade may increase with contact with plutons.

The tectonic settings proposed for the formation of greenstone belts can be divided into subduction-related and subduction-unrelated (e.g. Furnes et al., 2015, Table 1 gives a summary of selected greenstone sequences and their suggested tectonic setting; Smithies et al., 2005; Smithies et al., 2018; Tomlinson & Condie, 2001; Van Kranendonk & Pirajno, 2004). Again, the answer to the question of how greenstone belts were formed is not an unambiguous topic of ongoing research, as there is not one unique mechanism to be identified for all greenstone belts.

Nonetheless, volcanic rocks comprise an essential component of greenstone belts (de Wit & Ashwal, 1995) and are an example of the earliest preserved volcanic rocks.

Concluding remarks

Hazen (2012) and Stüeken et al. (2013) concluded that geochemical complexity, especially thermal and compositional gradients, fluid fluxes, cycles and interfaces, are the essential features of an early Earth environment to promote chemical complexification and, by doing so, the emergence of life (Hazen, 2012; Hazen & Sverjensky, 2010). All those features are given in an active volcanic setting, making this environment worth investigating for the emergence of life.

1.4 Volcanic lightning

Today's explosive volcanism is often accompanied by volcanic lightning (VL) (**Figure 1-6**), electric discharges within the eruption column. VL was observed for several volcanoes like Sakurajima (Aizawa et al., 2016; Cimarelli et al., 2016; Vossen et al., 2021), Anak Krakatau (Prata et al., 2020), Mount St. Augustine (Thomas et al., 2007; Thomas et al., 2010), Eyjafjallajökull (Behnke et al., 2014), Redoubt Volcano (Behnke et al., 2013) and many more (see supplementary Table 1 in Cimarelli and Genareau (2022) for a more exhaustive list of occurrence of VL in historical and recent eruptions).

Figure 1-6. Photography of volcanic lightning at Sakurajima volcano (2013). Photography by courtesy of Bettina Scheu. The photography is reproduced with the permission of the copyright holder.

Although volcanic lightning has been described in the literature for a very long time (for example, by Pliny the Younger during the catastrophic eruption of Mount Vesuvius (Italy), which destroyed Pompeii), it gained more attention quite recently as a parameter which allows scientists to gain information about volcanic eruption dynamics and allows the monitoring of the ongoing eruptions.

1.4.1 Charging mechanism and charge structure of a plume

Despite the similarities between volcanic lightning and atmospheric lightning, or lightning during a thunderstorm, volcanic plumes differ from thunderstorm clouds

based on the presence of volcanic tephra, their aerosol and the typical volcanic gas contents (James et al., 2008; Mather & Harrison, 2006). As thunderstorms mainly develop their charge because of collisional ice-graupel charging, the addition of silicate particles adds or modifies the charging mechanism within a volcanic plume (Mather & Harrison, 2006).

Mechanisms of electrification

Several charging mechanisms contribute to the charging and discharging of a complex volcanic plume during an explosive eruption which is either proximally to the vent or at varying altitudes in the plume. Proposed mechanisms for the electrification of ash are, for example, fracto-electrification (James et al., 2000), triboelectrification (Cimarelli et al., 2014; Méndez Harper et al., 2021; Méndez Harper & Dufek, 2016), interaction with water and ice particles (Arason et al., 2011; Williams & McNutt, 2005) and natural radioactivity (Nicoll et al., 2019).

Fractoemission describes the electrification process due to the brittle failure of the erupting material and the ejection of ions and atomic particles during fracture events (James et al., 2000; James et al., 2008). It is proposed as one dominant charging process in the volcanic conduit at the vent exit, where fragmentation occurs (Cimarelli & Genareau, 2022; Smith et al., 2018). Electrons, positive ions, neutral atoms, and electromagnetic radiation will be released during the fracturing, hence promoting the charging of the resulting fragmented particles (Cimarelli & Genareau, 2022; Mather & Harrison, 2006). For example, experimental fracto-emission has been observed on colliding pumice particles (James et al., 2000). Triboelectrification, or contact electrification (Lacks & Sankaran, 2011), describes the charging of two bodies by collision and friction with each other and has been observed in a wide range of industrial powders, e.g. during pneumatic transport (Boschung & Glor, 1980). Charge transfer in insulator systems composed of the same material demonstrates the tendency of small particles to charge more negatively than large particles, whereas large particles tend to charge more positively (Lacks & Levandovsky, 2007). The tendency of size-dependent bipolar charging has been experimentally observed in shock tube experiments simulating overpressured volcanic jets (Méndez Harper et al., 2021).

Fragmentation and collision are two processes taking place simultaneously in the volcanic conduit and close to the vent and near-vent region. Therefore, it is difficult to isolate the corresponding charging mechanism without any influence from the other charging mechanisms.

Charge structure of a plume

Miura et al. (2002) proposed the PNP charge distribution model as a schematical description of the typical electric charge distribution of a volcanic plume, where the plume is composed of three parts: the upper part consists of the positively charged volcanic gas and aerosols, the middle part contains the negatively charged fine ash fraction, and the lower part consists of the positively charged coarse ash particles

(see **Figure 1-7**). In granular flows, size-depending charging is a well-observed mechanism: larger particles tend to charge more positively, and finer particles tend to charge more negatively (Bilici et al., 2014; Lacks & Sankaran, 2011; Méndez Harper et al., 2021). Bilici et al. (2014) did not only observe a particle segregation by charge but also a segregation of particles due to the flow. Hence, several mechanisms contribute to the PNP model within a volcanic plume.

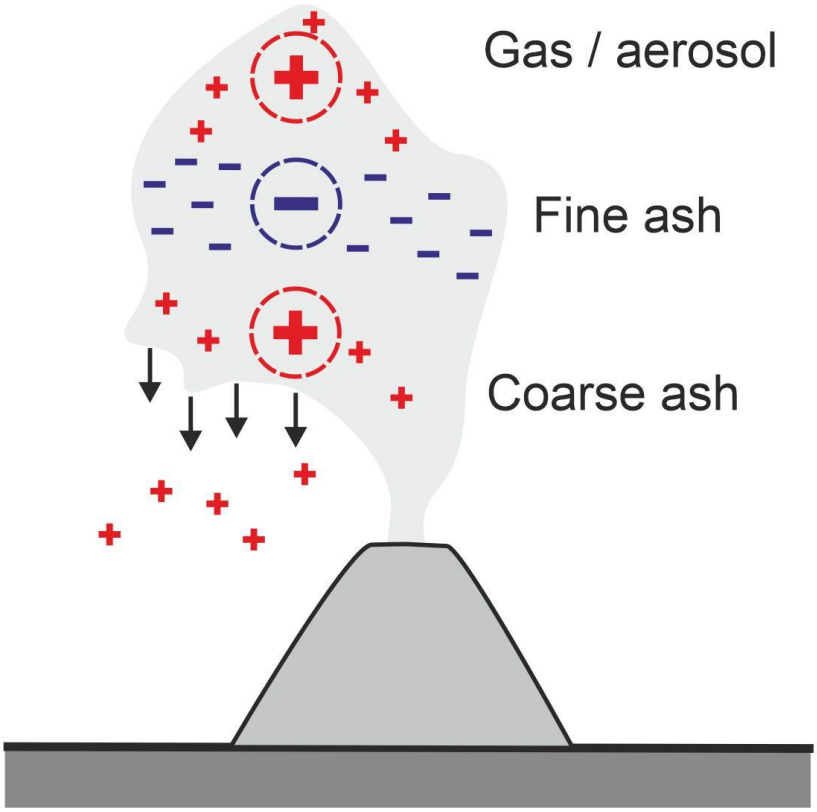

Figure 1-7. Schematic drawing of the typical electric charge distribution in a volcanic plume as proposed by Miura et al. (2002): the PNP model. The plume is composed of three parts. 1) The upper part of volcanic gas and aerosols is positively charged (P). 2) The middle part contains dominantly negatively charged fine ash particles (N). 3) The lower part consists dominantly of positively charged coarse ash particles. The illustration is modified from Miura et al. (2002).

The types of discharges within the eruption, the volcanic lightning, have been subdivided into three different types. The separation between the three types depends on the flash size, location and duration. Conceptually, each type is distinct, but there is very likely a continuum between them (McNutt & Thomas, 2015). Thomas et al. (2010) classified the lightning as 1) vent discharges, 2) near-vent lightning and 3) plume lightning (**Figure 1-8**). Vent discharges are close to the conduit and 10 to 100 m small sparks at rates as great as 10,000 s^{-1}. Near-vent lightning appears within the developing cone; those discharges are small in scale and short in duration, 1 – 7 km in length and 0.01 to 0.1 sec in duration. Plume lightning is the type of volcanic lightning most similar to thunderstorm lightning and shows flashes more than 10 km in span and 0.5 s in duration (Thomas et al., 2010).

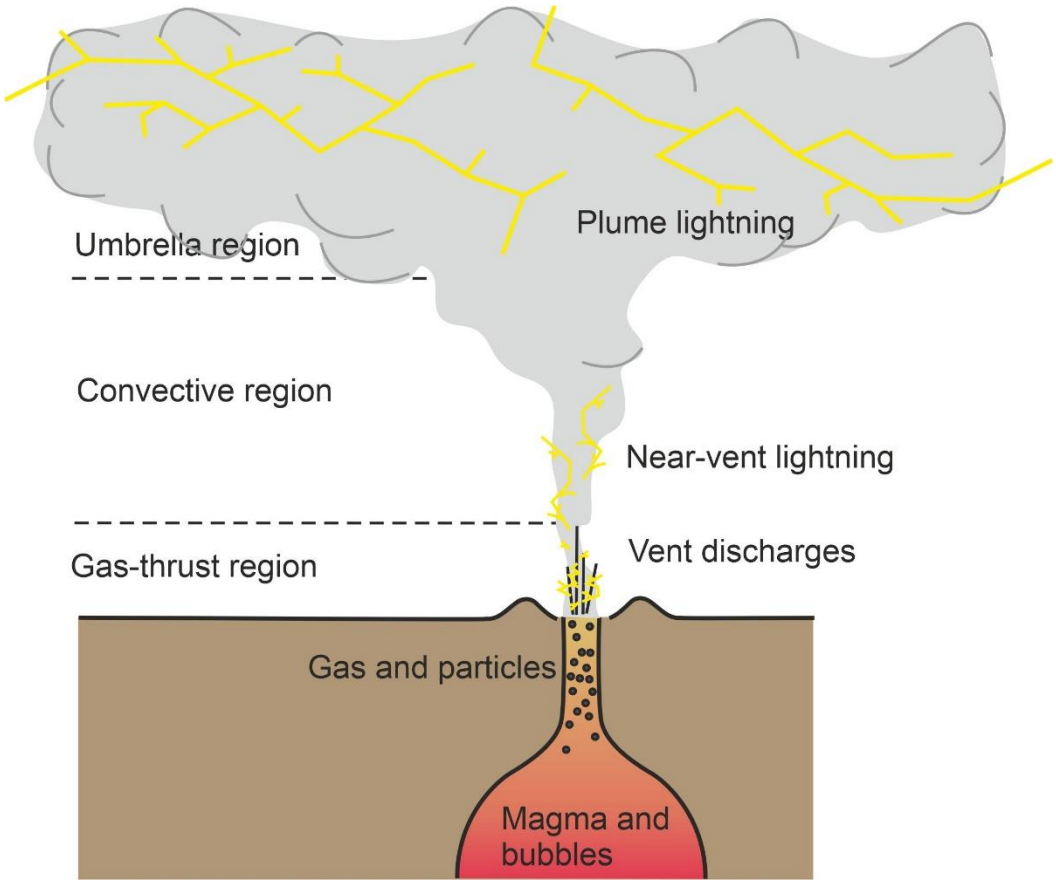

Figure 1-8. Three types of discharges were observed in volcanic plumes: Plume lightning, near-vent lightning and vent discharges. Plume lightning is observable in the upper region of the plume. Close to the conduit are vent discharges observable, near-vent lightning appears within the developing plume. The illustration is modified after Thomas et al. (2010) and Cimarelli and Genareau (2022).

Parameters governing the intensity of volcanic lightning

Several parameters and their influence on VL have been observed and investigated in field observations, laboratory experiments, and numerical modelling to explore the parameters controlling the magnitude and frequency of volcanic lightning. Parameters like the influences of mass eruption rate (Hargie et al., 2019), plume height (Behnke et al., 2013; Bennett et al., 2010; Vossen et al., 2021), water content and temperature (Méndez Harper et al., 2020; Stern et al., 2019), and grain size distribution (GSD) (Gaudin & Cimarelli, 2019; Méndez Harper et al., 2021; Rayborn & Jellinek, 2022) have been addressed in previous studies.

As the grain size distribution has a significant influence on the distribution and residence time of ash in the atmosphere and governs the charging mechanisms, charge density and charge separation, the particle size distribution within volcanic eruptions is of major interest. In general, an increase in fine ash increases discharges, as observed for volcanoes such as Yasour (McNutt & Thomas, 2015) and experimentally investigated for rapid decompression experiments (Gaudin & Cimarelli, 2019).

Influence of material composition

So far, VL has been observed for the full spectrum of magmatic compositions, from basaltic to rhyolitic eruptions (McNutt & Thomas, 2015). This observation concurred with the observation of the eruption of Parícutin (1943-1952, Mexico), where the composition of the ejecta changed progressively from basaltic to andesitic (Luhr & Simkin, 1993), and lightning was reported throughout the eruption for ash-rich eruptions (Foshag & González, 1956; Fries Jr & Guttiérrez, 1950; Mather & Harrison, 2006). Although VL does not appear to correspond to a particular magma composition, the fragmentation properties of a magma, its proportion of inhomogeneities, eruption style, water content, and capability to produce fine ash during eruption depends on the magma composition and hence govern the magnitude and intensity of volcanic lightning. As more silica-rich magma compositions tend to erupt more violently and ash-rich, more silicic magmas might be prone to produce more VL during an eruption. Basaltic volcanoes generally do not produce ash-rich plumes. The magma's lower viscosity allows the gases to escape less explosively (James et al., 2008). Nonetheless, violently explosive basaltic eruptions can occur, especially when the magma gets in contact with significant amounts of water, for example, in phreatomagmatic eruptions. An example of an eruption of basaltic composition resulting in an eruption column displaying VL is the Grímsvötn eruption from 2011 (Houghton et al., 2013). Laboratory experiments with ash from this eruption further emphasize the role of the grain size distribution within the sample (Houghton et al., 2013). Recent observations of VL during recent basaltic explosive eruptions at Stromboli (Vossen et al., 2022), Etna and Cumbre Vieja, show that also low silica magma is able to produce sufficient electrification to generate lightning (Cimarelli, Vossen, et al., 2022).

1.4.2 Extra-terrestrial discharges

As volcanism is also expected on other planetary bodies, the question arises if VL can also be expected on other extra-terrestrial bodies. Evidence for lightning/discharges exists, for example, for Jupiter, Saturn, Uranus and Neptune and possibly on Mars, Venus and Titan (Aplin, 2006; Desch et al., 2002). The existence of extra-terrestrial lightning implies that discharges are probably possible in other extra-terrestrial settings and atmospheres. The existence of electric discharges on other planetary bodies poses the question of extra-terrestrial VL and how it might work on other volcanically active planetary bodies. Concerning this question, Mather and Harrison (2006) argue that at least two fundamental mechanisms are required to cause a mechanism like volcanism: a source of heat and something to melt. The material does not necessarily need to be silicates. For example, ice or for some satellites of the outer planets, sulfur and nitrogen need to be considered (Mather & Harrison, 2006). As we are most interested in planets with a solid surface, with possible volcanism, we do not focus on Jovian planets and their electric discharges but on solid surface bodies.

Venus

For our nearest solar system neighbours, especially Venus and Mars, volcanically active history has been investigated with great curiosity.

Venus is covered by a dense CO_2-rich atmosphere, and its average surface pressure is much higher (~ 93 bar) than on Earth (Basilevsky & Head, 2003). Venusian atmospheric clouds of the uppermost layer are not composed of liquid or solid water droplets but of concentrated sulfuric acid (Basilevsky & Head, 2003), which limits visible observations of the planet's surface. The surface morphology of Venus is dominated by basaltic volcanism, but Venus's volcanic history remains debated (D'Incecco et al., 2021; Stanley, 2021; Teffeteller et al., 2022). Although it also stays still controversial how and if lightning occurs on Venus (e.g. Fischer et al., 2011; Russell, 1991; Russell, 1993; Yair et al., 2008), conclusions by Gurnett et al. (2001) emphasize that those crucial differences in atmospheric conditions are a possible explanation for the differences in radio emission characteristics (e.g. impulsive low-frequency (10 to 80 kHz) radio signals and separate very-low-frequency (~ 100 Hz) radio 'whistler' signals) detected on Venus. The observations point to the conclusion, that potential Venusian lightning is unlike terrestrial lightning, not showing cloud-to-ground discharges but that cloud-to-cloud discharges are prevalent (Gurnett et al., 2001). How and if those differences were also visible in the electrification of particles in either volcanic eruptions or dirty thunderstorms (dirt devils) is still highly speculative and under-investigated. Although some early speculations indicate that Venusian lightning shows clustering depending on surface features that could possibly be associated with volcanism (Scarf & Russell, 1983), it was later declared unlikely (Russell et al., 1988).

Mars

The Martian atmosphere consists mainly of CO_2 (Franz et al., 2017; Haberle, 2015; Owen et al., 1977). The importance of volcanism for Martian topography is spectacularly demonstrated by Olympus Mons, the highest volcano in our solar system (Greeley & Spudis, 1981; McCauley et al., 1972). On Mars, the effusive mafic volcanism dominated the volcanic eruption style (Greeley & Spudis, 1981), but there is also evidence for explosive volcanism (e.g. Horvath et al., 2021; Michalski & Bleacher, 2013) and even phreatomagmatic eruptions (Wilson & Mouginis-Mark, 2003) which is debated in the literature. Navarro-Gonzalez and Basiuk (1998) proposed VL in Martian volcanic eruptions in early Martian history as a potential prebiotic synthesis mechanism. Another explanation for volcanic structures on Mars is mud volcanism. Brož et al. (2020) investigated the behavior of mud volcanism experimentally under Martian conditions (with one exception: the experiments do not account for the lower gravity on Mars compared to Earth) to overcome missing information about land-scape structures on Mars that might have formed. Magmatic activity could also be a potential source of transient methane emission, as discussed in Formisano et al. (2004) and Fonti and Marzo (2010). Especially serpentinization reactions are regarded as the most plausible methane release mechanism by Atreya

et al. (2007). However, as Martian volcanism was active in its past and is considered quiescent today, VL is not likely to happen on modern Mars. Nevertheless, as Mars is exceptional in the solar system because of the significance of dust in its climate, dust storms are a likely source for electrification in Mars's atmosphere (e.g. Aplin, 2006; Farrell & Desch, 2001; Yair et al., 2008). In terrestrial dust storms or dust devils, similar charging mechanisms are responsible for the charging of the particles, as in VL. Convective dust devils will blow small and negatively charged particles upwards (e.g. Lacks & Sankaran, 2011; Stow, 1969), where the coarser and positively charged particles will reside in the lower part of the saltation/suspension cloud. Martian cloud tribo-charging is likely to be effective (for example, simulated by Melnik & Parrot, 1998).

Mars and Venus are examples spatially close to Earth for potential extra-terrestrial electrification. There are many more examples, like Saturn's moon Titan which has potential cryovolcanism and is especially interesting as its atmospheric composition resembles prebiotic Earth's atmosphere (Aplin, 2006; Molina-Cuberos et al., 2002).

1.4.3 Synthesis reactions by electric discharges

Prebiotic synthesis by volcanic lightning

Lightning, or in general electrical discharges, gained significant attention in 1953 as a potential energy source for the first prebiotic synthesis of organic molecules because of the famous experiments performed by Stanley Lloyd Miller and Harold Clayton Urey (Miller, 1953). Miller (1953) built an apparatus to boil water and circulate the gas and water vapour mixture (CH_4, NH_3, H_2O and H_2) past an electric discharge, and after that the vapor condenses again (**Figure 1-9**).

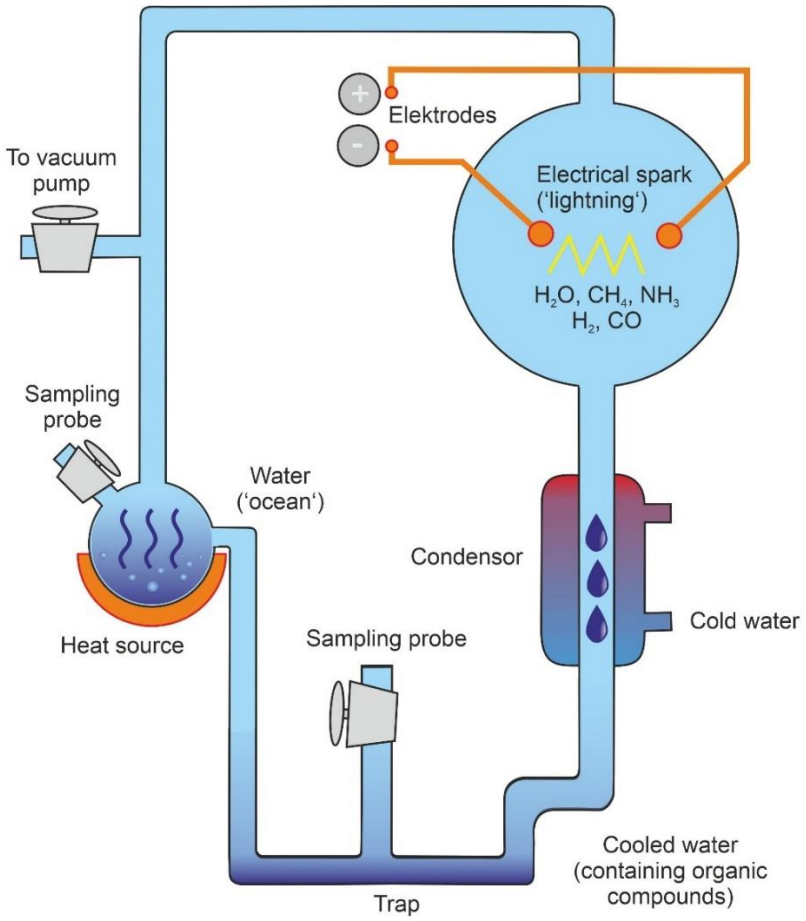

Figure 1-9. The spark-discharge apparatus used in the Miller-Urey experiments. Modified after McCollom (2013) and Miller (1953).

The solution was sampled, and glycine, α-alanine, β-alanine, aspartic acid, α-amino-n-butyric acid and two unidentified phases (A and B) were analyzed. At this time, this gas mixture was regarded as an accurate representation of early Earth's atmosphere.

Those findings sparked several investigations on the emergence of life and opened a new modern experimental epoch of research. The mystery of the emergence of life seemed to be closely unraveled. In the following decades, several experiments and models with electrical discharges as an energy source (Hirose et al., 1990; Honda et al., 1989; Lavrentiev et al., 1984; Miller, 1955, 1957; Navarro-González et al., 1998; Plankensteiner et al., 2004; Sanchez et al., 1966; Toupance et al., 1975) and other energy sources in primitive atmospheres (Bar-Nun et al., 1970; Fox & Harada, 1961; Harada & Fox, 1964) have been performed.

As ongoing research about the early Earth atmosphere developed more into a less reducing composition than proposed by Miller (1953), so prebiotic experiments were also performed with less reducing conditions than initially proposed by Miller (1953). Hirose et al. (1990), for example, performed experiments where a gas mixture of CO, N_2 and water vapour was subjected to discharges. Also, in an extra-terrestrial context

discharge experiments and models on several gas compositions were performed (Gupta et al., 1981; McDonald et al., 1994; Navarro-Gonzalez & Basiuk, 1998; Thompson et al., 1991). Gupta et al. (1981) performed discharge experiments in a gas composition relevant to Titan's atmosphere. A gas composition containing N_2 and CH_4 was subjected to discharges and analyzed by GC and GC/MS, and the results indicate that lightning might represent a possible source of producing C_2H_2 and HCN (next to other energy sources).

The similarity between ash-gas clouds and various biochemical experiments motivated scientists to analyze freshly erupted juvenile volcanic material for possible organic compounds. Markhinin and Podkletnov (1977) and Podkletnov and Markhinin (1981) found organic compounds on freshly erupted ash and bombs, like hydrocarbons, amino sugars and amino acids and concluded that volcanic processes are capable of producing representatives of the major groups of chemical compounds necessary for the functioning of a living cell (Podkletnov & Markhinin, 1981). Volcanic lightning was examined as a nitrogen fixation mechanism by Navarro-González et al. (1998). An Archean gas composition (estimated to be similar to volcanic gas exhalation of modern volcanism in Hawaii) flowed in a microwave discharge cavity where the gases were excited (Navarro-González et al., 1998). Based on their results, they concluded that volcanic lightning might represent a source of nitrogen fixation on early Earth, which is a fundamental prerequisite for the emergence and early evolution of life on Earth (Navarro-González et al., 1998).

The role of geomaterials in discharge experiments was investigated by Lavrentiev et al. (1984). A vapour-gas mixture composed of water vapor, nitrogen, carbon dioxide and ammonia (in a volume ratio 4:1:1:0.1) and 30 g pulverized volcanic bombs from Tolbachik volcano were put into a reactor and exposed to electric discharges between two platinum electrodes. The amino acid analysis of the condensates showed that the yield was substantially higher with the present volcanic material than without (Lavrentiev et al., 1984).

All those previous experiments indicate that the setting of active volcanism with ash as mineral catalysts, heat and volcanic lightning represents a fascinating environmental setting for potential prebiotic synthesis on early Earth.

Chapter 2 – A gas-tight shock tube apparatus for experimental volcanic lightning under varying atmospheric conditions

2.1 Abstract

Explosive volcanic eruptions often generate discharges within the eruption column, a phenomenon termed volcanic lightning (VL). VL is increasingly well investigated and monitored for modern eruptions, but volcanism has been active on Earth since its origin. Thus, investigating VL under different atmospheric conditions is relevant for studies of early atmospheric chemistry and potential prebiotic chemical synthesis reactions. Here, we have developed an experimental setup to investigate VL in varying atmospheres to mimic conditions relevant to studying early Earth and other terrestrial planets and exoplanets. We term this new setup the 'Tiny Tank' and present the first experiments of laboratory discharges in particle-laden jets in varying atmospheric conditions. The new experimental setup is a mobile fragmentation bomb erupting into a gas-tight particle collector tank. This setup enables the testing of different atmospheric conditions, involving changes in the carrier gas of the jet, changes in the pressure within the tank, monitoring of the jet behaviour and sampling of the gaseous atmosphere of the experiment together with the ‘erupted’ (decompressed) solid materials.

2.2 Introduction

On Earth, volcanic lightning (VL) is a phenomenon observed in various volcanic active geological settings and over a wide range of magma composition (McNutt & Williams, 2010). In general, the electrical activity within a volcanic plume accompanying explosive, ash-rich volcanic eruptions is classified as 1) plume lightning, 2) vent discharges, and 3) near-vent lightning (Aizawa et al., 2016; Behnke et al., 2013; Cimarelli et al., 2016; Méndez Harper et al., 2021; Thomas et al., 2010; Van Eaton et al., 2020). For electrical charging within the plume close to the vent, the interaction of the ash particles is especially essential for charge buildup. Previous studies have investigated and described the mechanisms that contribute to the electrical activity within the plume. The process of fracto-electrification (James et al., 2000) describes the buildup of charge due to the fragmentation of magma and the pyroclasts. The process of triboelectrification (Lacks & Levandovsky, 2007) contributes to the buildup of charge caused by the frictional interaction of different-sized particles. The afore mentioned mechanisms that cause the charging of the particles during volcanic eruptions also contribute to other types of atmospheric electrification, for example, the charge buildup in dust storms (Esposito et al., 2016; Stow, 1969). Thus, investigating those mechanisms is relevant for VL and other scenarios where particles interact turbulently.

Lightning or discharges are one mechanism for nitrogen fixation and are considered a potential prebiotic synthesis mechanism on early Earth (Chameides & Walker, 1981; Miller, 1953; Stribling & Miller, 1987; Toupance et al., 1975). In recent years, the detection of VL, e.g., by the emission of radio-frequency impulses, has become important as a potential monitoring tool for volcanic eruptions. However, VL is also a phenomenon that might have accompanied the Earth since its earliest beginnings

and might have played a crucial role in the occurrence of the first organic molecules (Bada, 2004; Navarro-González & Segura, 2004).

As the Earth's atmosphere has changed over time (Catling & Zahnle, 2020; Kasting, 1993), further understanding of how VL might have generated prebiotic synthesis requires a new experimental setup to investigate VL under varying atmospheric conditions.

One disputed point about prebiotic synthesis created by lightning activity is that the electrical current might not merely produce molecules but also destroy them immediately after production. Different zones of discharges characterize VL: In the near-vent region, the discharges are smaller in length and move smaller amounts of charge than meteorological lightning (Cimarelli & Genareau, 2022; Méndez Harper et al., 2021; Thomas et al., 2010) and might represent a potential geological setting for the synthesis of first organic molecules.

The process of electrification is not uncommon in planetary atmospheres. Pieces of evidence for lightning exist, for example, for Jupiter, Saturn, Uranus, and Neptune and discharges are considered possible for Mars, Venus and Titan (Aplin, 2006; Desch et al., 2002). Earth is not the only volcanically active planetary body, for example, Mars was volcanically active in its past (Greeley & Spudis, 1981; Horvath et al., 2021; McCauley et al., 1972). VL might occur in other volcanically active extra-terrestrial environments, and discharges might be generated by other dust-based charging mechanisms. In all these scenarios, early Earth and various forms of extra-terrestrial volcanism, oxygen is unlikely a major constituent of the atmosphere. Especially important is the influence of carbon volatiles on the charging and discharge behaviour of particles. For example, the Martian atmosphere consists mainly of CO_2 (Franz et al., 2017; Owen et al., 1977), the main constituents of early Earth's atmosphere were CO_2 and N_2 (Catling & Zahnle, 2020), and Venus' atmosphere also consists mainly of CO_2 (Basilevsky & Head, 2003). Other essential parameters that require further investigation to evaluate particle charging behaviour on extra-terrestrial bodies are temperature and atmospheric pressure. For example, Wurm et al. (2019) investigated the influence of pressure on potential charging mechanisms in Martian analog dust. Additionally, the gas composition of the plume itself can locally change significantly the composition of the gas in which the discharge might occur and also needs to be addressed in future studies on VL.

Although factors influencing VL have already been investigated experimentally as well as in the field, the same for mass eruption rate (Hargie et al., 2019), plume height (Behnke et al., 2013; Bennett et al., 2010; Vossen et al., 2021), water content and temperature (Méndez Harper et al., 2020; Stern et al., 2019) and grain size distribution (Gaudin & Cimarelli, 2019; Springsklee, Scheu, et al., 2022a), to the best of our knowledge, the impact of an oxygen-free atmosphere on VL has not yet been investigated in shock tube experiments.

To enable the investigation of controlled atmosphere VL studies, we present a new experimental setup ('Tiny Tank') which is a smaller, mobile version of the shock tube

apparatus first developed by Alidibirov and Dingwell (1996). The setup allows to simulate VL in the lab under varying atmospheric conditions (so far CO_2, CO-CO_2 and air), with different transporting gases (so far Ar and N_2) and varying atmospheric pressures (up to 4 bar). The setup enables us to detect the magnitude and the number of discharges and to survey the particles' eruption behaviour with a high-speed camera (Vision Research Phantom V711) through a transparent glass window. The pressure within the setup is displayed by an external pressure gauge that allows the measurement of pressure increase inside the tank caused by the decompression of the particle-laden jet into the particle collector tank. The small size of the apparatus enables the transport of the setup to different external locations (e.g., an explosion-safe-chamber to test more explosive gas mixtures). The ash can be sampled after the experiment from the particle collector tank, and the fine particles are filtered from the atmosphere within the tank by a filtering system in the exhaust air exit containing a Whatman Grade EPM 2000 Air Sampling Filter. Sampling the gas is also possible by attaching crimp cap bottles to an extra line of the exhaust air exit. Using a Faraday cage as the particle collector tank, we can compute the net electric charge associated with the particle gas mixture along with the number and intensity of discharges. The processing code to compute the results was developed by Gaudin and Cimarelli (2019).

2.3 Instrument Design

The shock tube apparatus originally developed by Alidibirov and Dingwell (1996) has been used successfully for decades to investigate and characterize the central mechanisms of explosive volcanism. The setup was consequently improved to enhance the understanding of concepts like the fragmentation threshold, the speed of the fragmentation front, fragmentation efficiency, resulting grain size distribution, the role of permeability, and many more tested concepts. The newest versions of the setup were further developed and improved to analyze experimentally generated VL (Cimarelli et al., 2014; Gaudin & Cimarelli, 2019; Stern et al., 2019). The upper part of the setup, the particle collector tank, became a Faraday cage by insulating it from the grounded autoclave. The new setup enables us to measure the discharges and sample the ash and gas-phase pre- and post-experiment.

The autoclave contains the sample and is pressurized by a system of imprinted diaphragms (**Figure 2-1**). The diaphragms form (in combination with the diaphragm holders) individual chambers in which pressure can be built up to a certain empirically determined burst pressure of the diaphragms. For a rapid rupture, the pressure in the chamber is increased rapidly, causing the rupture of all the diaphragms. We used argon and nitrogen gas to pressurize the sample chamber, but other gases might be used as well as pressurizing medium. After rupturing the diaphragms, the gas and the gas-particle mixture within the autoclave are ejected through the diaphragm system and the nozzle into the particle collector tank (86 cm in length and 27 cm in diameter). The diameter of the autoclave used in our experiments is 26 mm, and the

nozzle diameter is 28 mm. Two diaphragm holders with iron diaphragms were used to pressurize the sample to 10 MPa. The pressure control unit (**Figure 2-1**) supplies the autoclave system with pressure and is equipped with three gas lines to supply up to three diaphragm holders with gas.

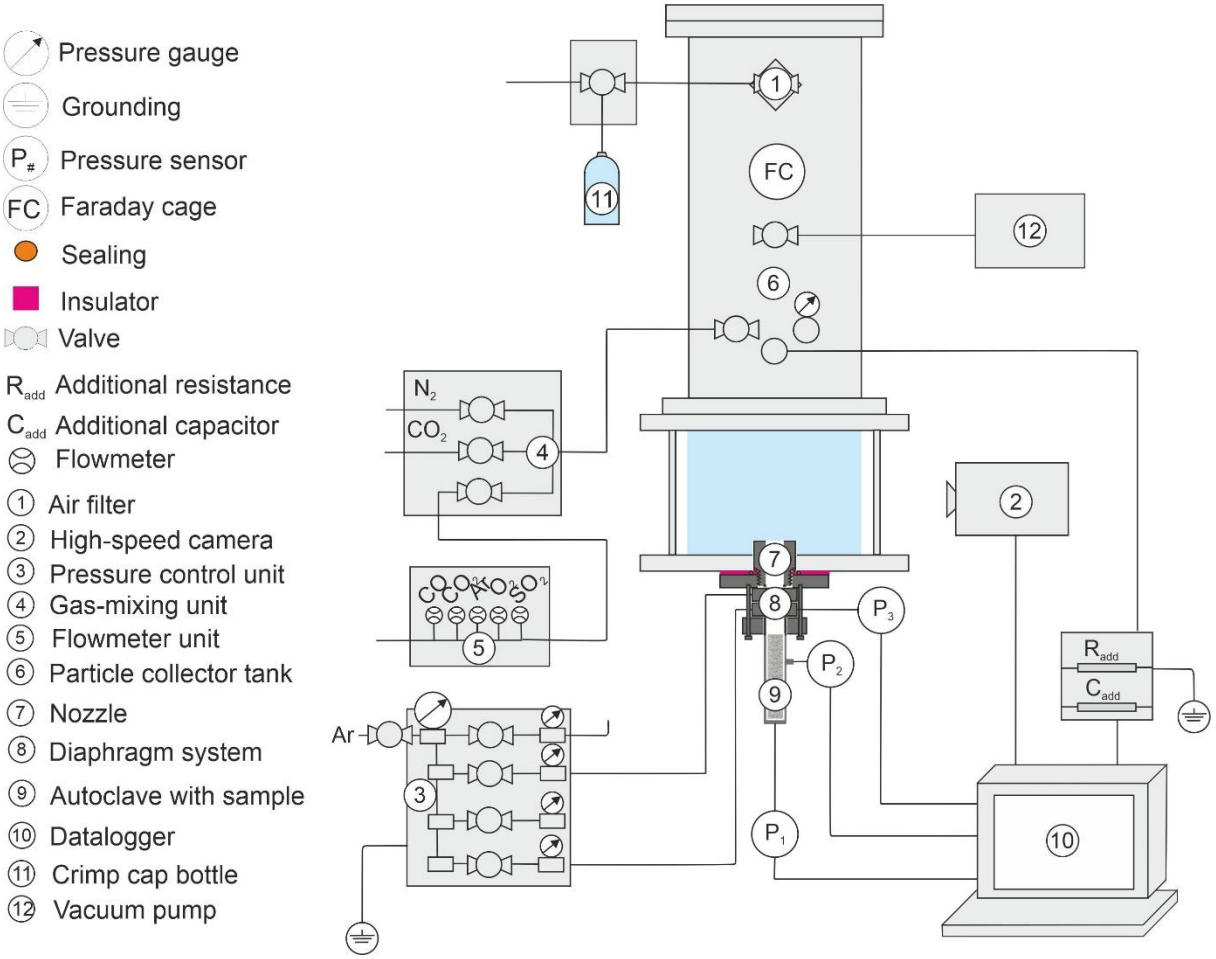

Figure 2-1. Experimental apparatus. The particle collector tank's upper part is insulated from the ground and the decompression system by a plastic flange (purple). The particle collector tank serves as a Faraday cage, and the datalogger records discharges from the jet to the nozzle. An additional resistor allows computing the electrical current (I) by measuring the voltage (V). The additional resistor decreases the amplitude of the signal and avoids saturation. The lower part of the particle collector tank is a transparent glass inlet, which enables the recording of the jet behaviour during decompression with a high-speed camera.

As the sample is ejected from the autoclave into the particle collector tank, the eruption behavior can be recorded with a high-speed camera because the lower part of the particle collector tank is composed of transparent glass (17.5 cm in height). A precision digital pressure gauge (model CPG 1500 by WIKA) is attached to the particle collector tank to determine the pressure before and after experimenting. The autoclave can be flushed with the pressurizing gas phase before performing the experiments to remove the initial air. The gas composition within the particle collector tank is determined by the gas mixing unit and a flowmeter unit (by Bronkhorst Deutschland Nord GmbH) with flowmeters for CO, CO_2, argon, oxygen and SO_4. The flowmeter unit allows a precise gas flow. The software used to control the flowmeter unit is provided by Bronkhorst (FLOWDDE, FLOWVIEW and FLOWPLOT). The

particle collector tank is conditioned by a vacuum pump before performing experiments. We performed experiments in CO_2 and CO_2-CO atmospheres in two different modes: either by flushing the tank three times or vacuuming the particle collector tank and filling the particle collector tank with the desired gas composition before an experiment. The final gas composition before decompression was analyzed for its gas composition. Gas samples were analyzed using a Thermo Fisher Trace 1310 gas chromatograph equipped with an Agilent CP-Sil 5 CB column and a thermal conductivity detector (TCD). The gas mixing unit is used to switch between the gas flow of the flowmeter and a simple supply of N_2 and CO_2. Here, the only way to measure the gas inlet is the pressure increase within the particle collector tank, surveyed by the pressure gauge. The particle collector tank can be sealed gas-tight during the experiments, and an exhaust air outlet will release the gas composition. A sampling system for crimp cap bottles is attached to the exhaust air outlet. Before sampling, the bottles are evacuated three times and in between, filled with helium gas. We insulated the particle collector tank from the ground and the diaphragm system in the tradition of previous setups. The autoclave is electrically grounded, whereas the particle collector tank is grounded during the experiments with an additional resistor set between the Faraday cage and the ground. The total resistance of this additional resistor (2500 Ω) and the datalogger (Yokogawa WE7000), and the voltage measurement allows for computation of the electrical current. Also, as described by Gaudin and Cimarelli (2019), the additional resistor is used with an extra capacitor to decrease the amplitude and avoid saturation of the electrical system. For the data evaluation, the data processing code developed by Gaudin and Cimarelli (2019) was implemented, and the capacitance for the Faraday cage of this setup was determined as described by Gaudin and Cimarelli (2019).

For the experiments, we used synthetic soda-lime glass beads (GB) as sample materials. The synthetic soda-lime glass beads were purchased from the MHG Strahlanlagen GmbH as fractions of 150 - 250 µm and 40 - 70 µm. The grain size fraction of 40 - 70 µm was ground in a disc mill and sieved to achieve a grain-size fraction < 25 µm. The glass beads have an average density of 2.45 g/cm^3.

The grain size distribution of the samples was analyzed with a Bettersizer S3 plus (3P Instruments GmbH & Co. KG) to determine the precise grain size distribution (GSD). Each sample used in the experiments is a mixture of fine (< 25 µm or 40 – 70 µm) and coarse loose sample powder (150 - 250 µm) that were mixed in varying compositions. Each experiment contains a total mass of ~ 113 g, so the sample mixture's weight and volume were almost kept constant.

2.4 Results

In total, we performed 39 experiments in atmospheres of varying amounts of CO_2-CO and air and with two different pressurizing gases, argon and nitrogen (**Table 2-1**).

Table 2-1. Summary of the experimental conditions of the 39 experiments performed in this study. The total atmospheric composition was determined by partial pressure. Two modes of removing the air from the particle collector tank were applied, flushing (Vacuum: N (no)) or flushing and conditioned by vacuum between the flushing (Vacuum: Y (yes)). Total removal of the air was not achieved, 7 vol% air was still measured in the gas sampling by conditioning the tank with flushing and vacuum.

Nr.	EXP	Total mass [g]	Autoclave pressure [MPa]	Very fines [wt%]	Atmosphere				Transporting gas	Vacuum
					Air	N_2	CO_2	CO		
1	EXP266	113.01	10.48	0.00	24	0	76	0	Ar	N
2	EXP267	113.05	10.49	0.00	24	0	76	0	Ar	N
3	EXP268	113.00	10.51	0.05	24	0	76	0	Ar	N
4	EXP269	113.00	10.48	0.05	24	0	76	0	Ar	N
5	EXP270	113.00	10.42	0.05	24	0	76	0	Ar	N
6	EXP271	113.01	10.26	0.16	24	0	76	0	Ar	N
7	EXP272	112.99	10.48	0.16	24	0	76	0	Ar	N
8	EXP273	113.00	10.44	0.16	24	0	76	0	Ar	N
9	EXP274	113.01	10.50	0.26	24	0	76	0	Ar	N
10	EXP275	113.00	10.41	0.26	24	0	76	0	Ar	N
11	EXP276	113.00	10.50	0.00	24	0	76	0	Ar	N
12	EXP277	113.01	10.28	0.00	24	0	76	0	Ar	N
13	EXP336	113.01	10.25	0.09	100	0	0	0	Ar	N
14	EXP368	113.00	10.37	0.09	100	0	0	0	N2	N
15	EXP369	113.00	10.46	0.13	100	0	0	0	N2	N
16	EXP370	113.00	10.26	0.13	100	0	0	0	N2	N
17	EXP371	113.00	10.13	0.13	100	0	0	0	Ar	N
18	EXP372	113.00	10.35	0.13	100	0	0	0	Ar	N
19	EXP384	112.91	10.30	0.12	100	0	0	0	Ar	N
20	EXP393	112.99	10.07	0.24	100	0	0	0	N2	N
21	EXP395	113.00	9.27	0.24	100	0	0	0	Ar	N
22	EXP396	113.00	10.13	0.34	100	0	0	0	Ar	N
23	EXP397	113.00	10.16	0.24	100	0	0	0	N2	N
24	EXP398	113.00	10.29	0.24	100	0	0	0	N2	N
25	EXP399	113.22	10.26	0.34	100	0	0	0	N2	N
26	EXP400	113.00	10.47	0.34	100	0	0	0	N2	N
27	EXP401	113.00	10.04	0.15	100	0	0	0	N2	N
28	EXP402	113.00	10.18	0.15	100	0	0	0	N2	N
29	EXP405	113.00	10.10	0.24	100	0	0	0	Ar	N
30	EXP406	113.00	10.36	0.25	7	0	93	0	Ar	Y
31	EXP407	113.00	10.16	0.05	100	0	0	0	Ar	N
32	EXP408	113.00	10.24	0.05	7	0	93	0	Ar	Y
33	EXP409	113.00	10.27	0.05	7	0	93	0	Ar	Y
34	EXP410	113.00	10.32	0.24	7	0	93	0	Ar	Y
35	EXP411	113.01	10.26	0.00	7	0	93	0	Ar	Y
36	EXP412	113.00	10.33	0.05	7	0	88.35	4.65	Ar	Y
37	EXP413	113.00	10.09	0.24	7	0	88.35	4.65	Ar	Y
38	EXP414	113.00	10.28	0.24	7	0	88.35	4.65	Ar	Y
39	EXP415	113.00	10.35	0.05	7	0	88.35	4.65	Ar	Y

Two different modes of supplying the particle collector tank with gas were tested: either flushing the particle collector tank or flushing and vacuuming the tank in between. We tested the discharge behavior for both operational modes in a CO_2 atmosphere to investigate potential differences by changing the atmosphere's composition. The crimp cap bottle sampling showed that the atmosphere within the particle collector tank only by flushing still contained ~ 24 vol% of air, whereas by vacuuming the tank before, the amount of air within the tank was reduced to ~ 7 vol%.

We performed two experiments (EXP266 and EXP276) with a mixture of the coarse grain size of 150 – 250 µm and fine grain size of 40 – 70 µm in a CO_2 atmosphere. Those two experiments produced no discharges. The same behavior is observable in experiments conducted in air, emphasizing the importance of very fine particles in the initial grain size distribution for generating discharges during decompression (Springsklee, Scheu, et al., 2022a). All other experiments represent a mixture of a coarse grain size fraction and a fine fraction of < 25 µm. We conducted all experiments with an applied pressure of ~ 10 MPa

We compared our experimental data with a previous dataset (Springsklee, Scheu, et al., 2022b), where the same experiments were performed under atmospheric conditions in air (**Figure 2-2**). As already investigated by Gaudin and Cimarelli (2019), the magnitude and the number of discharges increase with the increasing content of fines within the bimodal grain size distribution.

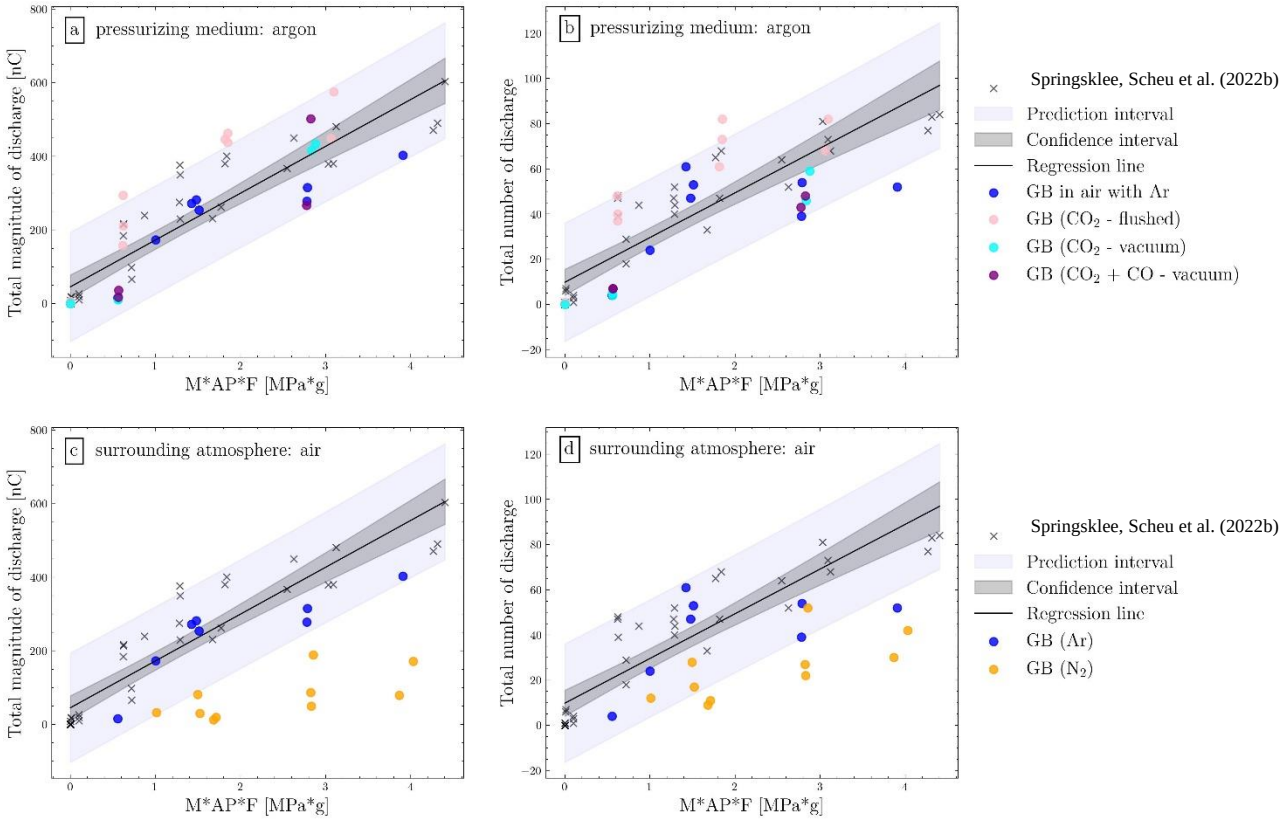

Figure 2-2. Results of the experimental generation of discharges during decompression with glass beads. The prediction interval, the confidence interval and the regression line are based on the dataset Springsklee, Scheu, et al. (2022b). In 2a and 2b, the pressurizing gas was always argon, and the surrounding atmosphere was changed. In 2c and 2d, the surrounding atmosphere was air, whereas the pressurizing gas was either argon or nitrogen. The total magnitude of discharge is displayed as a function of mass times autoclave pressure times the percentage of very fines (< 10 µm) in 2a and 2c, whereas the total number of discharges as a function of mass times autoclave pressure times the percentage of very fines (< 10 µm) is displayed in 2b and 2d. All experiments of this study represent a mixture of the coarse grain size fraction (150 – 250 µm) mixed with varying amounts of a fine grain size fraction < 25 µm or 40 – 70 µm.

Comparing the experiments conducted in an atmosphere containing air, CO_2 or CO_2-CO do not show significant differences in magnitude and number of discharges (**Figures 2-2a** and **2-2b**). The measured magnitude and number of discharges fall within the prediction interval for experiments conducted in air atmosphere. The experiments containing a CO-bearing atmosphere were not conducted in an explosion-safe laboratory; therefore, the content of CO was held below 5 vol%.

The discharge behaviour of the sample does not change, corresponding to the surrounding atmosphere. We changed the pressurizing medium to investigate changes in the transporting gas-phase and exchanged the argon gas as a carrier gas with nitrogen (**Figure 2-2c** and **2-2d**). The comparison of the carrier gases, argon and nitrogen, shows that in both cases, the particles are charging during the eruption, demonstrated by an increase in the net charge of the Faraday cage, but discharges are less commonly observed in a jet with nitrogen as a carrier gas. **Figure 2-3** shows the different discharge behaviour of an experiment with argon as carrier gas (EXP371) and an experiment with nitrogen as carrier gas (EXP370). For both experiments, by decompression, there is a resulting increase in charge of the

Faraday cage evident, but in the experiment with argon as a carrier gas, the discharges cause a decrease in the net charge of the Faraday cage which does not happen in the jet containing nitrogen as a carrier gas.

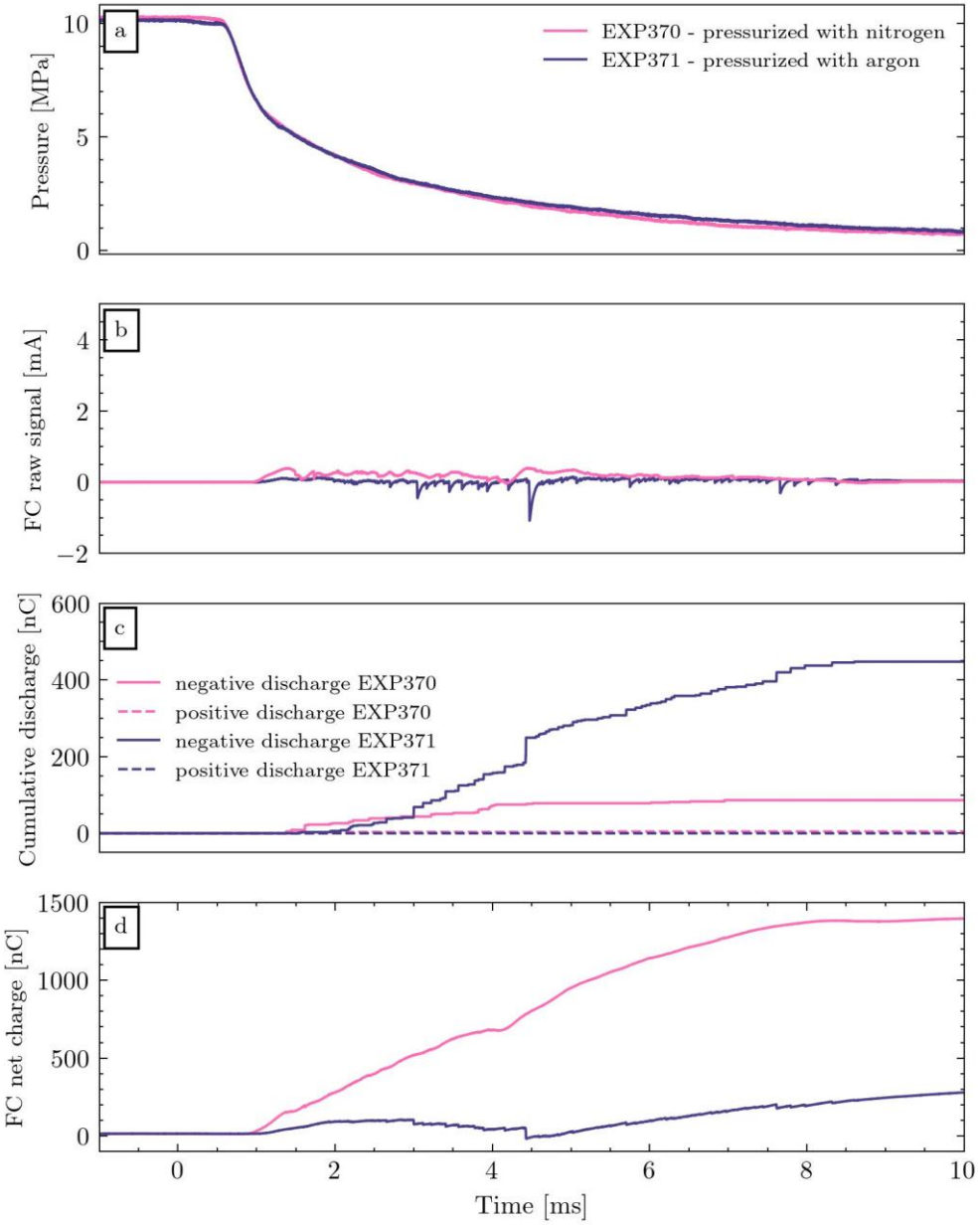

Figure 2-3. Signals from experiment 370 (carrier gas N_2) and experiment 371 (carrier gas Ar).

Gas samples were analyzed using a Thermo Fisher Trace 1310 gas chromatograph equipped with an Agilent CP-Sil 5 CB column and a thermal conductivity detector (TCD). The temperature program for separation started with a plateau at 50 °C for 2 minutes. The temperature was then raised to 100 °C at a rate of 20 °Cmin^{-1}. A constant flow of 2 mLmin^{-1} of helium was used as a carrier and reference gas.

Prior to injection, a Hamilton Gastight™ 1750 syringe was first purged with pure CO_2 three times and then with the sample itself another three times. An aliquot of 300 µL

was then sampled and locked inside the syringe. The needle was purged inside the helium flow of the GCs inlet for 20 s. After that 100 µL were injected to flush out any remaining air, and the syringe was locked again. After 60 s the remaining 200 µL were rapidly injected and acquisition was started. Every sample was analyzed three times. Removal of any of these purging steps led to additional contamination of the sample with air in the range of 0.5 % to 5 % (partial pressures). Even with this procedure, a residue of 0.44 % of air could be detected. This enabled us to distinguish between CO_2 and the remaining components of air (**Figure 2-4**).

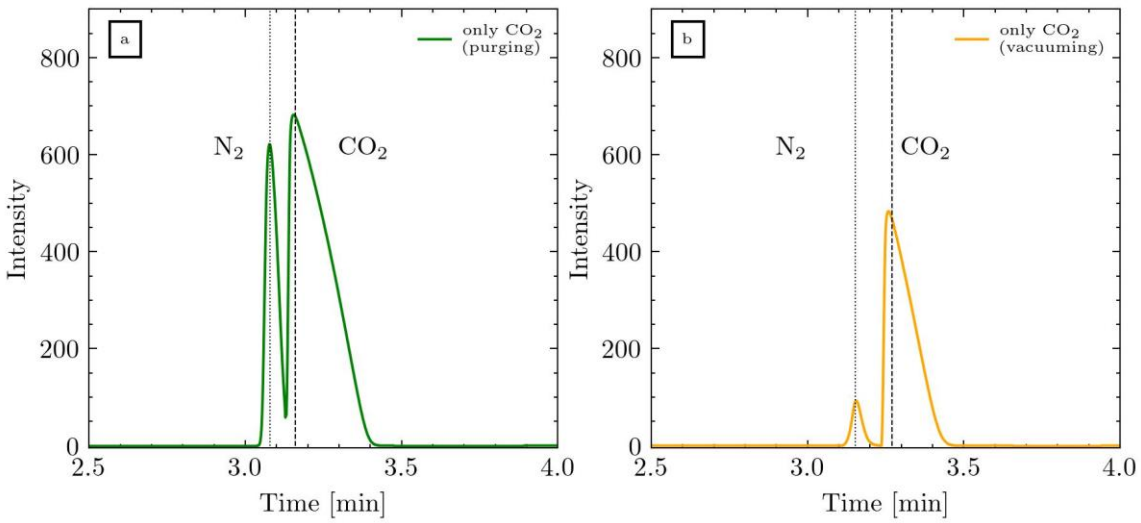

Figure 2-4. Separation of carbon dioxide and remaining components of air by GC. Gas samples were analyzed using a Thermo Fisher Trace 1310 gas chromatograph equipped with an Agilent CP-Sil 5 CB column and a thermal conductivity detector (TCD). Nitrogen and CO_2 show separate peaks, and the amount of air within the sample was determined by calibration. In a) the gas within the collector tank purged with CO_2 was analyzed, whereas is b) the gas composition within the particle collector tank conditioned by vacuum was analyzed.

Quantification of the remaining air was obtained by calibration with different partial pressures of air added to CO_2. The analysis of the gas composition within the particle collector tank before decompression shows that flushing the tank three times with the desired gas phase is not sufficient to remove all the initial air within a tank.

We measured a remaining volume of ~ 24 vol% in the samples for experiments conducted with flushing. Vacuuming the chamber before decompression is a necessity as the remaining volume of air was decreased to ~ 7 vol%.

2.5 Conclusion and outlook

The experiments show that near-vent discharges are possible in an oxygen-free atmosphere and the mechanism seems similarly effective in causing discharges as in air. Under our experimental conditions, the discharge experiments demonstrate that the surrounding atmosphere does not significantly affect the magnitude and number

of discharges in experimental near-vent lightning, as it is observable by comparing experiments conducted in air and CO_2. This observation was made concerning the low resolution and high variability within the experiments themselves. In general, the electrical breakdown threshold between two charged objects where a discharge occurs is described by the Paschen law and depends on the pressure of the enveloping gas and the distance between the charged objects. Because the Paschen curve of air and CO_2 deviate from each other (e.g. Helling et al., 2013 Figure 1), we expected to see differences in the magnitude or number of the discharges. In our experiments, although we can observe optically by a high-speed camera the jet behavior and individual discharges during the experiments, many discharges are hidden in the turbulent suspension of the jet. Therefore, a quantitative and qualitative evaluation of the length of individual discharges is impossible. Méndez Harper and Dufek (2016) investigated the effects of dynamics on the triboelectrification of volcanic ash and tested and concluded that the surface charge density seems to be capped by atmospheric conditions, specifically by the breakdown characteristics of the gas. The charge density of particles fluidized in an argon and nitrogen atmosphere was investigated to test this idea. They observed that the peak of the surface charge density distribution in nitrogen occurs at a value twice that in argon. This difference in charge density distribution does not stem from the side effects of the particles but instead supports the premise that atmospheric properties, not dynamics, dominate the saturation in charge in a granular flow (Méndez Harper & Dufek, 2016). Therefore, the charging of the particles should vary with the properties of the surrounding gas. Compared to their experimental setup, we have to consider the interaction with an expanding jet (particles and argon gas) with a surrounding atmosphere. The jet can be described as a gas-particle mixture where the distribution of the particles within the jet is governed by the particle's tendency to become coupled to the transporting gas phase. The frictional interaction of the small grains is based on turbulent collisions with the coarse grain size fraction and is most likely the charging mechanism causing the charging of the particles within our experimental setup. The jet behaves turbulently as eddies are observable in the high-speed images but more likely in the upper region of the jet than close to the nozzle. The results of the experiments demonstrate that gas entrainment of the atmospheric gas phase is less efficient close to the nozzle as in the upper parts of the jet and emphasize the importance of the transporting gas phase for near-vent discharges. Experiments conducted with nitrogen as a carrier gas compared to those with argon are less efficient in generating discharges following the Paschen law for those two gases. Therefore, the influence and interaction of the surrounding atmosphere and the volatile content of a plume for several eruption types should be investigated to provide deeper insights into volcanic eruptions and their accompanying VL. The influence of atmospheric pressure on such processes also requires further investigation.

The new experimental setup present in this study should make such further studies possible soon. This newly developed setup significantly broadens the range of potential gases available for prebiotic synthesis experiments and emphasizes the

importance of the transporting gas phase for VL. Different gases can be used to pressurize the sample, and the gas-tight tank allows a controlled decompression into the desired atmospheric conditions. The investigation of prebiotic synthesis in a volcanic eruption column based on volcanic near-vent lightning will also profit from this new experimental setup with reducing gases in the erupting jet.

Chapter 3 – The Influence of Grain Size Distribution on Laboratory-Generated Volcanic Lightning

3.1 Abstract

Over the last decades, remote observation tools and models have been developed to improve the forecasting of ash-rich volcanic plumes. One challenge in these forecasts is knowing properties at the vent including the mass eruption rate and grain size distribution. Volcanic lightning is a common feature of explosive eruptions with high mass eruption rates of fine particles. The grain size distribution (GSD) is expected to play a major role in generating lightning in the gas thrust region via triboelectrification. Here, we experimentally investigate the electrical discharges of volcanic ash as a function of varying GSD. We employ two natural materials, a phonolitic pumice and a tholeiitic basalt, and one synthetic material (soda-lime glass beads). For each of the three materials, coarse and fine grain size fractions with known GSDs are mixed, and the particle mixture is subjected to rapid decompression. The experiments are observed using a high-speed camera to track particle-gas dispersion dynamics during the experiments. A Faraday cage is used to count the number and measure the magnitude of electrical discharge events. Although quite different in chemical composition, tholeiitic basalt and soda-lime glass beads show similar vent dynamics and lightning properties. The phonolitic pumice displays significantly different ejection dynamics and a significant reduction in lightning generation. We conclude that particle-gas coupling during an eruption, which in turn depends on the GSD and bulk density, plays a major role in defining the generation of lightning. The presence of fines, a broad grain size distribution, and dense particles all promote lightning.

Plain Language Summary

Explosive volcanic eruptions are accompanied by volcanic lightning, which are electrical discharges resulting from particles that become electrically charged during eruption. We investigated experimentally the discharge behavior of three different materials by performing shock-tube experiments. We used different rocks and analogue material. We focused on the abundance of particle sizes smaller < 10 µm (very fine ash) by testing individual grain size fractions mixed with coarser grains. The jet behavior was recorded by a high-speed camera. We find that the presence of very fine particles has a major influence on the probability to produce electrical discharges within the particle laden jet. Based on our experiments, more volcanic lightning is expected when 1) fine ash is abundant, 2) there is a wide grain size distribution, and 3) the particles are dense.

3.2 Introduction

Explosive volcanic eruptions deliver volcanic ash (< 2 mm) to the atmosphere. Ash grain size has a large effect on the residence time and dispersal of ash in the atmosphere (Ayris & Delmelle, 2012), and thereby influences the distribution and duration of impacts on the Earth System. Ash electrification and associated volcanic lightning (VL) are common phenomena accompanying explosive volcanism. They

create opportunities to monitor and characterize vent properties in real time (Cimarelli & Genareau, 2022). Spectacular recent examples include the eruptions of Eyjafjallajökull in 2010 (Bennett et al., 2010), Calbuco in 2015 (Van Eaton et al., 2016), ongoing Sakurajima eruptions (e.g. Aizawa et al., 2016; Cimarelli et al., 2016; Vossen et al., 2021), Bogoslof in 2016 – 2017 (Van Eaton et al., 2020), Anak Krakatau in 2018 (Prata et al., 2020), Stromboli in 2019 (Vossen et al., 2022), and Hunga Tonga – Hunga Ha'apai in 2022 (Yuen et al., 2022).

Following the classification of Thomas et al. (2010), volcanic lightning can be broadly subdivided into plume lightning, near-vent lightning, and vent discharges (Aizawa et al., 2016; Behnke et al., 2018; Behnke et al., 2013; Cimarelli et al., 2016) each of which may be generated by a different combination of electrification mechanisms. Several studies have investigated the mechanisms that contribute to the build up of electrical charge and to charge separation in the volcanic plume: both processes that are required for the generation of electrical discharges (Arason et al., 2011; Björnsson et al., 1967; Cimarelli et al., 2014; James et al., 2000; Méndez Harper et al., 2021; Nicoll et al., 2019; Prata et al., 2020; Thomas et al., 2010; Van Eaton et al., 2020). The mechanisms include fracto-electrification due to the fragmentation of magma and pyroclasts (James et al., 2000) and triboelectrification by frictional interaction of particles of different sizes (Cimarelli et al., 2014; Gaudin & Cimarelli, 2019; Méndez Harper et al., 2021).

Field observations, laboratory experiments, and numerical modelling have all been employed to investigate VL generation in different plume regions and to explore the parameters controlling the magnitude and frequency of volcanic lightning. Investigations have focused on the influences of mass eruption rate (Hargie et al., 2019), plume height (Behnke et al., 2013; Bennett et al., 2010; Vossen et al., 2021), water content and temperature (Méndez Harper et al., 2020; Stern et al., 2019), and grain size distribution (GSD) (Gaudin & Cimarelli, 2019; Méndez Harper et al., 2021). In the context of the present study, the experiments performed by Gaudin and Cimarelli (2019) are particularly relevant. They concluded that the number of discharges is proportional to the amount of fine-grained particles < 63 µm ('fines') in the sample, with an increase in the amount of fines in a bimodal GSD sample generating an increase in the number of discharges.

The common occurrence of VL is a clear demonstration of the fact that it is not restricted to a single composition of magma (McNutt & Williams, 2010). The chemical compositions of magmas vary over a wide range, which does however affect magma properties and their eruption styles and thus the probability of VL. In this study, three materials with different chemical compositions and bulk densities were tested under the same eruption conditions to isolate the effect of the particle size and composition on VL.

Méndez Harper and Dufek (2016) concluded that composition does not have a significant effect on charging behavior. In contrast, Forward et al. (2009b) investigated triboelectric charging of granular synthetic materials, demonstrating

differences in the triboelectric charging behavior for different materials. We also investigate explicitly the importance of fines by using different fractions of fines (particles < 63 µm) to very fines (particles < 10 µm). We evaluate how the GSD influences the electrical charging behavior with a focus on the very fine fraction, and discuss the influence of chemical composition and bulk density on VL.

3.3 Experimental procedure

3.3.1 Sample preparation

We employed three materials: 1) soda-lime glass beads (GB), 2) tholeiitic basalt (TB), and 3) Laacher See phonolitic pumice (LSB). The materials differ in composition and texture and have been extensively characterized in previous studies (Cimarelli et al., 2011; Douillet et al., 2014; Gaudin & Cimarelli, 2019).

Soda-lime glass beads (GB)

Soda-lime glass beads (GB) manufactured by the MHG Strahlanlagen GmbH consist of 70 - 75 % SiO_2, 12-15 % Na_2O, 7-12 % CaO, max. 5 % MgO, max. 2.5 % Al_2O_3, max. 1.5 % K_2O and max. 0.5 % Fe_2O_3. The glass beads have a density of 2.45 g/cm^3. As this material lacks porosity, bulk density and matrix density are equivalent. The grain size fractions used during the experiments were 150 – 250 µm, 40 – 70 µm, and < 50 µm. The grain size fraction 40 – 70 µm was ground in a vibratory disc mill and sieved for 15 min to achieve fractions of 32 – 63 µm, 25 – 32 µm, < 32 µm and < 25 µm. To remove any finer particles adhering to the size fraction of interest, the size fractions of 32 – 63 µm and 25 – 32 µm were wet sieved under running distilled water and then dried in a furnace for ~ 12 h at 90 °C. An overview of the GSD of each fraction, and a representative image of particles from each material, are presented in **Figure 3-1** and **Table 3-1**. A summary of the composition of the particle mixture that was used in each of the 96 experiments is given in more detail in the dataset (Springsklee, Scheu, et al., 2022b).

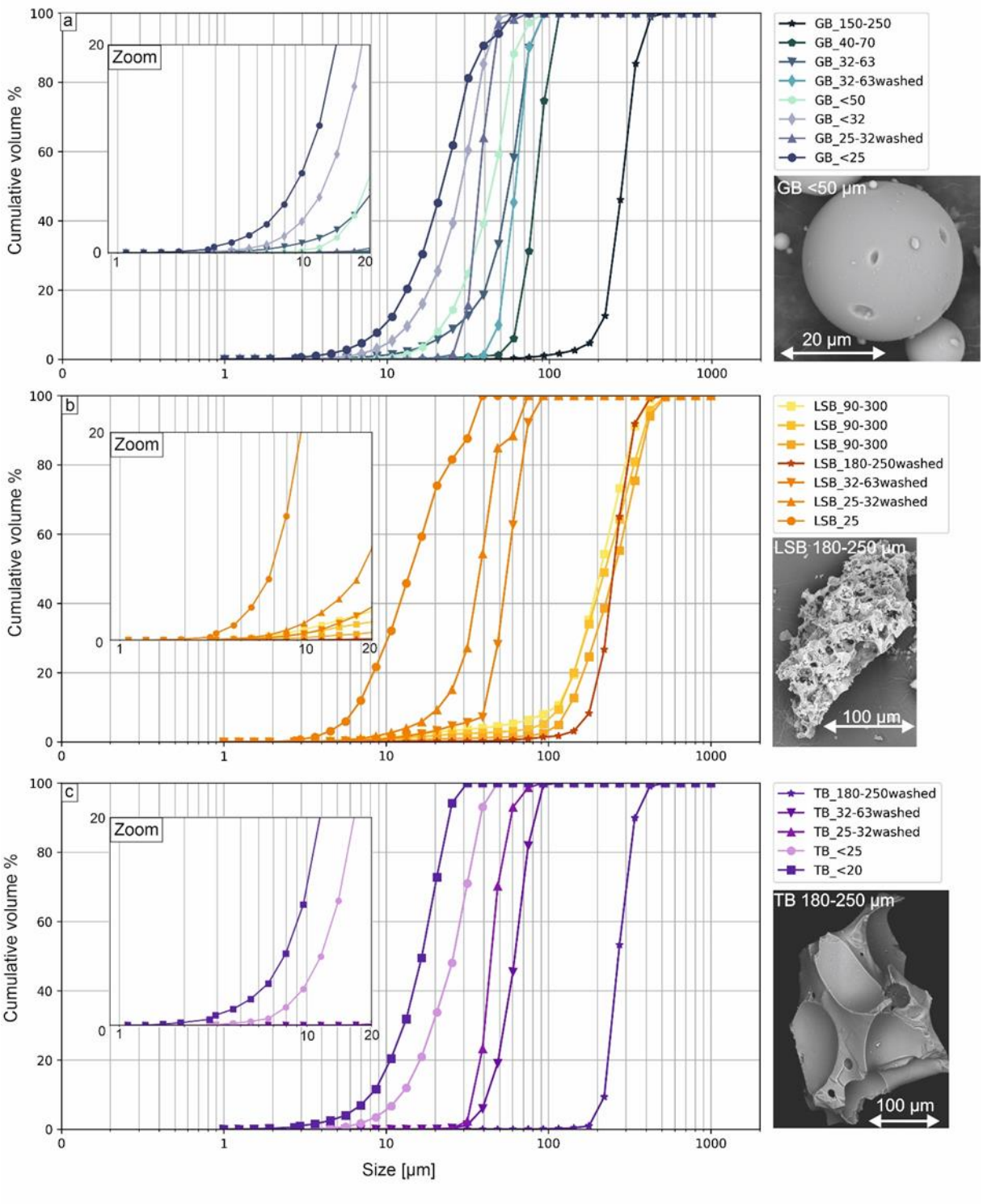

Figure 3-1. Grain size distribution (GSD) of the sample fractions used in this study. a) Overview of all fractions of soda lime glass beads (GB) and an SEM image of a glass bead < 50 µm in size; b) overview of all fractions of Laacher See phonolitic pumice (LSB) and an SEM image of a grain in the washed 180 - 250 µm fraction; c) overview of all fractions of tholeiitic basalt (TB) and an SEM image of a particle in the 180 – 250 µm size fraction. A close-up of the size distribution of the very fines' fractions is included as insets for all three materials.

Table 3-1. Summary of all grain-size fractions used in this study. For each sample, the grain size distribution is given by cumulative volume %. The samples were mixed to obtain the experimentally investigated grain size distribution comprising higher fractions of coarse vs. fine particles.

Sample	Cumulative volume %							
	10.0 µm	20.0 µm	25.0 µm	75.0 µm	100.0 µm	200.0 µm	300.0 µm	500.0 µm
GB_150-250	0.00	0.00	0.01	0.52	1.20	7.96	64.78	100.00
GB_40-70	0.00	0.18	0.37	31.19	89.59	100.00	100.00	100.00
GB_32-63	1.22	5.46	8.71	89.85	100.00	100.00	100.00	100.00
GB_32-63_washed	0.00	0.06	0.15	90.15	100.00	100.00	100.00	100.00
GB_<50	0.34	7.27	14.31	97.19	100.00	100.00	100.00	100.00
GB_<32	4.39	24.09	39.32	100.00	100.00	100.00	100.00	100.00
GB_25-32_washed	0.03	0.42	1.34	100.00	100.00	100.00	100.00	100.00
GB_<25	10.42	43.26	61.81	100.00	100.00	100.00	100.00	100.00
LSB_90-300_C41	1.30	2.79	3.25	6.34	8.53	45.33	81.24	99.94
LSB_90-300_C42.1	0.81	1.75	2.27	3.67	5.88	41.96	71.30	99.59
LSB_90-300_C42.2	0.31	0.74	0.95	1.70	2.83	31.96	63.43	99.31
LSB_180-250_washed	0.02	0.13	0.19	0.90	1.46	16.16	80.53	99.86
LSB_32-63_washed	0.85	3.19	4.63	92.20	100.00	100.00	100.00	100.00
LSB_25-32_washed	2.28	8.78	15.02	100.00	100.00	100.00	100.00	100.00
LSB_<25	28.42	72.72	81.54	100.00	100.00	100.00	100.00	100.00
TB_180-250_washed	0.00	0.00	0.01	0.04	0.11	3.99	74.93	99.93
TB_32-63_washed	0.00	0.09	0.30	81.93	100.00	100.00	100.00	100.00
TB_25-32_washed	0.00	0.03	0.16	98.64	100.00	100.00	100.00	100.00
TB_<25	5.33	32.01	48.05	100.00	100.00	100.00	100.00	100.00
TB_<20	17.13	69.66	94.22	100.00	100.00	100.00	100.00	100.00

Laacher See pumice (LSB)

The LSB particles come from the lower unit of the Laacher See eruption (East Eifel volcanic field, Germany). The LSB has been used in previous experiments (e.g., Gaudin & Cimarelli, 2019; Mueller et al., 2018; Stern et al., 2019) to simulate volcanic processes, including the generation of VL. The LSB is phonolitic in composition. The bulk density of the Laacher See pumice has been determined for different GSDs by Douillet et al. (2014) to be ~ 1.4 g/cm^3 for particles ranging in size from 0.125 – 16 mm. For particles in the range of 40 - 90 µm we determined a bulk density of 2.4

g/cm^3. This higher value corresponds to the matrix density of LSB, and the increase in bulk density likely results from these smaller size fractions being made from the melt surrounding larger bubbles. For the scaling to compare natural and experimental processes presented below, we adopt the value of 1.4 g/cm^3 as the coarse particles used in this experiment lie within the grain size range 180 – 300 µm. The LSB was provided by ROTEC GmbH in an initial 90 – 300 µm bulk distribution. Four fractions were separated from the bulk sample. Three of them (90 – 300 µm) were used directly in experiments after determining their GSD. A fourth fraction was sieved to 180 – 250 µm and sieved under distilled water and dried. The remaining material was ground and sieved for 15 min to the grain size fractions of 32 – 63 µm, 25 – 32 µm and < 25 µm. The grain size fractions (180 – 250 µm, 32 – 63 and 25 – 32 µm) were cleaned by sieving them under distilled water and dried in a furnace for ~ 12 h at 90 °C. For LSB wet sieving had to be repeated to ensure sufficient removal of adhering 'very fines' (< 10 µm fraction). The grain size fraction 90 – 300 µm was used unmodified in the experiments, whereas the grain size fraction 180 – 250 µm was mixed in different proportions with the other finer grain size fractions for the experiments.

Tholeiitic Basalt (TB)

The tholeiitic basalt (TB) is from the 1975 – 1984 Krafla fires (Iceland) eruption. The coarse samples (180 - 250 µm) have an average bulk density of 2.87 g/cm^3. For particles < 63 µm a density of 2.92 g/cm^3 was measured. In TB, we observed only a minor increase in density with decreasing grain size. TB samples are typically dense with very low porosity, therefore bulk density is similar to the matrix density of 2.92 g/cm³, and only minor changes occur between grain sizes. The scaling was done with the density of the coarse grain size fraction (180 – 250 µm). TB, collected in 2019, showed surface organic contamination. Thus, we performed a thorough cleaning process. The first step was to clean the rocks with distilled water and dry overnight at 90 °C. Next, the sample was immersed in H_2O_2 (10 vol%) for a week to remove organic matter. Finally, the rocks were again rinsed with distilled water and dried overnight at 90 °C. To achieve the desired grain size fractions (180 – 250 µm, 32 – 63 µm, 25 – 32 µm, < 25µm and < 20 µm), the rocks were ground with a disc mill and sieved for 15 min. The grain size fractions (180 – 250 µm, 32 – 63 µm and 25 – 32 µm) contained small amounts of a very fine fraction attached to the larger grain surfaces (despite sieving). We therefore we cleaned those fractions by wet sieving to remove any adhering very fine fraction.

The grain size fractions of all three materials were analyzed using a Bettersizer S3 plus (3P Instruments GmbH & Co. KG) using two high-speed cameras (10x and 0.5x magnification). The grain size analysis by image analysis allows a combined size and shape analysis. A comparison between the circularity and the aspect ratio (length over diameter, L/D, ratio) of the analyzed particles is given in the supplementary **Figure A-7** and **Figure A-8**. The particles exhibit similar circularities as well as L/D ratios. All grain size fractions, which were sieved under distilled water are hereafter referred to as 'washed'. For the TB and the LSB, the grain size fraction 180 – 250

µm, and for the GB, the fraction 150 – 250 µm was mixed homogenously with varying weight per cent of the smaller grain size fractions of the same material.

3.3.2 Experimental apparatus

The experimental setup is a vertical shock-tube apparatus designed to perform rapid decompression experiments. Our apparatus is a modified version of the setup first described by Alidibirov and Dingwell (1996). Modifications have enabled the detection and quantification of experimental VL during rapid decompression of loose samples (Cimarelli et al., 2014; Gaudin & Cimarelli, 2019; Stern et al., 2019). In this study, a mobile gas-tight version of this apparatus was developed (**Figure 3-2**) where the upper part, the particle collector tank, serves as a Faraday cage (FC) to measure discharges.

We performed 96 experiments: 29 using LSB, 31 using TB, and 36 using GB. The experiments were carried out using an autoclave 26 mm in diameter and 160 mm in length. The particle mixture was inserted into the autoclave after weighing the sample (90 g for TB, 113 g for GB, and 30 g for LSB). The volume used was approximately kept the same for all samples, by keeping the initial sample weight constant for each material. The change in packing and grain size distribution yielded differences in the filling height (f_h) of the autoclave (~ 130 mm for TB, ~ 148 mm for GB, ~ 132 mm for LSB 180 - 250 µm and ~ 115 mm LSB 90 – 300 µm). The average volume of all samples used in this study is 71.1 ±6.4 cm^3. Compaction of the sample was carefully avoided by abstaining from shaking or knocking the autoclave. The filled autoclave was attached to the diaphragm system, and the sample was slowly pressurized by argon gas up to an average pressure of 10.37 ±0.16 MPa (1 standard deviation). Autoclave pressure was monitored by a series of pressure sensors. The diaphragm system, which separates the pressurized sample from the low-pressure particle collector tank, consists of two scored diaphragms each with a burst pressure below the experimental target pressure. The controlled rupture of the diaphragms results in rapid decompression of the pressurized sample. The sample was ejected through the nozzle into the particle collector tank. The gas-tight particle collector tank is equipped with a pressure gauge that monitors tank pressure during the autoclave decompression.

The lower part of the particle collector tank is made of transparent glass and enables the recording of the ejection of the sample using a high-speed camera (Vision Research Phantom v711). We used the high-speed camera to monitor changes in the vent exit behavior of the expanding gas and gas plus particles mixture during the vertical expansion of the experimental jets. In particular, we monitored the expansion angle to identify the occurrence of a turbulent annulus of fine particles surrounding the collimated flow of larger particles in the core of each jet. The video recordings also captured some electrical discharge events but cannot be used to reliably quantify all discharges because some were obscured by particles in the jet.

The signal of the pressure sensors attached to the autoclave and the diaphragm system, the high-speed camera, and the FC connected to a data logger (Yokogawa WE7000) are synchronized and recorded simultaneously.

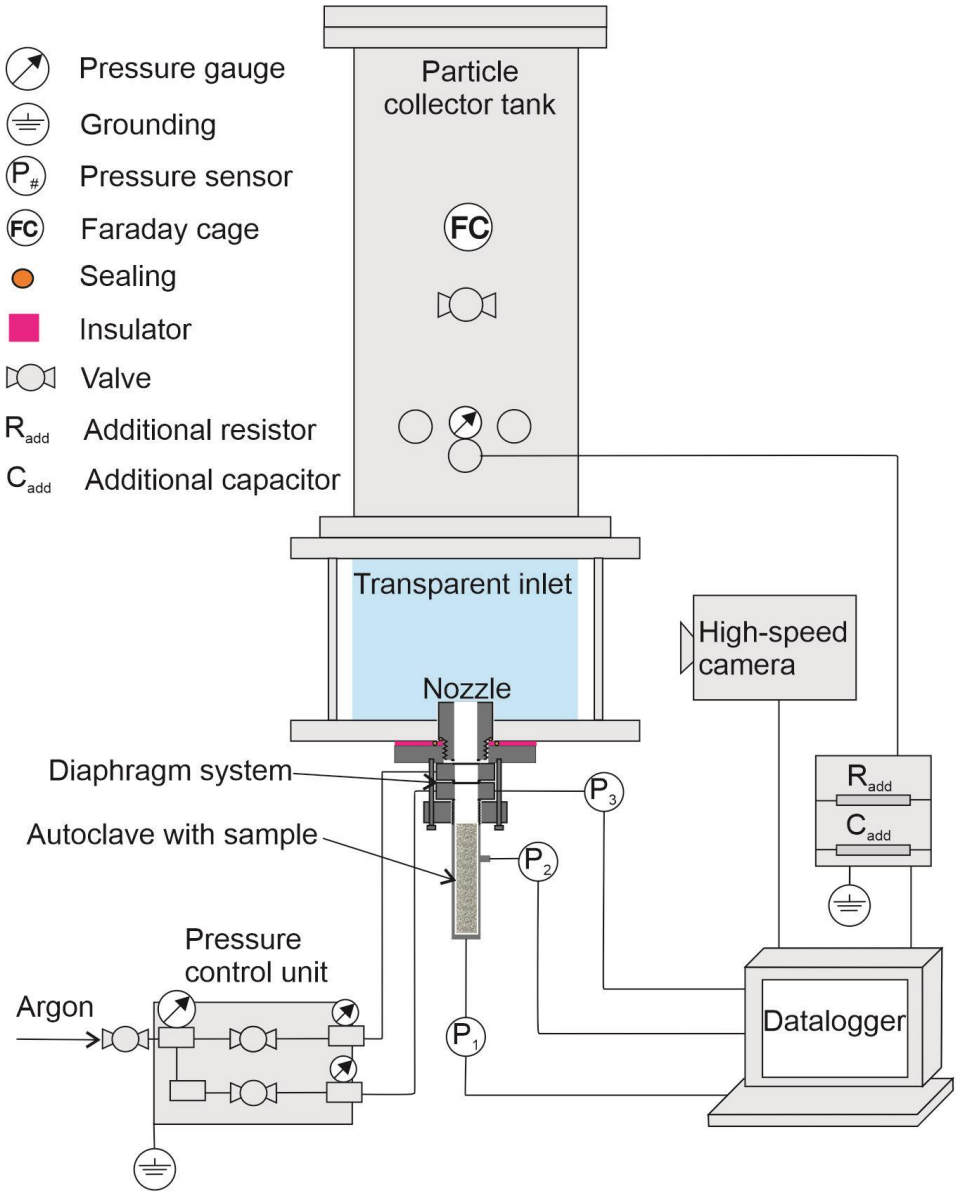

Figure 3-2. Experimental apparatus. The upper part, the particle collector tank, is insulated from the ground and the decompression system by a plastic flange (pink). It serves as a Faraday cage, and discharges from the jet to the nozzle are recorded by the datalogger. An additional resistor allows computing the electrical current (I) by measuring of the voltage (V). The additional resistor decreases the amplitude of the signal and avoids saturation. The lower part of the particle collector tank is a transparent glass inlet, which enables the recording of the jet behavior during decompression with a high-speed camera.

Once the flow has started, the interaction of the differently sized particles in the jet results in electrical charging, and charge separation will result in discharges. Discharges from the jet to the nozzle were detected and recorded by the data logger. Discharges within the jet were not recorded as they are not detected by the data logger.

We avoided any potential disturbances by particles reflected from the lid of the tank in the discharge signal by restricting our observations to the discharges within the first 5 ms of the experiments. Assuming that the gas and particle mixture travelled at the speed of sound in dry air, ~ 4.8 ms is the two-way travel time between the nozzle and the lid. Indeed, the analysis of the high-speed videos showed that after 4.4 – 4.8 ms, some very fine particles were moving downwards. The collector tank in all experiments was initially at ambient air pressure and room temperature. The conditions in the lab were kept constant at a temperature of 20.3 ±0.9 °C and relative humidity of 29.1 ±8.6 % RH. The decompression of the sample resulted in a pressure increase of ~ 0.2 MPa in the particle collector tank.

The detected charging decays approximately exponentially with time. We analyzed the raw signal (the measured electrical current) with a processing code developed by Gaudin and Cimarelli (2019) that deconvolves the instrument response from the raw data and counts the number of individual events and computes their magnitude. The capacitance of the setup was calculated as described in Gaudin and Cimarelli (2019). To evaluate the jet behavior after expansion, we used MTrackJ, an ImageJ plug-in, to determine the exit angle of the gas and particle mixtures at the vent during the experiments from the high-speed recordings. The gas opening angle was determined after the upper diaphragm opened and the jet was expanded, meaning it reached the top of the visible field of view, typically, five frames after the opening. 41 experiments were recorded with a frame rate of 14,217 frames per second (fps), and eight experiments were recorded with a frame rate of 50,000 fps. The particle opening angle was determined 20 frames after the first particles were visibly ejected through the nozzle when the frame rate was 14,217 fps and 70 frames after the first visible particles when the frame rate was 50,000 fps.

3.3.3 Scaling

In order to understand the physical processes that lead to charging of particles and discharge in the jet, and to enable some comparison with volcanic eruptions, we use the following calculations and dimensionless numbers.

In order to compare measurements of the number and magnitude of discharge events between experiments with different materials and properties, we compare these measures with the energy density (ρE) multiplied by the percentage of very fine (< 10 µm) particles. The energy E for an adiabatically expanding gas was calculated after Scheu and Dingwell (2022) as:

$$E = \frac{P_0 V_{gas}}{\gamma - 1}\left[1 - \left(\frac{P_{atm}}{P_0}\right)^{\frac{\gamma-1}{\gamma}}\right] \quad (1)$$

where P_0 is the applied overpressure, P_{atm} is the atmospheric pressure, V_{gas} is the volume of the gas within the autoclave, and γ is the adiabatic coefficient of argon at 10 MPa and 21 °C (γ = 1.99).

The total volume of the gas (V_{gas}) is the difference in the volume filled with particles and the condensed volume (dense rock equivalent) of the particles calculated based on their weight and density. The filling volume was calculated based on the filling height (f_h) and the radius (r) of the autoclave. The volume of the sample is the mass of the sample divided by its matrix density ρ_m:

$$V_{gas} = \pi r^2 f_h - \frac{m}{\rho_m}. \quad (2)$$

A volume normalization allows us to compare experimental results for samples of different sizes and is expressed as the energy density ρE:

$$\rho E = \frac{E}{V_{sample}} \quad (3)$$

where E is the energy and V_{sample} is the sample's total volume in the autoclave.

To compare natural processes and experiments, and to understand dynamics within the experiments, it is essential to compare the dynamics of the natural and experimental processes by a non-dimensional analysis of the main controlling forces on the flow (e.g., Andrews & Manga, 2011, 2012; Burgisser et al., 2005; Cigala et al., 2017; Jessop & Jellinek, 2014; Roche, 2012; Roche & Carazzo, 2019; Weit et al., 2018; Weit et al., 2019). Here, following these previous studies, we determine the Reynolds number of the flow, the Froude number, and the Stokes number for a range of particle sizes and velocities to characterize the relevant processes we observe.

Following Weit et al. (2018), the Reynolds number Re of the biphasic mixture was calculated as:

$$\mathrm{Re} = \frac{2\rho_{mix} U_{mix} r}{\mu_{mix}} \quad (4)$$

where subscripts *mix* refer to properties of the gas+particle mixture. For similar experiments, but coarse GSD (i.e., 0.5 to 2 mm particle diameter), Cigala et al. (2017) measured particle velocities up to 300 m/s, while Gaudin & Cimarelli (2019) with GSDs similar to our GSD estimated flow velocities between 200 – 500 m/s. Based on these results, the velocity U_{mix} was estimated to vary between 200 – 300 m/s. The characteristic length $2r$ in equation (4) is the diameter of the nozzle. The density ρ_{mix} and viscosity μ_{mix} of the mixture were defined as:

$$\rho_{mix} = C\rho_s + (1 - C)\rho_f \quad (5)$$

where C is the mean volume concentration, ρ_s is the bulk density of the sample and ρ_f is the density of the transporting gas (Weit et al., 2018). The mean volume concentration C was calculated from:

$$C = \frac{\frac{m}{\rho_s}}{U_{mix} A\, t} \quad (6)$$

where *A* is the cross-sectional area of the autoclave. In this study, an experiment lasts over a time period of $t \sim 0.15$ s to eject almost all material, but this would lead to an underestimation of the concentration of the flow at the beginning of the experiment, which is the focus of this study. Because most of the material is ejected in the first 0.01 s and almost all discharges take place in this time range, the concentration was calculated with $t = 0.01$ s. Given these approximations, the concentration is slightly overestimated.

The viscosity of the mixture, μ_{mix}, was calculated (Weit et al., 2018) from:

$$\mu_{mix} = \left(1 + \frac{5}{2} C\right) \mu_f \tag{7}$$

where μ_f is the viscosity of the fluid.

The Froude number, which compares the inertia of the flow with the forces from gravity, was calculated (Andrews & Manga, 2011) from:

$$\mathrm{Fr} = \frac{U_{mix}}{\sqrt{2g'r}} \tag{8}$$

where *g'* is the reduced gravity, calculated as:

$$g' = g\left(\frac{\rho_{mix} - \rho_f}{\rho_{mix}}\right) \tag{9}$$

The Stokes number St describes how well particles are coupled to the time-varying flow. Since electrical discharge requires both collisions between particles and then separation of charged particles, the Stokes number is particularly important because it influences both collisions and subsequent particle motions. St was calculated as the ratio of the particle drag response time, τ_p, to the overturn time of an eddy, τ_f:

$$St = \frac{\tau_p}{\tau_f} \tag{10}$$

The particle drag response time τ_p was calculated from:

$$\tau_p = \frac{(\rho_s - \rho_f) d^2}{18 \mu_f} \tag{11}$$

where *d* is the particle diameter. The overturn time of an eddy τ_f was determined experimentally by Jessop and Jellinek (2014) as:

$$\tau_f \sim \frac{10 r_0}{U_{mix}} \tag{12}$$

where r_0 is the nozzle radius. The factor of 10 in equation (12) and other approximations, lead to uncertainties in our estimates of the various ratios of forces and time scales. However, these dimensionless parameters provide the order of magnitude of the dynamics and thus the relationship between our experiments and volcanic eruptions.

3.4 Results

3.4.1 Discharge Experiment

Figure 3-3 summarizes the electrical discharge measurements. The experiments with GB and a GSD of 150 – 250 µm and 40 – 70 µm showed no discharges. To test the impact of increasing polydispersity, one experiment with GB (EXP 168) including 10 wt% of particles 40 – 70 µm in size was performed and did not have any detected discharge. The next smaller grain size fraction tested for GB was 32 – 63 µm. One fraction of this grain size was washed, whereas another fraction was not. Experiment 227 was performed with 5 wt% of the washed grain size fraction 32 – 63 µm, and this GSD did not generate any discharges during the first 5 ms of ejection. The same mixture was prepared with the unwashed fraction 32 - 63 µm and was used in experiments 217 and 221. During experiments 217 and 221, there were 18 and 29 discharges detected, respectively. Experiments containing the washed grain size fraction 25 – 32 µm only led to small amounts of discharge. In the experiments that included the grain size fraction < 25 µm, sample mixture is correlated with discharges (**Figure 3-3**). The variation in the proportion of the very fine fraction in the sample changes the total number and the total magnitude of discharges.

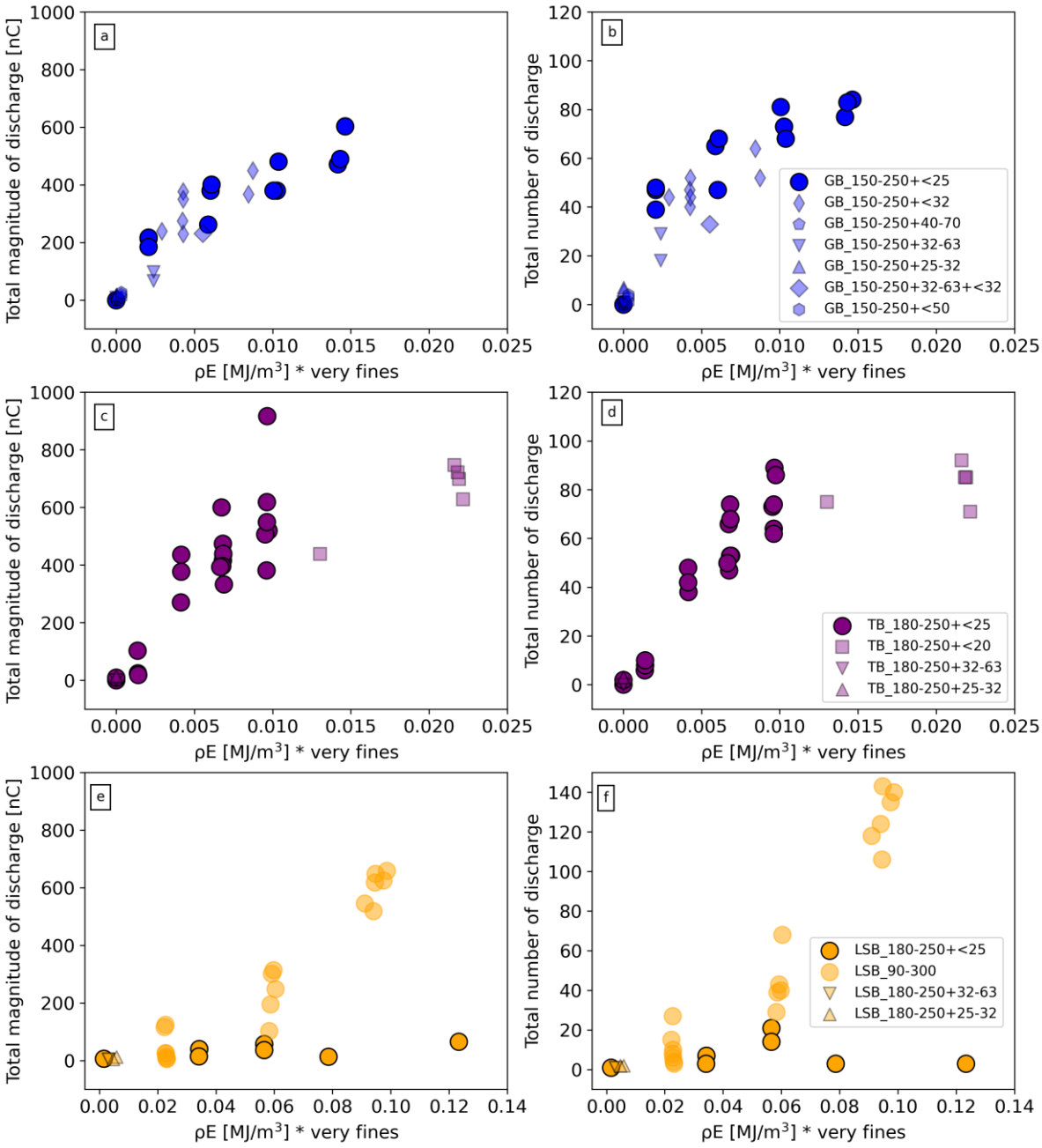

Figure 3-3. Measurements of volcanic lightning for TB, GB and LSB. The total magnitude of discharge is displayed as a function of the energy density multiplied by the percentage of very fine fraction (< 10 µm) in 3-3a, 3-3c and 3-3e, and the total number of discharges as a function of energy density multiplied by the percentage of very fines is displayed in 3-3b, 3-3d and 3-3f.

Similar behavior can be observed for the experiments conducted with the TB particles (**Figure 3-3**c and d). For this material, fewer GSDs were tested compared to

the GB. However, also in this case, samples containing no particles < 10 µm produced almost no discharges. The samples containing particles < 25 µm with a significant fraction of very fines (< 10 µm) were accompanied by discharges. Additionally, a sample containing a fraction < 20 µm was prepared and tested, and a significant number of discharges were measured. These experiments show that increasing the fraction of very fine particles produces an increase in the number of electrical discharges (**Figure 3-3**). We observe an apparently asymptotic behavior of the number of discharges versus fine particle concentration (**Figure 3-3**d) that may indicate a charge saturation limit for which further increments of very fine particles in the mixture will cause no increase in discharge number. The same asymptotic behavior is observed in the magnitude of discharge as a function of increasing fraction of very fine particles (**Figure 3-3**a and c).

LSB particles behave significantly differently compared with GB and TB (**Figure 3-3**)**.** As for GB and TB, LSB does not show discharges for the sample with the added size fractions 32 – 63 µm and 25 – 32 µm. Yet, the charging behavior for LSB differs from GB and TB, as adding a fine grain size fraction of < 25 µm does not generate significant discharge (**Figure 3-3**). Three unwashed samples with a GSD of 90 – 300 µm were tested for comparison. The grain size fractions 90 – 300 µm showed a significant amount of discharge and displayed a linear increase in the magnitude of discharge with increased very fines (< 10 µm). The variability of the discharge measured in the experiment increased relative to GB, perhaps because of the higher variance in the GSD.

Comparing the three different materials, TB and GB particles both display an increase in total magnitude of discharge by increasing the number of very fines (< 10 µm) (**Figure 3-3**). The total discharge magnitude of TB is slightly higher than that of the GB particles. For LSB, only the unwashed and broader grain size fraction 90 – 300 µm shows a similar behavior. However, the increase in total magnitude of discharge with increasing fraction of very fines is less pronounced and no asymptotic behavior could be observed (**Figure 3-3**).

3.4.2 Vent exit behavior

High-speed video enable the determination of the exit angle of the experimental jet (**Figure 3-4**). The video recordings of the nine experiments are provided as supplementary Movie S1, S2, S3, S4, S5, S6, S7, S8 and S9 in Springsklee, Scheu, et al. (2022a). The vent exit angle of the gas-particle mixture α_{gp} was measured and compared to the vent exit angle of the preceding expanding particle-free gas α_g. The value of α_g is approximately constant for all experiments at a value of 28.6 ±1.9°, i.e., independent of material or original GSD. We note that the applied pressure and temperature in all experiments was very similar, and the carrier gas is the same for all experiments.

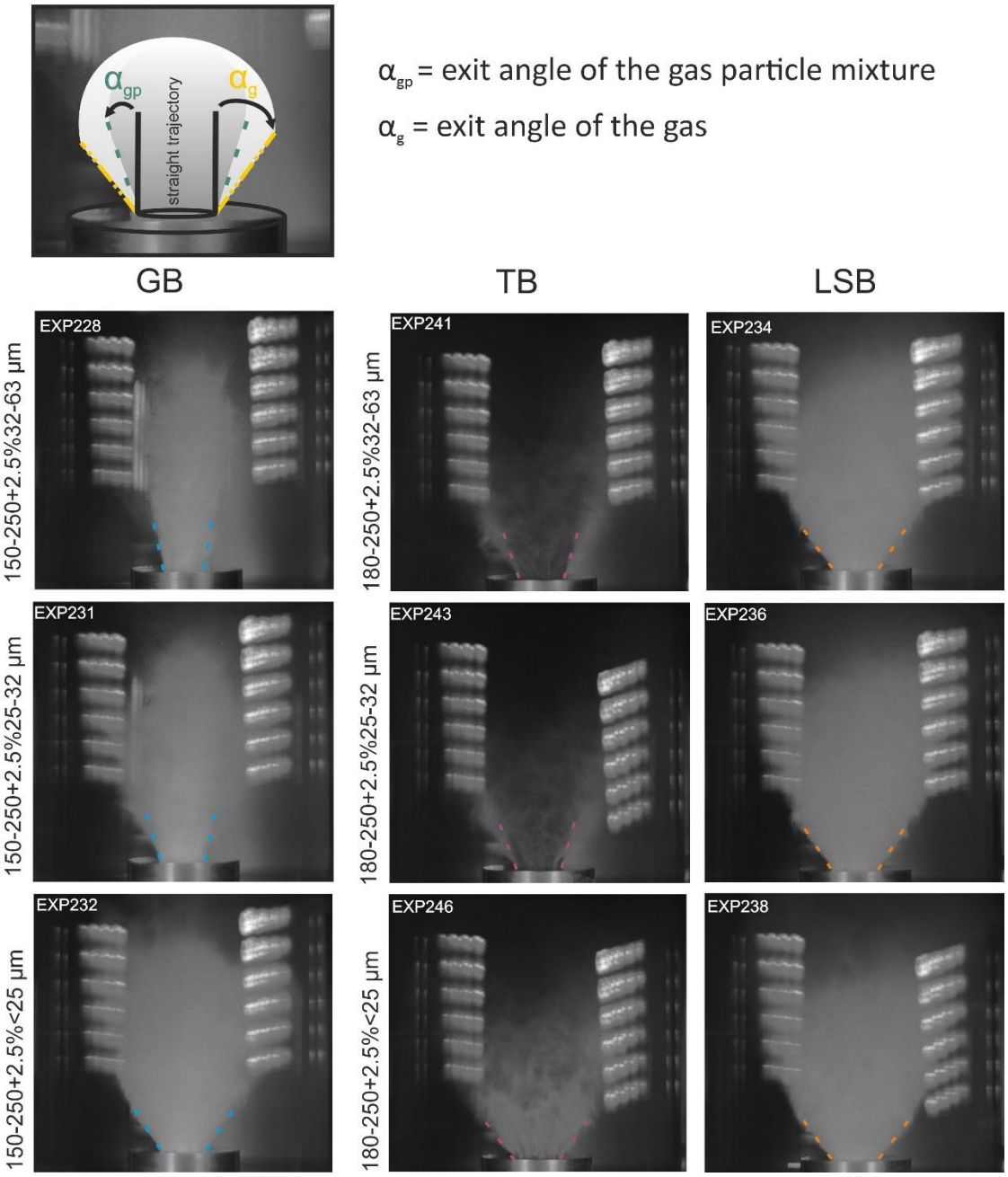

Figure 3-4. Illustrations of the vent exit behavior of the different materials after decompression. The schematic drawing in the upper left defines the exit angles. The exit angle of the gas-particle suspension was measured 20 frames (for a frame rate of 14,217 fps) or 70 frames (frame rate of 50,000 fps) after the first particles were ejected through the nozzle. The exit angle of the gas-particle mixture (α_{gp}) is drawn in the images with the dashed coloured lines.

The value of α_{gp} varies much more widely. The TB and GB particles exhibit similar trends in their vent exit behavior; i.e., α_{gp} increases with increasing fraction of very fines (**Figure 3-5**). In order to capture the evolution of the vent exit behavior of the gas-particle mixture, we define a ratio Γ between the exit angles of gas-particle mixtures divided by the exit angle of the gas phase only: $\Gamma = \alpha_{gp} / \alpha_g$. A ratio $\Gamma < 1$ describes a narrowing of jet exit angle, which is observed for no to very minor fractions of very fine particles. We speculate here that for the case of a small number very fine fraction, (TB with 0.5 wt% of fines (ρE [MJ/m^3] * very fines = 0.0014), the fine particles form a mixed layer surrounding the collimated flow in the middle of the jet. As this mixed layer is likely highly diluted and thus cannot be identified in the high-speed video recordings (especially when the very fines fraction is low), it might lead to a bias in the measured α_{gp}. $\Gamma > 1$ describes an enhanced expansion of the jet (**Figure 3-5**). For GB and TB, we observe that Γ is most sensitive to small amounts of very fines and seems to become increasingly insensitive to the addition of further amounts of very fine particles once a value of ~ 1.3 is reached.

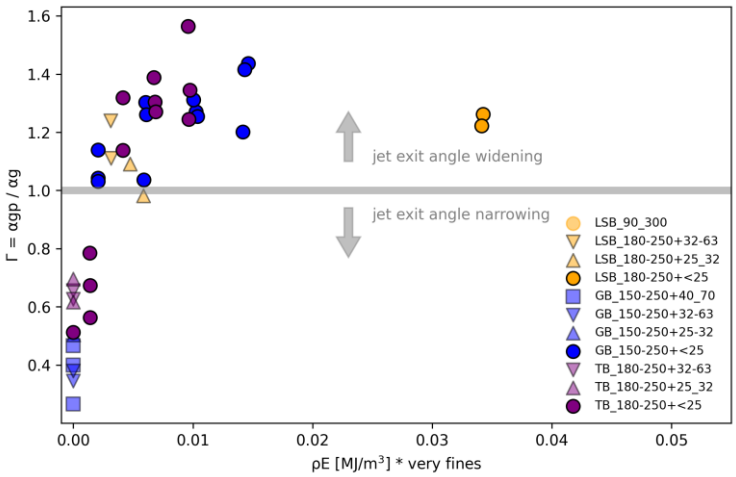

Figure 3-5. The vent exit behavior of the jet was characterized by the ratio of the vent exit angle of the gas-particle mixture and the vent exit angle of the gas ($\Gamma = \alpha_{gp} / \alpha_g$, where α_{gp} is the exit angle of the particle laden jet and α_g is the exit angle of the gas, as illustrated in **Figure 3-5**) as a function of the energy density multiplied by the percentage of very fines (< 10 µm). A value for $\Gamma < 1$ indicates a narrowing of the jet, whereas a value for $\Gamma > 1$ indicates a widening. The grey line $\Gamma = 1$ indicates that the gas exit angle and the gas-particle mixture angle are equal.

This trend could not be confirmed or refuted for the LSB, because we could not completely quantitatively remove the very fine fraction. Here, values for α_{gp} and thus Γ are quite similar for all experiments. In addition, after decompression, the less dense LSB particles appear to be more coupled to the expanding gas phase than the denser TB and GB particles of the same size.

3.5 Discussion

Triboelectrification has been found to be the dominant charging process for near-vent discharges in shock-tube experiments (Gaudin & Cimarelli, 2019; Rayborn & Jellinek,

2022). Gaudin and Cimarelli (2019) also used LSB under similar applied pressure conditions as in this study, and did not observe a significant grain size reduction in their experiments using a 4 m long particle collector tank. We can thus exclude primary sample fragmentation as a significant mechanism for electrification. Hereafter, triboelectrification will be considered the key mechanism in charging particles compared to fracto-electrification, though the contribution of other charging mechanisms cannot be fully excluded. Non-disruptive interaction or collision between particles produces charging where charge of opposite polarity is separated between large and fine particles (Forward et al., 2009a; Kikuchi & Endoh, 1982; Méndez Harper et al., 2021), and leads to a size-dependent bipolar charging mechanism.

The interaction of particles with each other depends on their coupling to the gas phase and whether the flow is turbulent. The Reynolds number Re_{mix}, the ratio of inertial to viscous forces within the fluid, for natural volcanic plumes usually ranges between 10^7 and 10^9 (see **Table 3-2**) and implies turbulent conditions ($Re > 10^4$). Burgisser et al. (2005) highlight the importance that experiments reach $Re > 10^4$ to investigate volcanic processes in jets, plumes and pyroclastic density currents. In this study, a similarly high Reynolds number ($Re \sim 10^6$- 10^7) is reached based on the high velocities achieved during the initial phase of decompression. The empirical principle called ‘Reynolds-number independence’ states that provided Re is high enough, its exact value does not strongly influence the overall dynamics (Paola et al., 2009).

Table 3-2. Summary of common ranges of the dynamic variables relevant for volcanic plume systems and this study. Values were obtained from Carazzo and Jellinek (2012), Burgisser et al. (2005), Roche and Carazzo (2019), and the references therein. The Froude number was determined from $Fr = 1/Ri^{1/2}$ (Roche & Carazzo, 2019).

Variable [Unit]	Experiments		Common ranges of the dynamic variables
	Gaudin and Cimarelli (2019)	This study	
Main parameter			
Velocity [m/s]	200 – 500	200 – 300	150 – 500
Particle size [m]	10^{-6} – 3 x 10^{-4}	10^{-6} – 3 x 10^{-4}	10^{-6} – 10^{-2}
Vent diameter [m]	2.2 x 10^{-2} – 3.7 x 10^{-2}	2.8 x 10^{-2}	100 – 400
Gas viscosity [Pa s]	2.23 x 10^{-5}	2.24 x 10^{-5}	3 x 10^{-5}
Fluid density [kg/m^3]	1 – 33	20 – 108	2 – 90
Jet dimensionless numbers			
Reynolds number Re	3 x 10^5 – 3 x 10^7	7 x 10^6 – 3 x 10^7	10^7 – 10^9
Stokes number St	10^{-2} – 10^2	10^{-2} – 10^2	10^{-4} – 10^3
Froude number Fr	3 x 10^2 – 10^3	4 x 10^2 – 6 x 10^2	3 x 10^{-1} – 3 x 10^1

Given the importance of particle collisions for triboelectrification, and the need for charge separation to enable electric discharge, the Stokes number (St) is central to understanding our experimental results and for scaling to volcanic eruptions. St describes the degree to which particle velocity is coupled to the gas velocity. **Figure 3-6** shows that the particles smaller than 10 µm used in this study have a St less than about unity, so they are well-coupled to the turbulent gas motions, whereas larger particles are not. As in volcanic eruptions, our experiments span the range for St from much less than, to much greater than, unity (**Table 3-2**).

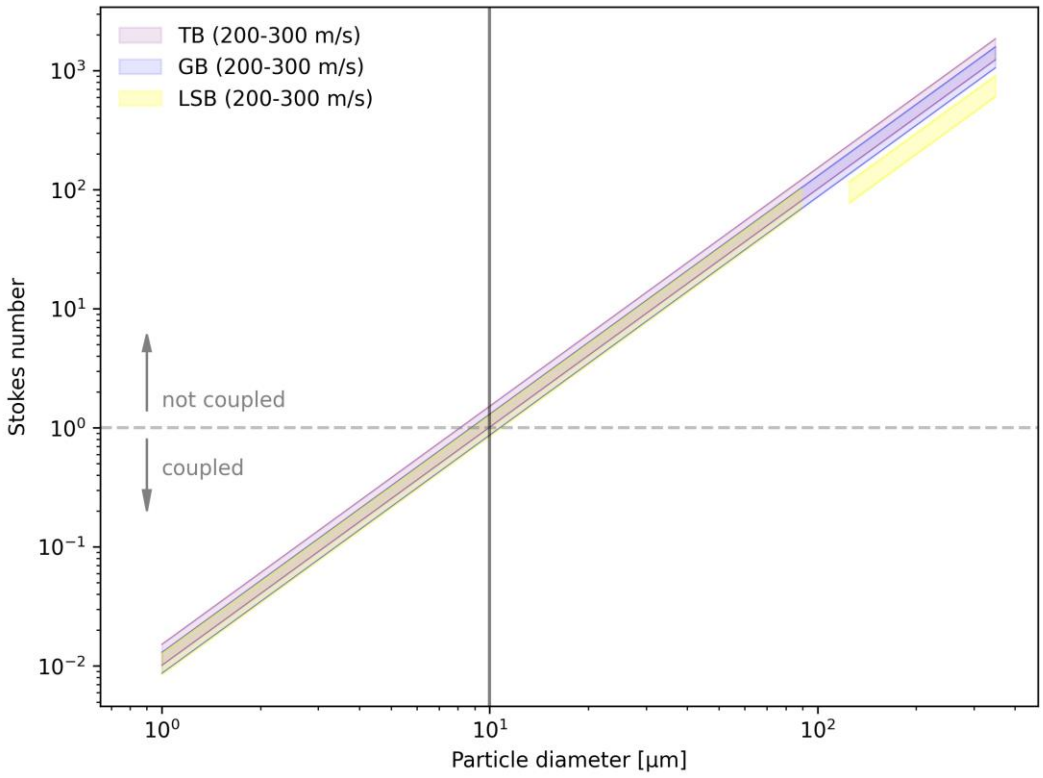

Figure 3-6. Stokes number (St) as a function of particle diameter for the particles used in this study. The particles are well-coupled to gas motions when St is smaller than 1, which is the case for particles with diameters < 10 µm for TB and GB. For LSB, St is calculated with the matrix density for diameters < 90 µm and the bulk density for coarse particles > 125 µm.

For the glass beads, the discharge behavior of the experiments containing a grain size fraction < 50 µm (**Figure 3a and b**) shows that the grain size fraction < 10 µm is most likely responsible for the observed discharges. The grain size fraction < 50 µm includes ~ 7.3 % of grains smaller than 20 µm but only 0.34 % smaller than 10 µm, resulting in an almost negligible amount of particles < 10 µm in the total particle mixture. A sample mixture containing coarse particles (150 – 250 µm) and the grain size fraction < 50 µm but no particles < 10 µm caused no discharges. Although different in chemical composition, TB and GB show similarities in their discharge behavior. TB and GB also have similar St for a given grain size (**Figure 3-6**). **Figure 3-3** shows that TB and GB display an increase in the magnitude of discharge with increasing very fine fraction. It appears, however, that there may be a threshold fraction of very fine particles at which the gas-particle mixture becomes electrically saturated and cannot charge/discharge further at the given flow conditions (total mass of particles, particles vs gas volume, initial pressure).

The LSB particles have a smaller St number for a given size due to the lower density of the coarse porous fraction. However, the fine fraction of LSB has a density similar to TB and GB and thus the size of coupled particles is similar to TB and GB. We

might therefore expect a somewhat different behavior of the coarse, uncoupled particles in the expanding jet due to their lower density.

The generation of electric discharge requires separation of the charged particles within the jet. The model by Cimarelli et al. (2014) explains why a monodisperse GSD will not cause substantial charging upon rapid decompression as separation of charged particles following different trajectories in the jet is required to generate electrical discharges. Consistent with the predictions of this model, our experiments with solely coarse grain size fractions yielded no discharges.

High-speed camera observations provide information about the gas-particle mixture behavior at the vent. With decreasing grain size and / or decreasing density, the particles are better coupled to the turbulent gas motions, which is visible in the high-speed recordings as a mixed layer surrounding the collimated flow in the middle of the jet. This behavior is illustrated schematically in **Figure 3-7**. Charging can occur when particles of different sizes collide in the core of the jet. The entrainment of the small Stokes number particles (very fines) by the turbulence enables the charge separation.

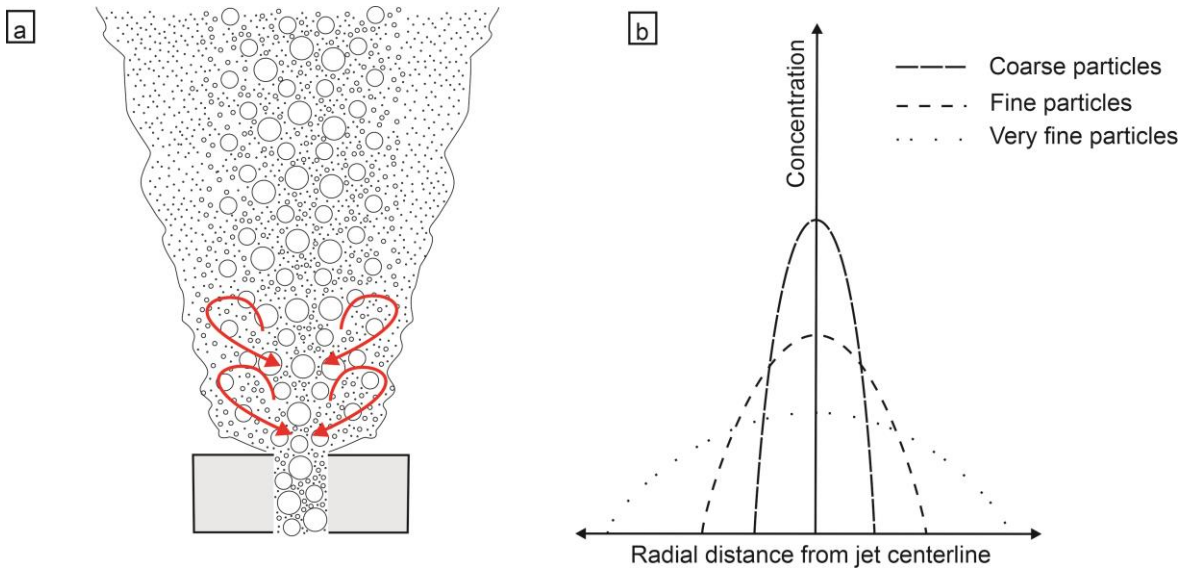

Figure 3-7. Illustration of particle transport in the jet. The red arrows indicate schematically the turbulent motions generated by shear at the edge of the jet. The very fine particles (St < 1) are coupled to the turbulent gas flow. Depending on their Stokes number, the coarser particles (St > 1) are less coupled to the flow and form a more collimated flow in the middle of the jet. Finer and coarser particles interact with each other by colliding which charge the particles. The different transport of small and large St particles enables the separation of very fines from larger particles leading to charge separation.

From our experimental results, it appears that for TB and GB, the presence of a very fine fraction is necessary to generate discharges during the experiment. Under the same experimental conditions, LSB does not show significant discharges during decompression despite containing particles < 10 µm, whereas grain size mixtures of LSB exhibiting a broader variance in their distribution produce discharges during decompression: The grain size fractions of LSB 90 – 300 µm differ from the washed

grain size fractions 180 – 250 µm mixed with added amounts of fines in still containing grains sizes in the intermediate range 63 – 180 µm (**Figure 3-1**). Several phenomena might explain the different discharge behavior of LSB. Firstly, very fine particles might adhere to the high internal surface area of the highly vesicular clasts or even get trapped in the pore space of the coarse LSB particles, thereby suppressing separation of particles and their charges. Secondly, the LSB fraction 90 – 300 µm contains moderately fine particles and thus has a broader grain size distribution. Particle collision frequencies are highest for intermediate St, typically between about 1 and 10 (details depend on the type of flow and flow Re), owing to feedback between coupling to turbulent motions and particle concentration in regions with low vorticity (e.g., Sundaram & Collins, 1997; Wang et al., 2000; Zhou et al., 1998). Thus, a broader GSD with more particles having St with order of magnitude 1 to 10 may enhance the collisions between particles, leading to more charging. The moderately fine particles (63 – 180 µm) may also provide less internal surface that could trap very fines. Taken together, these dynamics would promote particle charging and separation and, as a result, discharges.

All three samples analyzed in this study are chemically distinct. In addition, they vary texturally: LSB is highly vesicular whereas TB and GB are dense; LSB and TB are irregularly shaped whereas GB particles are mostly spherical. Despite their chemical differences, the TB and GB show similar numbers and intensities in their near-vent discharges (**Figure 3-3**), and they also have similar coupling to the gas (**Figure 3-5**). For LSB, electric discharge has a different dependence on the GSD; to achieve near-vent discharges, different grain size fractions of LSB have to interact compared to GB and TB. Common to all samples, however, is the need for the presence of very fines to cause discharges. The key characteristics discriminating LSB particles from TB and GB particles is the high vesicularity at moderate and coarse sizes. Based on these observations, acknowledging the small range of compositions and textures we were able to explore, we suggest that textural properties, especially vesicularity, do affect near vent lightning whereas samples' chemistry seems to have a minor influence. We hypothesize that near vent lightning is dominated by the motion of particles in response to the transporting gas phase and their interaction with the other particles of the ejected particle mixture, processes that are more affected by textural differences than by chemical differences.

The experimental results and interpretations presented in this study provide some insights into how particle interactions and particle-gas coupling lead to electrical charging and discharge. There are, however, several important limitations, some of which could possibly be addressed in the future with additional experiments and modifications to the experimental methods. First, although the velocity of the particles is a crucial parameter to understand collisions and particle separation, velocities of individual particles could not be determined. The high-speed recordings (up to 50,000 fps) show the motion of the jet, but it was not possible to obtain the speed of individual particles due to the small grain size. Second, although particle clustering is pervasive in flows of solid particles, creating dense regions of concentrated particles

surrounded by more dilute regions (Fullmer & Hrenya, 2017), addressing this phenomenon is beyond the scope of our study because we could not image clustering in the jet. Clustering might play a crucial role in the process of particle charging and separation to cause discharges. Thirdly, all experiments in this study were performed at room temperature. Stern et al. (2019) performed shock-tube experiments to investigate the influence of temperature (25 - 320 °C) and water content (0 - 27 wt%) on the charging and discharging behavior of a particle-laden jet. With increasing temperature, they observed a decrease in the jet exit angle, which could result in a higher particle concentration, but only a minor increase in cumulative discharge was observed. They pointed out that an increase in temperature does change the solid and gas properties and therefore the jet dynamics, which could be related to a decrease in net charge at the onset of the discharging activity. Méndez Harper et al. (2020) also investigated the role of humidity and temperature on the charging of particles and observed a decrease in the amount of charge gained by a particle by increasing the temperature. Fourthly, the circularity and the L/D ratio of the samples measure some aspects of particle shape and are similar to each other. Nonetheless, the effect of the surface roughness of the particles was not addressed in this study. As we attribute triboelectrification as the key mechanism to build up charge in the experiments, charging could depend on the roughness of surfaces that interact frictionally and during collisions. Further, particle density, shape, and roughness can affect coupling with the gas. The LSB, for example, has a significantly different mobility in the jet and differs significantly in its discharge behavior. The ability to collide and build up charge depends on the differences in particle motion. The role of Stokes number distributions could be explored more thoroughly. Finally, the experimental apparatus allows the detection of discharges from the jet to the nozzle but not discharges within the jet itself, and thus charge transfer between particles.

3.6 Conclusion

Shock-tube experiments provide an opportunity to investigate processes in volcanic jets under controlled conditions in the laboratory (Alatorre-Ibargüengoitia et al., 2011; Cigala et al., 2017; Gaudin & Cimarelli, 2019). The presence of very fine to fine particles is observed here to be essential for the production of discharges. Experiments with a monomodal grain size distribution do not produce any discharges. We thus infer that near-vent lightning may be diagnostic of an ash-rich eruption, especially very fine ash.

Despite their chemical differences, TB and GB produce similar numbers of discharges, supporting the hypothesis that chemical composition does not significantly affect discharge behavior (at least for silicates). A similar conclusion was drawn from charging experiments where particles with different compositions had similar charging rates and charge densities (Méndez Harper & Dufek, 2016) as well

as from field observations where volcanic lightning was observed in different geological settings with varying magma compositions (McNutt & Williams, 2010).

We find that the vesicularity and thus the bulk density of the particles affects the generation of near-vent lightning. Other textural properties such as shape and surface roughness also may affect the charging and discharging behavior but require further study. While particle composition does not appear to affect discharging, the vesiculation processes as well as vesicle sizes that affect bulk density are influenced by magma composition. Thus, composition may indirectly affect near-vent lightning by changing clast density. Comparison of the highly vesiculated LSB, compared to the dense GB and TB, demonstrates this effect.

As noted above, we conclude that the presence of very fine particles (< 10 µm) is was required in our experiments to generate discharges during decompression. Particle size and density affect the coupling between gas and the particles and therefore their ability to collide with other particles and to follow different trajectories. In our experiments, particles smaller than 10 µm for GB and TB are well-coupled to the gas-phase enabling turbulence in the gas to separate very fines from larger particles after triboelectrification. LSB has a change in density due to the loss of vesicularity with reduced grainsize, which affects the coupling of the particles.

VL is increasingly established and recognized as a tool to monitor volcanic eruptions (Cimarelli, Behnke, et al., 2022). Observations from controlled experiments provide insights into the mechanisms that lead to near-vent lightning and hence what features of the eruption can be inferred (qualitatively and quantitatively) for VL and thereby inform monitoring strategies. As an example, for a given GSD, electrical discharge is approximately proportional to the mass eruption rate of very fine particles. Equally, the GSD has a major influence on electrical discharge. Thus monitoring near-vent lightning may help constrain in real time some combination of the two key vent parameters, mass eruption rate and GSD (e.g., Beckett et al., 2015; Bonadonna et al., 2012; Dioguardi et al., 2020), that control the height of plumes created by explosive eruptions and the long distance transport and residence time of very fine ash in the atmosphere. While volcanic lightning has not traditionally been viewed as a tool for assessing tephra grain size and mass eruption rate (see table 2 in Bonadonna et al., 2012) our experimental results show volcanic lightning is sensitive to both parameters and, hence, holds the potential for real-time monitoring of changing conditions at the vent.

Open Research

Experimental data are online at the GFZ Data Services (Springsklee, Scheu, et al., 2022b). The obtained data were analyzed using the Pandas Data Analysis Library (McKinney, 2010; Reback et al., 2022) and visualized using the Matplotlib Library (Caswell et al., 2021; Hunter, 2007).

Chapter 4 – Volcanic lightning as a potential ignition mechanism in mud volcanoes

4.1 Abstract

Self-ignition during the explosive eruption of mud volcanoes can create flames that in some cases reach heights that exceed hundreds of meters. To study the controls on electrical discharge in natural mud, we performed laboratory experiments using a shock-tube apparatus to simulate explosive eruptions of mud. We vary the water content of the mud and proportions of fine particles. We measure electric discharge within a Faraday cage, and we use a high-speed video camera to image the eruption of mud and some of the electric discharge events. We find that 1) decreasing the proportion of fine particles and 2) increasing water content each suppress the number and magnitude of electric discharge events. Experimentally observed mud volcano lightning occurs where particles exit from the vent and within the jet of erupting particles.

4.2 Plain Language Summary

Vigorous mud volcano eruptions are often accompanied by large flames, which are the result of the self-ignition of natural gas blasted with the erupting mud. The mechanisms for this gas ignition are not yet understood. We study a potential self-ignition mechanism: volcanic lightning. We erupt mud in a laboratory setting and measure the conditions that promote lightning. We find that dry mud and mud with abundant fine particles create more lightning. For safety reasons, we studied mud samples with argon as the carrier gas for the eruption but expect that if a flammable gas was used, the lightning could ignite the gas.

4.3 Introduction

Mud breccias that erupt explosively at mud volcanoes are sometimes accompanied by flames produced by the self-ignition of methane and other hydrocarbons. Flames can reach heights up to one km (Planke et al., 2003), though are most often 60 to 100 m high (Bagirov et al., 1996). While most of these flaming eruptions are short-lived (Judd, 2005), once ignited, methane seeps can burn for millennia (e.g., Etiope et al., 2004) and in some cases burn hot enough and long enough to melt rock (Grapes et al., 2013) causing pyrometamorphism (Sokol et al., 2008). The spectacular flames garner widespread media attention and speculation about the reasons for the self-ignition. Sparks, other electric discharge, or spontaneous combustion are possible processes.

Self-ignition has long been attributed to collisions between rock fragments. Arnold and MacReady (1956) wrote that ‘sparks were probably formed by the striking together of some of the rocks, and the petroleum gas thus ignited’ and Snead (1964) wrote that in ‘violent eruptions enough friction is exerted between rock fragments to ignite methane gas escaping with the liquid mud.’ Electric discharge from erupting solids is, in fact, well documented. Volcanic lightning has been reported at least since

Pliny's account of the 79 AD eruption of Vesuvius. It accompanies nearly all styles of explosive eruption (e.g., Cimarelli & Genareau, 2022), from the small eruptions at Stromboli, Italy (McNutt & Williams, 2010; Vossen et al., 2022) to almost 600,000 detected lightning strikes during the 2022 Hunga Tonga-Hunga Ha'apai eruption that reached a height of > 50 km. Electrical activity can occur both near the vent and in the plume, with the former promoted by high velocities and the latter by high volume fluxes (Smith et al., 2021). Jetting of fine ash is thought to be a key for charging (McNutt & Thomas, 2015).

Not all mud eruptions self-ignite. Only 'the most vigorous of such outbursts uproot trees, ignite methane' (Kopf, 2003). The Shikhzarli mud volcano, Azerbaijan, has flames in 74% of its eruptions (Kokh et al., 2017). Lokbatan, Azerbaijan, has a number of well documented explosive eruptions. The 5th January 1887 eruption produced a flame that reached a height greater than 600 m (Dimitrov, 2002). An example flaming eruption from Lokbatan on 20th September 2012 is shown in **Figure 4-1** (Mazzini et al., 2021). Lokbatan erupted on 11th August 2022, with conflicting reports about whether the eruption was accompanied by flames. Investigations of the parameters which govern ignition can yield insights into eruption initiation and dynamics. Here, we study here the influence of grain size distribution and mud humidity (e.g., Springsklee, Scheu, et al., 2022a; Stern et al., 2019) on electrical discharge in erupting mud.

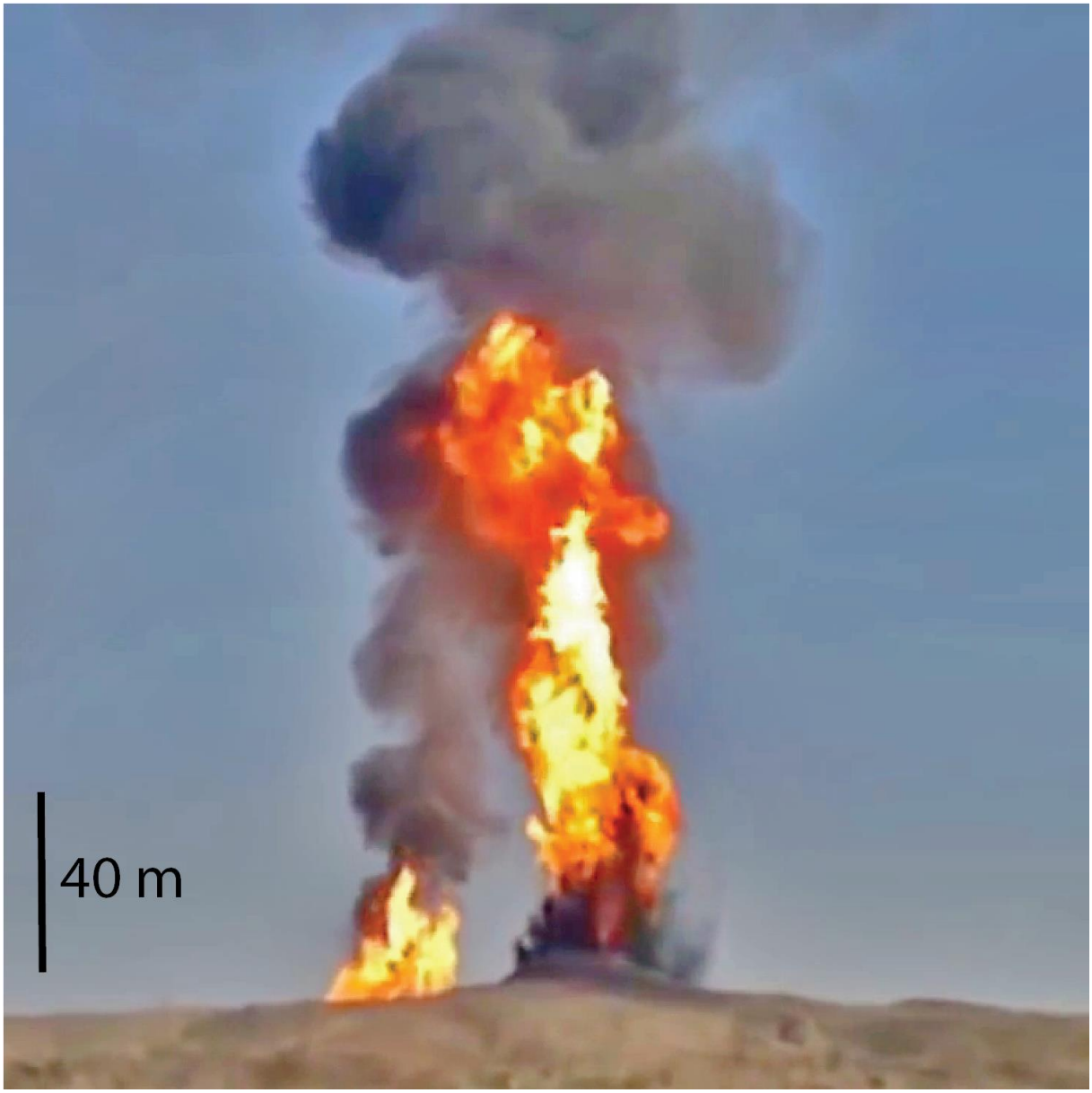

Figure 4-1. Mud eruption of Lokbatan, Azerbaijan on 20th September 2012. Two vents are active at this time. The flame in the foreground may have been ignited by flames at the vent in the background (adapted from Mazzini et al., 2021). Scale is obtained by triangulating the known vent locations and estimated location of the video recording.

Explosive eruptions are generally attributed to sealing of the vent between eruptions so that large overpressures are needed to initiate eruptions and unblock feeder channels and vents (Dimitrov, 2002; Mazzini & Etiope, 2017). Bagirov et al. (1996) compiled statistics of mud eruptions in Azerbaijan and found that gas self-ignites in 42% of eruptions. In a global assessment, Judd (2005) found that 30% of methane emitted at mud volcanoes ignites to produce flames. While explosive mud eruptions accompanied by flames are most abundantly documented in Azerbaijan, examples have also been reported in Trinidad (Anderson, 1911), New Zealand (Ridd, 1970), and Pakistan (Snead, 1964). Self-igniting gas explosions from permafrost have also been documented (e.g., Bogoyavlensky et al., 2022) and may share processes in common with mud volcanoes.

Here we use laboratory shock-tube experiments to study the conditions that lead to electrical discharge events in explosively ejected mud. In these experiments, mud held in an autoclave is subjected to a rapid decrease in pressure and it erupts through a vent to form an expanding jet. This simulates the brecciation of the seal that confines overpressured sediments (Mazzini et al., 2021). The jet is imaged with a high-speed video camera, and electric discharge is measured with a Faraday cage. Similar experiments have been used to simulate volcanic lightning to understand how properties of the erupted materials and environmental variables control electrical activity (Cimarelli et al., 2014; Gaudin & Cimarelli, 2019; Stern et al., 2019). For the case of mud, we first document that electrical discharge can occur. We then assess how particle size and water content affect electrical activity.

4.4 Materials and Methods

4.4.1 Samples

Mud was collected from the Davis-Schrimpf hydrothermal field in the Imperial Valley, California, USA. The mud extrudes from gryphons (cone-shaped vents) 1-2 m in height. Bubbles that burst in the vents or pools of mud can also eject spatter. This mud is composed of 41% quartz, 27% clay minerals (illite, montmorillonite and kaolinite), 24% feldspar, and 9% carbonates (Tran et al., 2015). **Figure A-10** shows the particle size distribution measured with a Bettersizer S3 Plus laser particle size analyzer. The sub-10-micron fraction comprises 30.7 vol% of the mud.

For the experiments in which the mud is not fully saturated with water, the mud was initially dried and then hydrated in an environmental chamber at controlled humidity and temperature. In the process of drying, the mud became consolidated and was thus mechanically disaggregated with a vibratory disc mill prior to being used in the experiments. We measured the grain-size distribution after disaggregation and found an increase in the volume fraction of fine particles (< 10 microns) (**Figure A-10**) from 30.7 vol% to 41.7 vol%. The proportion of fines is a crucial parameter in the number and intensity of discharges as demonstrated in experiments (Cimarelli et al., 2014; Gaudin & Cimarelli, 2019; Stern et al., 2019) and modelling predictions based on these experimental data (Rayborn & Jellinek, 2022).

The mineralogy and particle size distribution of the mud from the Davis-Schrimpf vents are similar to those of other mud volcanoes (Tran et al., 2015) which generally tend to erupt sediment deposited in deltaic and lacustrian settings. More deeply rooted mud volcanoes may have a greater proportion of illite among the clay minerals. The Davis-Schrimpf vents cannot ignite because the gas driving their eruptions (CO_2) is not flammable and there is no record of violent eruptions (Mazzini et al., 2011; Svensen et al., 2009).

To evaluate the potential role of particle size, we performed three additional experiments in which we added 0.17 mm diameter quartz sand. The grain size distribution of this sand is provided in **Figure A-10**.

4.4.2 Experimental facility

The experimental apparatus is shown and labeled in **Figure 4-2** and is adapted from the system used in previous studies (Alidibirov & Dingwell, 1996; Cimarelli et al., 2014; Gaudin & Cimarelli, 2019; Stern et al., 2019). Samples were placed in a cylindrical steel autoclave, with sample chamber dimensions of 26 mm in diameter and 160 mm in length; the entire autoclave was electrically grounded. The autoclave was completely filled in all experiments. At this constant volume, variable densities of the mud+sand+water mixtures resulted in differing sample masses.

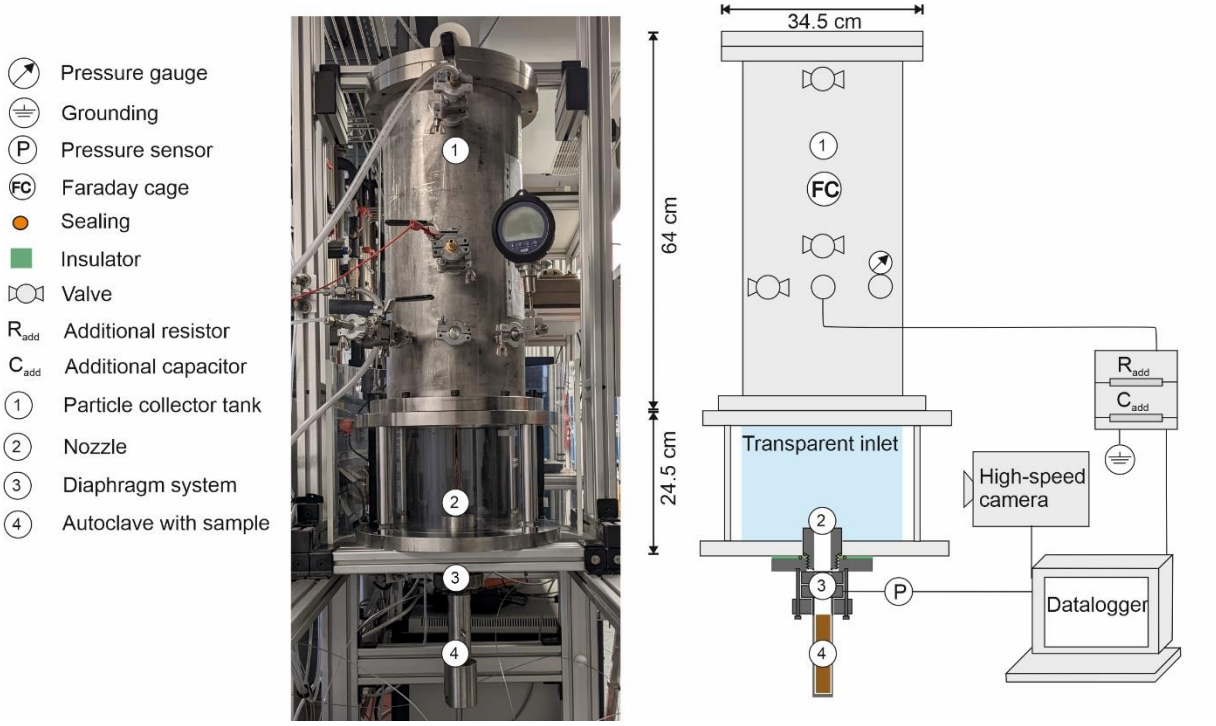

Figure 4-2. Photograph and illustration of the experimental apparatus. The upper part (light grey color) represents the Faraday cage that is insulated by a plastic flange (dark green color) from the decompression system including the nozzle and the autoclave. The autoclave is completely filled with the sample and grounded. Discharges from the jet to the nozzle are recorded by the datalogger and captured by a high-speed camera. The additional resistor and capacitor enable the calculation of the electrical current from the recorded voltage.

The samples were pressurized with argon gas to 10.2 ±0.1 MPa. The sample was then subjected to a rapid decompression by the controlled disruption of iron rupture diaphragms that sit between the autoclave and the capture tank. Upon diaphragm rupture, the sample was free to expand as a gas-particle jet into the capture tank which was instrumented to record optically the expanding jet as well as flashes of light from electrical discharges using a V711 Phantom high-speed video camera. The entire capture tank was electrically insulated and served as a Faraday cage such that changes in charge over the course of the experiment could be recorded and quantified (Stern et al., 2019).

The frame rate of the camera was set to 15,000 frames per second. The video camera was employed in three different modes. The shutter was left open for either 4

microseconds (6% of the time between individual frames), 10 microseconds (experiment 382 – completely water-saturated mud), or 66.66 microseconds (continuous mode). In the first case, the images captured sharply the ejection of mud fragments sand particles as well as the dynamics of the gas phase. However, the probability of capturing visible electrical discharges was greatly reduced as the shutter remained closed for 94% of the experiment. In the third case, all electrical discharges visible in the field of view of the camera were captured at a high focal depth but the long exposure times did not allow us to capture the motion of the initially rapidly expanding jet thus causing trails and streaks from the gas phase and particles and resulting in more blurred images. Owing to the high concentration of particles, only electrical discharge events near the outside of the jet and where the jet emerges from the vent were visible to the camera.

4.5 Results

Figure 4-3 shows the evolution of electric current and charge with time over the course of an experiment with mud containing 2.92 wt% water (experiment 378). Equivalent times series for all the experiments are plotted in **Figure A-11**.

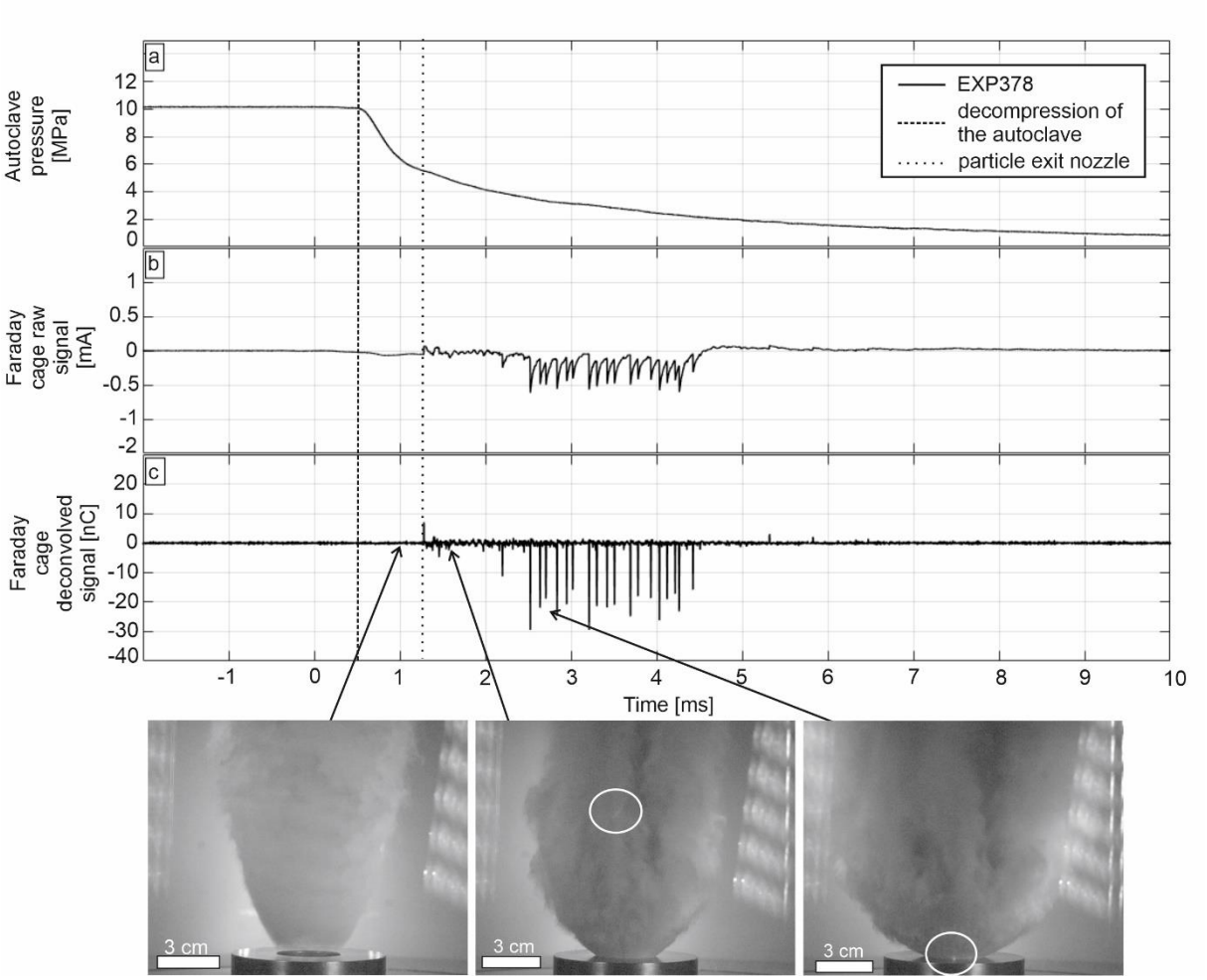

Figure 4-3. Example time series (experiment 378, mud containing 2.92 wt% water): a) decrease in pressure due to decompression, b) measured raw current signal, and c) the electric discharges obtained from the deconvolved signal. The photos show snapshots of the erupting mud during the progression of the experiment. The photos show the initial gas pulse that accompanies decompression experiments, followed by the gas-particle mixture. The high-speed camera detected discharges within the jet as well as discharges from the jet to the nozzle (circled). A complete set of images is in supplemental Movie S1 in Springsklee, Manga, et al. (2022a).

Following the rupture of the diaphragm, pressure in the autoclave drops (**Figure 4-3a**). Synchronized acquisition of pressure, electrical discharges and video recording is triggered as soon as the pressure in the autoclave drops below 6.5 MPa (falling edge trigger) and represents time = 0 in the raw data (shifted by 1 ms in the processed data to include potential discharges from the very beginning of decompression). A pre-trigger (~ 30%) ensures that we capture the decompression event in its entity. The decompression of the sample accelerates the mud upwards through the vent and into the capture tank, creating an expanding jet of gas and particles. **Figure 4-3b** shows the raw electrical current recorded by the Faraday cage. Each peak combined with an exponential decay identifies an electrical discharge event. The charging of the detector decays approximately exponentially with time. By fitting an exponential decay model to each event, it is possible to deconvolve the instrument response from the raw data in order to detect and count individual events and compute their magnitudes (Gaudin & Cimarelli, 2019).

Discharge events begin with the arrival of particles at the vent. Most, but not all, events generate a negative charge (**Figure 4-3** and **Figure A-11**). During the process of triboelectrification, large particles tend to be positively charged while small particles tend to acquire a negative charge (Forward et al., 2009a; Lacks & Levandovsky, 2007; Lee et al., 2015). In our experiments, the discharges are positive as well as negative.

Table 4-1. Summary of experiments. For experiment 390, no particle front velocity was measured because the video recording was not triggered.

EXP	Material	Water [wt%]	Sand [wt%]	Total mass [g]	Autoclave pressure [MPa]	Positive discharges 0 - 5 ms [nC]	Negative discharges 0 - 5 ms [nC]	Number of positive discharges 0 - 5 ms	Number of negative discharges 0 - 5 ms	Particle front velocity [m/s]
377	Mud	0.00	0.0	72.97	10.08	855.6	-1068.0	178	246	291.1 ± 7.8
378	Mud	2.92	0.0	70.01	10.16	5.5	-400.2	1	28	304.4 ± 15.1
379	Mud + Sand	0.00	10.0	60.34	10.15	397.0	-621.6	56	152	397.3 ±14.2
380	Mud + Sand	0.00	90.0	113.86	10.46	13.2	-100.4	6	22	292.6 ± 13.8
382	Mud	31.12	0.0	76.01	10.20	0.0	0.0	0	0	367.6 ± 2.9
383	Mud	5.06	0.0	62.03	10.23	0.0	-5.8	0	3	285.1 ± 5.1
385	Mud	0.00	0.0	78.95	10.30	226.5	-729.1	58	155	178.1 ± 44.1
386	Mud	0.00	0.0	60.77	10.14	75.8	-576.4	19	104	212.5 ± 14.7
387	Mud + Sand	0.00	50.0	82.93	10.20	24.4	-188.2	12	47	166.9 ± 8.0
388	Mud	0.62	0.0	57.01	10.30	38.1	-553.2	11	61	208.0 ± 39.1
389	Mud	0.62	0.0	57.60	10.11	4.3	-623.8	2	68	282.6 ± 19.8
390	Mud	3.49	0.0	47.03	10.35	0.0	-101.5	0	14	-
391	Mud	3.49	0.0	49.44	10.26	0.0	-96.9	0	11	286.2 ± 3.5

Table 4-1 summarizes for all 13 successful experiments the properties of sample used, the number and magnitude of discharge events, the total charge neutralized during each experiment and the detectable particle front velocity, observable by increased obscuration within the jet.

Figure 4-4a shows the number of detected discharge events and **Figure4-4c** shows the total charge accumulation, as a function of water content. Also shown for dry samples are the effects of adding sand (**Figure 4-4b**, **d**). The dry mud (without sand added) exhibits the greatest charging and the highest number of events (with a measurable variability in both parameters being observed in repeat experiments). The observations of the high-speed video reveal discharges within the upper part of the jet (Supplementary **Figure A-12**).

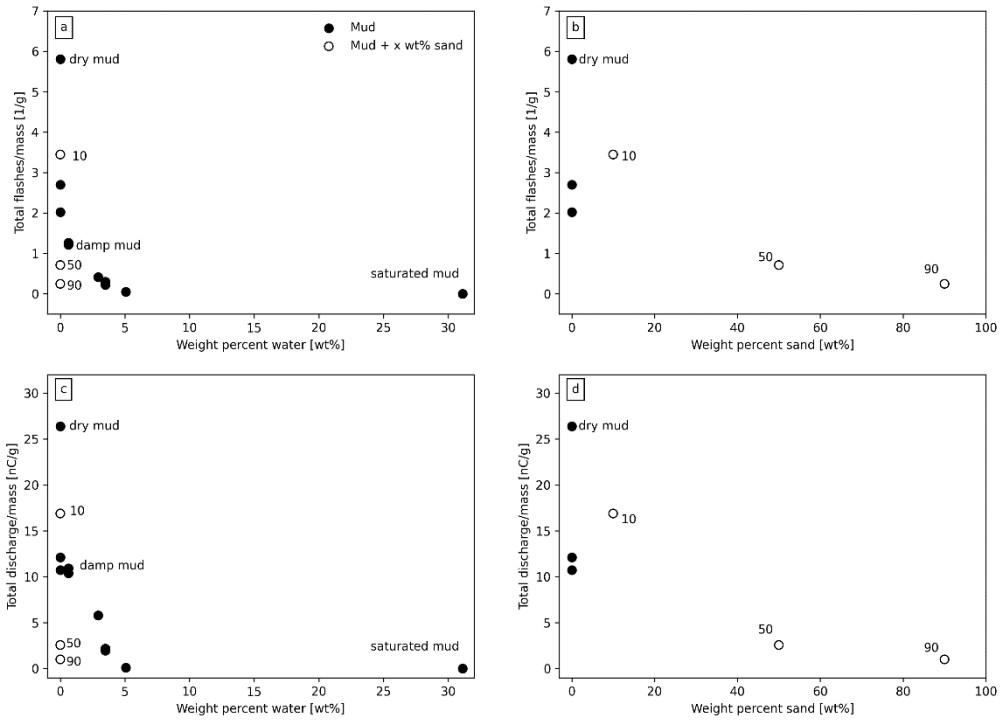

Figure 4-4. Total number of flashes and the total magnitude of discharge (both divided by sample mass) as a function of a,c) water content and b,d) weight fraction of sand for dry samples. Numbers next to the open circles indicate the weight percent of sand in the experimental run.

When sand or water has been added to the mud, the number of discharge events and the total charging both decrease. The addition of 2.9 wt% of water yielded a decrease of 93% of both the number of discharges observed, and the magnitude of the largest discharge event recorded. The addition of 5.1 wt% of water decreases the number of discharges observed by > 99%. A fully water-saturated mud experiment (31.1 wt% of water) produced no observed discharge events.

4.6 Discussion

Our experiments document that dry mud particles can become electrically charged and induce discharges during explosive mud volcano eruptions. Increasing water content of the mud, and decreasing fine fraction of mud particles by adding sand to the mud, both yield decreases in the number and magnitude of observed electrical discharge events.

The first stage in creating electric discharge is to charge particles. There are several particle charging mechanisms in natural particle-laden jets, and quantifying these processes remains the subject of active research (Arason et al., 2011; Björnsson et al., 1967; Cimarelli et al., 2014; James et al., 2000; Méndez Harper et al., 2021;

Nicoll et al., 2019; Prata et al., 2020; Thomas et al., 2010; Van Eaton et al., 2020). Ion transfer between colliding particles, triboelectrification, is generally thought to be the dominant process in thunderstorms (Mather & Harrison, 2006) and volcanic plumes (Cimarelli et al., 2014; Méndez Harper & Dufek, 2016). Fracto-electrification, in contrast, generated by fracturing particles (e.g., James et al., 2000) is likely insignificant in our experiments as we do not observe or expect significant fragmentation in these experiments since the particles are already very small and mostly non-porous (sand), and both of these particle attributes suppress further fragmentation during rapid gas expansion and / or particle collisions.

Next, prior to electrostatic discharging, charged particles need to be separated, and be surrounded by an electrically insulating medium to prevent charge transfer. The gas in the experiment fulfills the role of the low-conductivity medium. The turbulence in jets and plumes, and the differential velocity of particles of different sizes, enable the charge separation (Cimarelli et al., 2014; Gaudin & Cimarelli, 2019). In more detail, the dynamics of particles depends on whether their motion is well-coupled to the surrounding fluid. The inertial response time τ_p of particles with diameter *d* and density ρ_p in a fluid with density ρ and viscosity μ is $\tau_p \sim (\rho_p - \rho) d^2/18\mu$; the time characterizing eddy circulation is $\tau_f \sim 10 r_0/u_0$, with r_0 and u_0 the vent radius and initial jet velocity, respectively (Jessop and Jellinek (2014). The ratio of these time scales is the Stokes Number, $\mathrm{St} = \tau_p/\tau_f$. With our chosen definitions, $\rho_p = 2600$ kg/m^3 (Tran et al., 2015), measured $u_0 = 262$ m/s (±61m/s), and $r_0 = 1.4$ cm, then St < 1 for *d* < 10 microns and hence our fine particles will circulate in eddies. While details of particle-gas coupling depend on particle shape and drag coefficient, St is of order unity or less for particles smaller than 10 μm (**Figure A-13**).

In analogous experiments with volcanic ash it has also been observed that the number of discharge events increases with the fine fraction of volcanic ash (Gaudin & Cimarelli, 2019). The magnitude of individual discharge events in erupting volcanic ash is approximately linearly proportional to the erupted mass and the initial overpressure (Gaudin & Cimarelli, 2019). Thus, larger and more explosive eruptions will produce larger electrical discharges, and presumably this will increase the probability of ignition in the presence of methane or other flammable hydrocarbons. We note that natural muds and source rocks for mud breccia eruptions contain abundant fine particles (Dimitrov, 2002).

Our experiments show that even small amounts of water can suppress electric discharge. This may seem counterintuitive considering the common occurrence of lightning in clouds where ice particles and liquid water droplets are the charge carriers, but liquid water on particles can also enhance rapid charge leakage (Lorenz, 2018) and reduce charge accumulation (Méndez Harper et al., 2020). Wet volcanic eruptions also produce abundant volcanic lightning, such as the recent 2016-2017 Bogoslof, Alaska eruption (Van Eaton et al., 2020) and the 2022 Hunga Tonga-Hunga Ha'apai eruption. Lightning in the plumes of these large, wet explosive volcanic eruptions may be enabled by the formation of ice above the atmospheric

freezing level and hence electrification through mechanisms that operate in thunderstorms (Van Eaton et al., 2020). In fact, controlled laboratory experiments of volcanic particle jets reveal that as relative humidity and water content increase, the electrification of volcanic ash decreases (Méndez Harper et al., 2020). A mere 1.8 wt% water in volcanic ash has been observed to significantly decrease electrical discharge (Stern et al., 2019), quantitatively similar to our present findings with natural mud.

There are some limitations to generalizing from our experimental results. Firstly, for safety reasons, we employed argon rather than methane as the compressing gas phase. Thus, in the absence of flammable gases we could not assess whether the electrical discharge events actually generate ignition and combustion of the gas. Further, gas composition and pressure both affect the minimum breakdown distance for electric discharge and therefore our results are not quantitatively applicable to discharges within a methane-dominated jet. Hackam (1969) compares the electrical breakdown for gases including N_2, CH_4, and CO_2 and emphasizes the significance of the gas composition for electric discharge. The role of gas properties is also the subject of ongoing research into electrical discharge in extraterrestrial atmospheres, for example for brown dwarfs (Helling et al., 2013). Secondly, we have not yet systematically investigated the role of mineralogy on this phenomenon. Finally, we have not explored the effects of changing the overpressure that initiates the eruption. The value of 10 MPa was chosen as it is similar to the tensile strength of rocks, though even larger overpressures may develop in the source region of mud volcanoes at depths of a few kilometers (e.g., Blouin, Imbert, et al., 2019; Blouin, Sultan, et al., 2019). Complete conversion of the experimental overpressure ΔP into kinetic energy and then gravitational potential energy would lead to eruption heights of $\Delta P/\rho g$ where ρ is mud density and g is gravitational acceleration. This estimate neglects frictional losses and drag during eruption which would reduce height, but also acceleration of particles from gas expansion that increases height. If ΔP = 10 MPa, the ejection height would be 0.6 km for a bulk mud density of 1600 kg/m^3 (Tran et al., 2015); the mean ejection speed of 262 m/s in our experiments leads to ballistic heights of 3.5 km; these estimates are similar to heights of a few kilometers reported in large explosive mud volcano eruptions (Dimitrov, 2003).

4.7 Conclusions

Explosive eruption of dry mud creates electrical discharge events, and thus may be one mechanism to self-ignite methane in erupting mud. The conditions that promote electrification include the presence of fine particles and a limited amount of water. Although the mud and mud breccias that erupt during sustained eruptions generally have higher water contents that may dampen the propensity towards ignition, it may be an initial explosive venting through dry ground which provides the window of opportunity for self-ignition and initiation of prolonged flames.

Open Research

The data of the performed experiments is online at the GFZ Data Services (Springsklee, Manga, et al., 2022b). The obtained data was analyzed using the Pandas Data Analysis Library (McKinney, 2010; Reback et al., 2022) and visualized using the Matplotlib Library (Caswell et al., 2021; Hunter, 2007).

Chapter 5 – Conclusion

For this thesis, the shock tube apparatus originally developed by Alidibirov and Dingwell (1996) was further extended and modified into a new experimental setup to investigate discharges in shock tube experiments of particle-laden jets at varying atmospheric conditions. The variability in atmospheric pressure and composition enables the simulation of atmospheric conditions relevant to early Earth scenarios and extra-terrestrial conditions. Three different materials are compared in this thesis, a tholeiitic basalt, a phonolitic pumice and synthetic soda-lime glass beads, to investigate the potential difference in the behaviour of the three materials during decompression, visible in their charging and discharging behavior.

Extensions of the new setup

Although prior versions of the shock tube apparatus enabled the detection and quantification of experimentally generated near-vent discharges in decompressed particle-laden jets (Cimarelli et al., 2014; Gaudin & Cimarelli, 2019; Stern et al., 2019), the relevant modification of the setup is that it became gas-tight. The particle collector tank's upper part is sealed gas-tight to the nozzle system as surveyed by the high-precision pressure gauge applied to the particle collector tank. A gas-mixing unit, in combination with a flowmeter unit, allows a steady inflow of different gases to the particle collector tank. Additionally, the exhaust air system was tightly attached to the particle collector tank to ensure the removal of dangerous/poisonous gas compositions without any harm to the operator. A filter system and an extra-gas sampling pipe enabled the sampling of the very fine particles suspended in the gas as well as the gas itself. The glassy inlet mainly restricted the applied overpressure to the particle collector tank at the lower part of the particle collector tank. Due to the glassy inlet, the most pressure-sensitive material, the so far applied overpressure within the tank was 3 bar. The glassy part enables the observation of the jet exit behavior by a high-speed camera to gain insights into the spreading angle and the particle coupling behavior to the gas phase. An exchange of the glassy lower part of the particle collector tank for a steel inlet would enable the user to test even higher atmospheric overpressures and under pressures within a range of 200 mbar – 4 bar. Hence, the charging and the ejection behavior became observable, and the gas and particle samples became recoverable to be analyzed after conducting the experiments.

The influence of grain size distribution

A fundamental prerequisite for experimental laboratory studies is the reproducibility and evaluation of the parameters governing the experimental conditions. Therefore, the influence of grain size distribution for samples with bimodal grain size distributions was investigated in detail. The results demonstrate that the abundance of very fine particles (particles smaller than 10 µm) was necessary to generate near-vent discharges within the decompressed jets. This behavior was most evident for the less porous tholeiitic basalt and the fully dense soda-lime glass beads. The phonolitic Laacher See pumice (LSB), highly porous, demonstrates a different behavior. The sole addition of very fine-grained particles to a coarse sample did not

result in the expected charging and discharging behavior. The moderate grain size fraction was also required for the experimental generation of near-vent discharges with LSB. The observations of the discharge behavior were analogue to the observations of the jet exit behavior obtained by the high-speed recordings. They corroborated the conclusion that the coupling of the particles to the transporting gas phase governs the charging and discharging mechanisms.

The grain size distribution of the mud samples was modified by adding coarser sand grains to the sample to test the observed effect of grain size distribution additionally for these samples. An increase in coarse sand particles resulted in a decrease in detected discharge activity. The grain size distribution of the mud itself was not intentionally modified to preserve the natural grain size distribution of the sample and to preserve natural conditions to test the discharge potential of the material during decompression.

The influence of material properties

In this study, four materials were the subject of the conducted experiments (basalt, pumice, glass beads and mud). The tholeiitic basalt was employed as an analogue material for early Earth volcanism, which was supposedly predominantly mafic (e.g., basaltic) to ultra-mafic. Additionally, tholeiitic basalt was chosen to represent potential Martian volcanic conditions. An essential question of this study was if mafic material is as effective in causing charging in a volcanic plume as more silicic material. For this reason, the basaltic sample was compared against the recent phonolitic pumice and synthetic soda-lime glass beads to exclude natural variations. The soda-lime glass beads do not exhibit any variation in mineralogical content or chemical inhomogeneity.

In natural systems, magma composition does affect the eruption of a volcano. More volatile-rich compositions result in more vigorous and explosive eruptions, whereas more mafic compositions are known to exhibit explosive eruptions less often. This influence was excluded from the experiments, as the decompression conditions were comparable. Therefore, the decompression behavior of the sample materials was compared. The prediction and confidence interval of the results obtained from the experiments show a wide spread, minor effects of the material properties might not be detectable within our results. Nonetheless, within the wide spread of our experimental results, the composition (evident in the comparison of tholeiitic basalt and soda-lime glass beads) seems less significant than properties like porosity (evident by comparing tholeiitic basalt and soda-lime glass beads with the LSB). Therefore, the experiments demonstrate that volcanic lightning was possible under early Earth conditions for explosive mafic volcanism and represents a potential synthesis mechanism.

The influence of humidity

Previous studies on the influence of humidity on experimental volcanic lightning have shown that a significant decrease in discharge activity is observable with increasing

humidity. In our study with the mud samples, the samples were exposed to controlled humid conditions by moisturizing the samples with a minor amount of water. As expected, the discharge activity decreased tremendously for humid samples compared to the dry material.

The influence of the atmospheric composition and transporting gas phase

The goal of this study was further to investigate the environmental parameters at early Earth conditions to explore active volcanic settings as a potential environment for the emergence of life. Therefore, the atmospheric conditions enveloping the decompressed jet were changed to investigate the influence of modified atmospheric conditions on near-vent lightning. So far, only neutral to slightly reducing conditions were tested, so atmospheres composed of CO_2 and CO. Although the tank was proven to be gas-tight, the tank's purging and conditioning still resulted in air contamination within the tank of 7 vol%. Considering this contamination, the results for the discharge activity within the jet in CO_2 and CO_2-CO atmosphere are within the prediction limit of the results obtained for an enveloping atmosphere of air. The Paschen law predicts varying threshold values in charge to generate a discharge in varying atmospheric conditions. Discharge activity changes are visible for experiments for different transporting gas phases. Again, the jet dynamics might represent one potential explanation. The turbulent behavior of the particles close to the nozzle exit implies the entrainment of the surrounding gas phase, but the amount was not quantified. A potential explanation is that the charging and discharging occur in the transporting gas phase. This observation implies that for further studies concerning the prebiotic synthesis, not only a change in the atmosphere is of high interest, but rather a change in the transporting gas phase would be of high interest. As recent eruptions have shown, different types of eruptions demonstrate different compositions of volatile content. This observation significantly broadens the spectrum for possible gas compositions as the Archean atmosphere is regarded as less reducing than previously thought by early prebiotic synthesis experiments with discharges. Eruptions containing methane, like the investigated mud eruptions and eruptions containing H_2S, should obtain more attention.

Results of the ash and filter analysis

So far, the analyzed filter and ash samples were void of substantial evidence for any organic synthesis reaction. Most detected substances, like formic acid, were more likely the result of contamination than a product of a reaction taking place within the jet. One potential explanation for the lack of synthesis reactions might be that the air contamination prevented the synthesis reactions.

Another explanation is insufficient entrainment of the enveloping gas phase. The results obtained for discharges in enveloping CO_2 atmospheres compared to discharges with nitrogen as a carrier gas support this explanation. A substantial change in charging is observed in the case of changing the transporting gas phase. The entrainment of the surrounding gas phase into the decompressed jet seems not to be efficient enough to cause a change in charging as significantly as when the

transporting gas phase itself was changed. Therefore, the conclusion drawn from the results is that not enough of the reactive gas phase was entrained into the discharge-containing jet during decompression, so not close enough in spatial proximity to the discharges to take part in any potential synthesis reaction.

Limitations of this study

The particle collector tank of the new set up was proven to be gas-tight over the length of the experiment by the attached high-precision pressure gauge. Nonetheless, completely oxygen-free conditions weren't achieved. The analysis of the gas samples from the experiments showed that the remaining contamination of 7 vol% was achieved at best. Further improvement of the procedure to fill the atmosphere of the tank is needed to optimize the desired atmospheric conditions within the tank.

For safety reasons, more reducing gas compositions containing H_2 or CH_4 should be performed in an explosion-safe environment. So far, the first experiments were conducted with CO_2 and CO to test neutral to slightly reducing atmospheric conditions. The setup is mobile, so it can be moved to a safe explosion chamber.

The modified experimental setup cannot detect the analogue for plume lightning so far. Discharges within the jet, not moving from the jet to the nozzle, are not recorded by the datalogger and, therefore, not considered in the total magnitude budget of the eruption. In its current state, the setup can only detect near-vent discharges. An additional antenna that could detect the intra-jet discharges would require improvement. Not modifying the jet dynamics with such an antenna will be a challenge in applying such a system. Another limitation concerning the detection of the discharges is that there is no quantitative and qualitative procedure to gain insights about the length of the discharges within the jet. By chance, some discharges are visible in the turbulent obscured jet, but those are coincidental and obtained insights are insufficient to make a valid empirical statement about the discharge length.

The results obtained for the variable grain size distributions influencing laboratory-generated discharges in jets emphasize the importance of the fluid dynamics within the jet and the coupling and movement of the particles within the jet. Though the high-speed camera recorded videos with frame rates of up to 50000 fps, tracking the individual particles, especially for the fine fraction, was impossible. The recordings' resolution was insufficient to track the very fine particles. Although an image subtraction algorithm was applied to the recordings to enhance the visibility, the resolution remained insufficient to track individual particles. The individual particle movement and velocity would be required to improve the understanding of the charging and discharging behavior of the particles.

Chapter 6 – Outlook

The influence of grain size distribution for bimodally distributed grain size compositions was investigated. As demonstrated with the Laacher See pumice, the intermediate grain size fraction of the phonolitic highly porous material modified the discharge behavior of the material significantly. Therefore, a further detailed investigation of how the inclusion of other grain sizes resulting in more than bimodal grain size distributions affects the discharge and the coupling behavior of the particles to the jet.

Furthermore, this study does not address the clustering and collision of the particles within the decompressed jet. As explained before, tracking individual particles, especially the very fine particles and their individual behavior, movement and velocity, would be helpful for an improved understanding of jet dynamics. Collision rates depending on the Stokes number for the individual grains would be of high interest as the frictional non-destructive interaction of the particles is the primary mechanism for charging within the system and, ultimately, the intensity of discharges. The clustering would prohibit the separation of the particles, so in other terms, the separation of charge would hinder the probability of a discharge within the system. As the charged particles can also exhibit agglomeration due to their charging, those parameters need further evaluation to describe this highly diverse and interactive system in its entirety. Developing a particle track algorithm for the high-speed recordings would enable us to track individual particles and therefore is regarded as a necessary next step in this study.

One limitation of the experiments is that the analogue for plume discharges were not recorded. An additional antenna, a detection mechanism which is commonly used on active volcanoes, could be utilized to test for the experimental discharges as well. However, it will cause some jet disturbance. In the field, lightning is commonly monitored by the detection of the associated radio frequencies over a wide range (from very low (3 – 30 kHz) up to very high frequencies (30 – 300 MHz) (Cimarelli & Genareau, 2022). Detecting the potential radio frequencies caused by the experimental volcanic lightning might give first insight into the jet discharges and would be worthwhile investigating.

Experimental data provides the base for prediction models and helps to understand natural systems. Based on the experimental results of Stern et al. (2019) and Gaudin and Cimarelli (2019), a random forest prediction model was used by Rayborn and Jellinek (2022) to predict discharge behavior based on the abundance of fine ash. This thesis provides a significant number of new experimental data which could be used to improve this model regarding grain size distribution. The modelling and prediction of volcanic lightning is not only relevant for an experimental context and, more importantly as an indicator to predict ash-rich eruptions.

To thoroughly investigate the air entrainment and expansion behavior of jets close to the nozzle, a major improvement of the experiments would be to provide a longer supply of pressurized gas to obtain a long sustaining eruption column which can fully develop and does not terminate within milliseconds after formation. A longer lifetime

of the experiments would also result in more charges and discharges. The experimentally obtained data showed a possible saturation limit of charge and discharge, therefore, a longer lifetime of the experiments would help to investigate if this effect is only due to the experimental restrictions or based on the initial conditions within the system itself.

The modified setup did not only allow the testing of different gas compositions nor the enveloping surrounding pressure conditions. So far, the influence of underpressurized conditions (200 mbar) as well as overpressure (4 bar) was tested on the magnitude and number of discharges. The discharge behaviour of granular flows under different pressure conditions is essential for planetary science. In addition to a mechanism to detect the discharges within the jet and the extension of the pressure conditions, extra-terrestrial settings and their probability to exhibit discharges can be investigated. This modification can be easily done by exchanging the glassy part of the particle collector tank with a metallic part. This would prohibit video recordings of the jet but enables the user to apply higher pressure and higher vacuum to the tank safely.

One potential extra-terrestrial setting suggested for the formation of organic molecules is Enceladus, the biggest of Saturn’s moons. Geyser activity on this planet and its icy oceans are regarded as an environment with the potential for forming of first organic molecules. So far, our investigations have shown that an increase in humidity significantly decreases the probability of discharges. Nonetheless, investigations on geysers with electrical activity would be of high interest as discharges are in general a potential mechanism to initiate prebiotic synthesis. Ice particles are known to charge and cause discharges in atmospheric lightning on Earth. Therefore, further investigations on icy particles erupting and potentially causing discharges would be highly interesting for astrobiology. Again, the experiments need to consider that eruptions occur in a vacuum. The further modification of the setup to resist a very high vacuum within the particle collector tank ideally meets the requirements to perform such experiments.

As there were no prebiotic synthesis products detectable in our jets mobilized with argon, the reasonable next step in testing prebiotic synthesis in the setup will be to pressurize more reducing gases therefore more reactive gas phases like methane. For example, the ignition of methane requires some oxygen entrainment to cause ignition. No oxygen is required for the prebiotic synthesis reactions, but the reactive gas phase itself. Therefore, plausible mixtures of reducing gases pressurized together with the sample would be highly interesting. To ensure laboratory safety when working with highly reducing gas compositions, the purging procedure of the particle collector tank needs to be optimized, as with the procedure so far, contamination with air is not preventable. Highly reducing conditions will increase the probability of the formation of organic compounds by discharges. Those experiments need to be repeated with isotopically labelled gases to ensure that the obtained organics are no contamination but originate from the gas phase. Another mechanism

which could be investigated with the setup would be ammonia formation (NH_3) due to discharges.

References

Abbott, D. H., & Isley, A. E. (2002). The intensity, occurrence, and duration of superplume events and eras over geological time. *Journal of geodynamics*, *34*, 265-307. https://doi.org/10.1016/S0264-3707(02)00024-8

Aizawa, K., Cimarelli, C., Alatorre-Ibargüengoitia, M. A., Yokoo, A., Dingwell, D. B., & Iguchi, M. (2016). Physical properties of volcanic lightning: Constraints from magnetotelluric and video observations at Sakurajima volcano, Japan. *Earth and Planetary Science Letters*, *444*, 45-55. https://doi.org/10.1016/j.epsl.2016.03.024

Alatorre-Ibargüengoitia, M. A., Scheu, B., & Dingwell, D. B. (2011). Influence of the fragmentation process on the dynamics of Vulcanian eruptions: An experimental approach. *Earth and Planetary Science Letters*, *302*, 51-59. https://doi.org/10.1016/j.epsl.2010.11.045

Alidibirov, M., & Dingwell, D. B. (1996). An experimental facility for the investigation of magma fragmentation by rapid decompression. *Bulletin of Volcanology*, *58*, 411-416. https://doi.org/10.1007/s004450050149

Anders, E. (1989). Pre-biotic organic matter from comets and asteroids. *Nature*, *342*, 255-257. https://doi.org/10.1038/342255a0

Anderson, R. (1911). A new gas volcano in Trinidad. *Science*, *34*, 834-835. https://doi.org/10.1126/science.34.885.834

Andrews, B. J., & Manga, M. (2011). Effects of topography on pyroclastic density current runout and formation of coignimbrites. *Geology*, *39*, 1099-1102. https://doi.org/10.1130/G32226.1

Andrews, B. J., & Manga, M. (2012). Experimental study of turbulence, sedimentation, and coignimbrite mass partitioning in dilute pyroclastic density currents. *Journal of Volcanology and Geothermal Research*, *225-226*, 30-44. https://doi.org/10.1016/j.jvolgeores.2012.02.011

Aplin, K. L. (2006). Atmospheric electrification in the solar system. *Surveys in Geophysics*, *27*, 63-108. https://doi.org/10.1007/s10712-005-0642-9

Arason, P., Bennett, A. J., & Burgin, L. E. (2011). Charge mechanism of volcanic lightning revealed during the 2010 eruption of Eyjafjallajökull. *Journal of Geophysical Research: Solid Earth*, *116*. https://doi.org/10.1029/2011JB008651

Arndt, N., & Lesher, C. M. (2004). Komatiite. In *Encyclopedia of Geology.* (pp. 260-268). Elsevier. https://hal.archives-ouvertes.fr/hal-00101712

Arnold, R., & MacReady, G. A. (1956). Island-forming mud volcano in Trinidad, British West Indies. *AAPG Bulletin*, *40*, 2748-2758. https://doi.org/10.1306/5CEAE5E0-16BB-11D7-8645000102C1865D

Atreya, S. K., Mahaffy, P. R., & Wong, A.-S. (2007). Methane and related trace species on Mars: Origin, loss, implications for life, and habitability. *Planetary and Space Science*, *55*, 358-369. https://doi.org/10.1016/j.pss.2006.02.005

Avice, G., Marty, B., Burgess, R., Hofmann, A., Philippot, P., Zahnle, K., & Zakharov, D. (2018). Evolution of atmospheric xenon and other noble gases inferred from Archean to Paleoproterozoic rocks. *Geochimica et Cosmochimica Acta*, *232*, 82-100. https://doi.org/10.1016/j.gca.2018.04.018

Ayris, P. M., & Delmelle, P. (2012). The immediate environmental effects of tephra emission. *Bulletin of Volcanology*, *74*, 1905-1936. https://doi.org/10.1007/s00445-012-0654-5

Bada, J. L. (2004). How life began on Earth: a status report. *Earth and Planetary Science Letters*, *226*, 1-15. https://doi.org/10.1016/j.epsl.2004.07.036

Bada, J. L., & Korenaga, J. (2018). Exposed areas above sea level on Earth> 3.5 Gyr ago: Implications for prebiotic and primitive biotic chemistry. *Life*, *8*, 55. https://doi.org/10.3390/life8040055

Bagirov, E., Nadirov, R., & Lerche, I. (1996). Flaming eruptions and ejections from mud volcanoes in Azerbaijan: Statistical risk assessment from the historical records. *Energy exploration & exploitation*, *14*, 535-583. https://doi.org/10.1177/014459879601400603

Bar-Nun, A., Bar-Nun, N., Bauer, S. H., & Sagan, C. (1970). Shock synthesis of amino acids in simulated primitive environments. *Science*, *168*, 470-473. https://doi.org/10.1126/science.168.3930.470

Barge, L. M., & White, L. M. (2017). Experimentally testing hydrothermal vent origin of life on Enceladus and other icy/ocean worlds. *Astrobiology*, *17*, 820-833. https://doi.org/10.1089/ast.2016.1633

Basilevsky, A. T., & Head, J. W. (2003). The surface of Venus. *Reports on Progress in Physics*, *66*, 1699. https://doi.org/10.1088/0034-4885/66/10/r04

Basiuk, V. A., & Navarro-González, R. (1996). Possible role of volcanic ash-gas clouds in the Earth's prebiotic chemistry. *Origins of Life and Evolution of the Biosphere*, *26*, 173-194. https://doi.org/10.1007/BF01809854

Battistuzzi, F. U., Feijao, A., & Hedges, S. B. (2004). A genomic timescale of prokaryote evolution: insights into the origin of methanogenesis, phototrophy, and the colonization of land. *BMC evolutionary biology*, *4*. https://doi.org/10.1186/1471-2148-4-44

Beckett, F. M., Witham, C. S., Hort, M. C., Stevenson, J. A., Bonadonna, C., & Millington, S. C. (2015). Sensitivity of dispersion model forecasts of volcanic ash clouds to the physical characteristics of the particles. *Journal of Geophysical Research: Atmospheres*, *120*, 11,636-611,652. https://doi.org/10.1002/2015JD023609

Behnke, S. A., Edens, H. E., Thomas, R. J., Smith, C. M., McNutt, S. R., Van Eaton, A. R., Cimarelli, C., & Cigala, V. (2018). Investigating the origin of continual radio frequency impulses during explosive volcanic eruptions. *Journal of Geophysical Research: Atmospheres*, *123*, 4157-4174. https://doi.org/10.1002/2017JD027990

Behnke, S. A., Thomas, R. J., Edens, H. E., Krehbiel, P. R., & Rison, W. (2014). The 2010 eruption of Eyjafjallajökull: Lightning and plume charge structure. *Journal of Geophysical Research: Atmospheres*, *119*, 833-859. https://doi.org/10.1002/2013JD020781

Behnke, S. A., Thomas, R. J., McNutt, S. R., Schneider, D. J., Krehbiel, P. R., Rison, W., & Edens, H. E. (2013). Observations of volcanic lightning during the 2009 eruption of Redoubt Volcano. *Journal of Volcanology and Geothermal Research*, *259*, 214-234. https://doi.org/10.1016/j.jvolgeores.2011.12.010

Belousova, E. A., Kostitsyn, Y. A., Griffin, W. L., Begg, G. C., O'Reilly, S. Y., & Pearson, N. J. (2010). The growth of the continental crust: constraints from zircon Hf-isotope data. *Lithos*, *119*, 457-466. https://doi.org/10.1016/j.lithos.2010.07.024

Benner, S. A. (2014). Paradoxes in the origin of life. *Origins of Life and Evolution of Biospheres*, *44*, 339-343. https://doi.org/10.1007/s11084-014-9379-0

Bennett, A. J., Odams, P., Edwards, D., & Arason, Þ. (2010). Monitoring of lightning from the April–May 2010 Eyjafjallajökull volcanic eruption using a very low frequency lightning location network. *Environmental Research Letters*, *5*, 044013. https://doi.org/10.1088/1748-9326/5/4/044013

Bernal, J. D. (1949). The physical basis of life. *Proceedings of the Physical Society. Section B*, *62*, 597. https://doi.org/10.1088/0370-1301/62/10/301

Bilici, M. A., Toth III, J. R., Sankaran, R. M., & Lacks, D. J. (2014). Particle size effects in particle-particle triboelectric charging studied with an integrated fluidized bed and electrostatic separator system. *Review of Scientific Instruments*, *85*, 103903. https://doi.org/10.1063/1.4897182

Björnsson, S., Blanchard, D. C., & Spencer, A. T. (1967). Charge generation due to contact of saline waters with molten lava. *Journal of Geophysical Research*, *72*, 1311-1323. https://doi.org/10.1029/JZ072i004p01311

Blouin, A., Imbert, P., Sultan, N., & Callot, J.-P. (2019). Evolution model for the Absheron Mud Volcano: from in situ observations to numerical modeling. *Journal of Geophysical Research: Earth Surface*, *124*, 766-794. https://doi.org/10.1029/2018JF004872

Blouin, A., Sultan, N., Callot, J.-P., & Imbert, P. (2019). Sediment damage caused by gas exsolution: A key mechanism for mud volcano formation. *Engineering Geology*, *263*, 105313. https://doi.org/10.1016/j.enggeo.2019.105313

Bogoyavlensky, V., Bogoyavlensky, I., Nikonov, R., Sizov, O., Kishankov, A., & Kargina, T. (2022). Seyakha catastrophic blowout and explosion of gas from the permafrost in the Arctic, Yamal Peninsula. *Cold Regions Science and Technology*, *196*, 103507. https://doi.org/10.1016/j.coldregions.2022.103507

Bonadonna, C., Folch, A., Loughlin, S., & Puempel, H. (2012). Future developments in modelling and monitoring of volcanic ash clouds: outcomes from the first IAVCEI-WMO workshop on Ash Dispersal Forecast and Civil Aviation. *Bulletin of Volcanology*, *74*, 1-10. https://doi.org/10.1007/s00445-011-0508-6

Boschung, P., & Glor, M. (1980). Methods for investigating the electrostatic behaviour of powders. *Journal of Electrostatics*, *8*, 205-219. https://doi.org/10.1016/0304-3886(80)90007-8

Bowring, S. A., & Williams, I. S. (1999). Priscoan (4.00–4.03 Ga) orthogneisses from northwestern Canada. *Contributions to Mineralogy and Petrology*, *134*, 3-16. https://doi.org/10.1007/s004100050465

Bradski, G. (2000). The openCV library. *Dr. Dobb's Journal: Software Tools for the Professional Programmer*, *25*, 120-123.

Brasier, M. D., Matthewman, R., McMahon, S., Kilburn, M. R., & Wacey, D. (2013). Pumice from the∼ 3460 Ma Apex Basalt, Western Australia: A natural laboratory for the early biosphere. *Precambrian Research*, *224*, 1-10. https://doi.org/10.1016/j.precamres.2012.09.008

Brasier, M. D., Matthewman, R., McMahon, S., & Wacey, D. (2011). Pumice as a remarkable substrate for the origin of life. *Astrobiology*, *11*, 725-735. https://doi.org/10.1089/ast.2010.0546

Brož, P., Krýza, O., Wilson, L., Conway, S. J., Hauber, E., Mazzini, A., Raack, J., Balme, M. R., Sylvest, M. E., & Patel, M. R. (2020). Experimental evidence for lava-like mud flows under Martian surface conditions. *Nature Geoscience*, *13*, 403-407. https://doi.org/10.1038/s41561-020-0577-2

Burgisser, A., Bergantz, G. W., & Breidenthal, R. E. (2005). Addressing complexity in laboratory experiments: the scaling of dilute multiphase flows in magmatic systems. *Journal of Volcanology and Geothermal Research*, *141*, 245-265. https://doi.org/10.1016/j.jvolgeores.2004.11.001

Campbell, I. H., & Taylor, S. R. (1983). No water, no granites-No oceans, no continents. *Geophysical Research Letters*, *10*, 1061-1064. https://doi.org/10.1029/GL010i011p01061

Canup, R. M. (2004). Simulations of a late lunar-forming impact. *Icarus*, *168*, 433-456. https://doi.org/10.1016/j.icarus.2003.09.028

Canup, R. M., & Asphaug, E. (2001). Origin of the Moon in a giant impact near the end of the Earth's formation. *Nature*, *412*, 708-712. https://doi.org/10.1038/35089010

Carazzo, G., & Jellinek, A. M. (2012). A new view of the dynamics, stability and longevity of volcanic clouds. *Earth and Planetary Science Letters*, *325-326*, 39-51. https://doi.org/10.1016/j.epsl.2012.01.025

Casas, A. S., Wadsworth, F. B., Ayris, P. M., Delmelle, P., Vasseur, J., Cimarelli, C., & Dingwell, D. B. (2019). SO2 scrubbing during percolation through rhyolitic volcanic domes. *Geochimica et Cosmochimica Acta*, *257*, 150-162. https://doi.org/10.1016/j.gca.2019.04.013

Caswell, T. A., Droettboom, M., Lee, A., Sales de Andrade, E., Hoffmann, T., Hunter, J., Klymak, J., Firing, E., Stansby, D., Varoquaux, N., Hedegaard Nielsen, J., Root, B., May, R., Elson, P., Seppänen, J. K., Dale, D., Lee, J.-J., McDougall, D., Straw, A., . . . Ivanov, P. (2021). *matplotlib/matplotlib: REL: v3.5.1*. In (Version v3.5.1) Zenodo. https://doi.org/10.5281/zenodo.5773480

Catling, D. C., & Claire, M. W. (2005). How Earth's atmosphere evolved to an oxic state: a status report. *Earth and Planetary Science Letters*, *237*, 1-20. https://doi.org/10.1016/j.epsl.2005.06.013

Catling, D. C., & Kasting, J. F. (2017). *Atmospheric evolution on inhabited and lifeless worlds*. Cambridge University Press.

Catling, D. C., & Zahnle, K. J. (2020). The archean atmosphere. *Science Advances*, *6*, eaax1420. https://doi.org/10.1126/sciadv.aax1420

Cavosie, A. J., Valley, J. W., Wilde, S. A., & E.I.M.F. (2005). Magmatic δ18O in 4400–3900 Ma detrital zircons: A record of the alteration and recycling of crust in the Early Archean. *Earth and Planetary Science Letters*, *235*, 663-681. https://doi.org/10.1016/j.epsl.2005.04.028

Cawood, P. A., Chowdhury, P., Mulder, J. A., Hawkesworth, C. J., Capitanio, F. A., Gunawardana, P. M., & Nebel, O. (2022). Secular evolution of continents and the Earth system. *Reviews of Geophysics*, *60*, e2022RG000789. https://doi.org/10.1029/2022RG000789

Cawood, P. A., Hawkesworth, C. J., Pisarevsky, S. A., Dhuime, B., Capitanio, F. A., & Nebel, O. (2018). Geological archive of the onset of plate tectonics. *Philosophical Transactions of the Royal Society A: Mathematical, Physical and Engineering Sciences*, *376*, 20170405. https://doi.org/10.1098/rsta.2017.0405

Chameides, W. L., & Walker, J. C. G. (1981). Rates of fixation by lightning of carbon and nitrogen in possible primitive atmospheres. *Origins of Life*, *11*, 291-302. https://doi.org/10.1007/BF00931483

Channer, D. M. D., De Ronde, C. E. J., & Spooner, E. T. C. (1997). The Cl− Br− I− composition of∼ 3.23 Ga modified seawater: implications for the geological evolution of ocean halide chemistry. *Earth and Planetary Science Letters*, *150*, 325-335. https://doi.org/10.1016/S0012-821X(97)00101-5

Chyba, C. F., & McDonald, G. D. (1995). The origin of life in the solar system: current issues. *Annual Review of Earth and Planetary Sciences*, *23*, 215-250. https://doi.org/10.1146/annurev.ea.23.050195.001243

Chyba, C. F., & Phillips, C. B. (2001). Possible ecosystems and the search for life on Europa. *Proceedings of the National Academy of Sciences*, *98*, 801-804. https://doi.org/10.1073/pnas.98.3.801

Chyba, C. F., Thomas, P. J., Brookshaw, L., & Sagan, C. (1990). Cometary delivery of organic molecules to the early Earth. *Science*, *249*, 366-373. https://doi.org/10.1126/science.11538074

Cigala, V., Kueppers, U., Peña Fernández, J. J., Taddeucci, J., Sesterhenn, J., & Dingwell, D. B. (2017). The dynamics of volcanic jets: Temporal evolution of particles exit velocity from shock-tube experiments. *Journal of Geophysical Research: Solid Earth*, *122*, 6031-6045. https://doi.org/10.1002/2017JB014149

Cimarelli, C., Alatorre-Ibargüengoitia, M. A., Kueppers, U., Scheu, B., & Dingwell, D. B. (2014). Experimental generation of volcanic lightning. *Geology*, *42*, 79-82. https://doi.org/10.1130/G34802.1

Cimarelli, C., Alatorre-Ibargüengoitia, M. A., Aizawa, K., Yokoo, A., Díaz-Marina, A., Iguchi, M., & Dingwell, D. B. (2016). Multiparametric observation of volcanic lightning: Sakurajima Volcano, Japan. *Geophysical Research Letters*, *43*, 4221-4228. https://doi.org/10.1002/2015GL067445

Cimarelli, C., Behnke, S., Genareau, K., Méndez Harper, J., & Van Eaton, A. R. (2022). Volcanic electrification: recent advances and future perspectives. *Bulletin of Volcanology*, *84*, 78. https://doi.org/10.1007/s00445-022-01591-3

Cimarelli, C., Costa, A., Mueller, S., & Mader, H. M. (2011). Rheology of magmas with bimodal crystal size and shape distributions: Insights from analog experiments. *Geochemistry, Geophysics, Geosystems*, *12*. https://doi.org/10.1029/2011GC003606

Cimarelli, C., & Genareau, K. (2022). A review of volcanic electrification of the atmosphere and volcanic lightning. *Journal of Volcanology and Geothermal Research*, *422*, 107449. https://doi.org/10.1016/j.jvolgeores.2021.107449

Cimarelli, C., Vossen, C. E. J., & Bennett, A. J. (2022). Electrical Activity of Basaltic Explosive Eruptions at Stromboli, Etna and Cumbre Vieja. AGU Fall Meeting 2022, Chicago.

Clark, B. C. (1988). Primeval procreative comet pond. *Origins of Life and Evolution of the Biosphere*, *18*, 209-238. https://doi.org/10.1007/BF01804671

Cleaves II, H. J., Scott, A. M., Hill, F. C., Leszczynski, J., Sahai, N., & Hazen, R. (2012). Mineral–organic interfacial processes: potential roles in the origins of life. *Chemical Society Reviews*, *41*, 5502-5525. https://doi.org/10.1039/C2CS35112A

Cleland, C. E., & Chyba, C. F. (2002). Defining 'life'. *Origins of Life and Evolution of the Biosphere*, *32*, 387-393. https://doi.org/10.1023/A:1020503324273

Cleland, C. E., & Chyba, C. F. (2007). Does 'life'have a definition? In W. T. Sullivan III & J. A. Baross (Eds.), *Planets and life: The emerging science of astrobiology* (pp. 119-131). Cambridge University Press.

Cloud, P. (1972). A working model of the primitive Earth. *American Journal of Science*, *272*, 537-548. https://doi.org/10.2475/ajs.272.6.537

Cohen, K. M., Finney, S. C., Gibbard, P. L., & Fan, J.-X. (2013; updated). The ICS international chronostratigraphic chart. *Episodes Journal of International Geoscience*, *36*, 199-204. https://doi.org/10.18814/epiiugs/2013/v36i3/002

Condie, K. C. (1981). *Archean greenstone belts*. Elsevier.

Condie, K. C. (2013). *Plate tectonics & crustal evolution*. Elsevier.

Condie, K. C., & Kröner, A. (2008). When did plate tectonics begin? Evidence from the geologic record. In *When did plate tectonics begin on planet Earth* (Vol. 440, pp. 281-294). Geological Society of America Special Papers. https://doi.org/10.1130/2008.2440(14)

Conrad, P. G., & Nealson, K. H. (2001). A non-Earthcentric approach to life detection. *Astrobiology*, *1*, 15-24. https://doi.org/10.1089/153110701750137396

Corliss, J. B., Baross, J. A., & Hoffman, S. E. (1981). An hypothesis concerning the relationships between submarine hot springs and the origin of life on earth. *Oceanologica Acta, Special issue*. https://archimer.ifremer.fr/doc/00245/35661/34170.pdf

Crowe, S. A., Paris, G., Katsev, S., Jones, C., Kim, S.-T., Zerkle, A. L., Nomosatryo, S., Fowle, D. A., Adkins, J. F., Sessions, A. L., Farquhar, J., & Canfield, D. E. (2014). Sulfate was a trace constituent of Archean seawater. *Science*, *346*, 735-739. https://doi.org/10.1126/science.1258966

D'Incecco, P., Filiberto, J., López, I., Gorinov, D. A., Komatsu, G., Martynov, A., & Pisarenko, P. (2021). The geologically supervised spectral investigation as a key methodology for identifying volcanically active areas on Venus. *Journal of Geophysical Research: Planets*, *126*, e2021JE006909. https://doi.org/10.1029/2021JE006909

Dalrymple, G. B. (2001). The age of the Earth in the twentieth century: a problem (mostly) solved. In C. L. E. Lewis & S. J. Knell (Eds.), *The Age of the Earth: From 4004 BC to AD 2002* (Vol. 190, pp. 205-221). Geological Society of London. https://doi.org/10.1144/GSL.SP.2001.190.01.14

Damer, B., & Deamer, D. (2015). Coupled phases and combinatorial selection in fluctuating hydrothermal pools: A scenario to guide experimental approaches to the origin of cellular life. *Life*, *5*, 872-887. https://doi.org/10.3390/life5010872

Dauphas, N., Robert, F., & Marty, B. (2000). The late asteroidal and cometary bombardment of Earth as recorded in water deuterium to protium ratio. *Icarus*, *148*, 508-512. https://doi.org/10.1006/icar.2000.6489

De Ronde, C. E. J., Channer, D. M. d. R., Faure, K., Bray, C. J., & Spooner, E. T. C. (1997). Fluid chemistry of Archean seafloor hydrothermal vents: Implications for the composition of circa 3.2 Ga seawater. *Geochimica et Cosmochimica Acta*, *61*, 4025-4042. https://doi.org/10.1016/S0016-7037(97)00205-6

de Wit, M. J., & Ashwal, L. D. (1995). Greenstone belts: what are they? *South African Journal of Geology*, *98*, 505-520. https://hdl.handle.net/10520/EJC-943d19ff8

Deamer, D., & Damer, B. (2017). Can life begin on Enceladus? A perspective from hydrothermal chemistry. *Astrobiology*, *17*, 834-839. https://doi.org/10.1089/ast.2016.1610

Deamer, D., Singaram, S., Rajamani, S., Kompanichenko, V., & Guggenheim, S. (2006). Self-assembly processes in the prebiotic environment. *Philosophical Transactions of the Royal Society B: Biological Sciences*, *361*, 1809-1818. https://doi.org/10.1098/rstb.2006.1905

Deamer, D. W., & Georgiou, C. D. (2015). Hydrothermal conditions and the origin of cellular life. *Astrobiology*, *15*, 1091-1095. https://doi.org/10.1089/ast.2015.1338

Debaille, V., O'Neill, C., Brandon, A. D., Haenecour, P., Yin, Q.-Z., Mattielli, N., & Treiman, A. H. (2013). Stagnant-lid tectonics in early Earth revealed by 142Nd variations in late Archean

rocks. *Earth and Planetary Science Letters*, *373*, 83-92. https://doi.org/10.1016/j.epsl.2013.04.016

Desch, S. J., Borucki, W. J., Russell, C. T., & Bar-Nun, A. (2002). Progress in planetary lightning. *Reports on Progress in Physics*, *65*, 955. https://doi.org/10.1088/0034-4885/65/6/202

Dhuime, B., Hawkesworth, C. J., Cawood, P. A., & Storey, C. D. (2012). A change in the geodynamics of continental growth 3 billion years ago. *Science*, *335*, 1334-1336. https://doi.org/10.1126/science.1216066

Dimitrov, L. I. (2002). Mud volcanoes—the most important pathway for degassing deeply buried sediments. *Earth-Science Reviews*, *59*, 49-76. https://doi.org/10.1016/S0012-8252(02)00069-7

Dimitrov, L. I. (2003). Mud volcanoes—a significant source of atmospheric methane. *Geo-Marine Letters*, *23*, 155-161. https://doi.org/10.1007/s00367-003-0140-3

Dioguardi, F., Beckett, F., Dürig, T., & Stevenson, J. A. (2020). The impact of eruption source parameter uncertainties on ash dispersion forecasts during explosive volcanic eruptions. *Journal of Geophysical Research: Atmospheres*, *125*, e2020JD032717. https://doi.org/10.1029/2020JD032717

Dohm, J. M., & Maruyama, S. (2015). Habitable trinity. *Geoscience Frontiers*, *6*, 95-101. https://doi.org/10.1016/j.gsf.2014.01.005

Douillet, G. A., Rasmussen, K. R., Kueppers, U., Castro, D. L., Merrison, J. P., Iversen, J. J., & Dingwell, D. B. (2014). Saltation threshold for pyroclasts at various bedslopes: Wind tunnel measurements. *Journal of Volcanology and Geothermal Research*, *278-279*, 14-24. https://doi.org/10.1016/j.jvolgeores.2014.03.011

Driese, S. G., Jirsa, M. A., Ren, M., Brantley, S. L., Sheldon, N. D., Parker, D., & Schmitz, M. (2011). Neoarchean paleoweathering of tonalite and metabasalt: Implications for reconstructions of 2.69 Ga early terrestrial ecosystems and paleoatmospheric chemistry. *Precambrian Research*, *189*, 1-17. https://doi.org/10.1016/j.precamres.2011.04.003

Dupré, J., & O'Malley, M. A. (2009). Varieties of living things: life at the intersection of lineage and metabolism. *Philosophy, Theory, and Practice in Biology*, *1*. https://doi.org/10.3998/ptb.6959004.0001.003

Eriksson, P. G., Altermann, W., Nelson, D. R., Mueller, W. U., & Catuneanu, O. (2004). Precambrian volcanism: An independent variable through time. In *Developments in Precambrian Geology* (Vol. 12, pp. 271-358). Elsevier.

Esposito, F., Molinaro, R., Popa, C. I., Molfese, C., Cozzolino, F., Marty, L., Taj-Eddine, K., Di Achille, G., Franzese, G., Silvestro, S., & Ori, G. G. (2016). The role of the atmospheric electric field in the dust-lifting process. *Geophysical Research Letters*, *43*, 5501-5508. https://doi.org/10.1002/2016GL068463

Etiope, G., Feyzullayev, A., Baciu, C. L., & Milkov, A. V. (2004). Methane emission from mud volcanoes in eastern Azerbaijan. *Geology*, *32*, 465-468. https://doi.org/10.1130/G20320.1

Farquhar, J., Bao, H., & Thiemens, M. (2000). Atmospheric influence of Earth's earliest sulfur cycle. *Science*, *289*, 756-758. https://doi.org/10.1126/science.289.5480.756

Farrell, W. M., & Desch, M. D. (2001). Is there a Martian atmospheric electric circuit? *Journal of Geophysical Research: Planets*, *106*, 7591-7595. https://doi.org/10.1029/2000JE001271

Fischer, G., Gurnett, D. A., & Yair, Y. (2011). Extraterrestrial lightning and its past and future investigation. In M. D. Wood (Ed.), *Lightning: Properties, formation and types* (pp. 19-38). Nova Science.

Fleischaker, G. R. (1990). Origins of life: an operational definition. *Origins of Life and Evolution of the Biosphere*, *20*, 127-137. https://doi.org/10.1007/BF01808273

Fonti, S., & Marzo, G. A. (2010). Mapping the methane on Mars. *Astronomy & Astrophysics*, *512*, A51. https://doi.org/10.1051/0004-6361/200913178

Formisano, V., Atreya, S., Encrenaz, T., Ignatiev, N., & Giuranna, M. (2004). Detection of methane in the atmosphere of Mars. *Science*, *306*, 1758-1761. https://doi.org/10.1126/science.1101732

Forward, K. M., Lacks, D. J., & Sankaran, R. M. (2009a). Charge segregation depends on particle size in triboelectrically charged granular materials. *Physical Review Letters*, *102*, 028001. https://doi.org/10.1103/PhysRevLett.102.028001

Forward, K. M., Lacks, D. J., & Sankaran, R. M. (2009b). Methodology for studying particle–particle triboelectrification in granular materials. *Journal of Electrostatics*, *67*, 178-183. https://doi.org/10.1016/j.elstat.2008.12.002

Foshag, W. F., & González, J. (1956). Birth and development of Parícutin volcano, Mexico. *U.S.G.S. Bulletin*, *965–D*, 355-489. https://doi.org/10.3133/b965D

Fox, S., & Strasdeit, H. (2013). A possible prebiotic origin on volcanic islands of oligopyrrole-type photopigments and electron transfer cofactors. *Astrobiology*, *13*, 578-595. https://doi.org/10.1089/ast.2012.0934

Fox, S. W., & Harada, K. (1961). Synthesis of uracil under conditions of a thermal model of prebiological chemistry. *Science*, *133*, 1923-1924. https://doi.org/10.1126/science.133.3468.1923

Franz, H. B., Trainer, M. G., Malespin, C. A., Mahaffy, P. R., Atreya, S. K., Becker, R. H., Benna, M., Conrad, P. G., Eigenbrode, J. L., Freissinet, C., Manning, H. L. K., Prats, B. D., Raaen, E., & Wong, M. H. (2017). Initial SAM calibration gas experiments on Mars: Quadrupole mass spectrometer results and implications. *Planetary and Space Science*, *138*, 44-54. https://doi.org/10.1016/j.pss.2017.01.014

Fries Jr, C., & Guttiérrez, C. (1950). Activity of Paricutin volcano from August 1, 1948 to June 30, 1949. *Eos, Transactions American Geophysical Union*, *31*, 406-418. https://doi.org/10.1029/TR031i003p00406

Frost, D. J., Mann, U., Asahara, Y., & Rubie, D. C. (2008). The redox state of the mantle during and just after core formation. *Philosophical Transactions of the Royal Society A: Mathematical, Physical and Engineering Sciences*, *366*, 4315-4337. https://doi.org/10.1098/rsta.2008.0147

Frost, D. J., & McCammon, C. A. (2008). The redox state of Earth's mantle. *Annual Review of Earth and Planetary Sciences*, *36*, 389-420. https://doi.org/10.1146/annurev.earth.36.031207.124322

Fry, I. (1995). Are the different hypotheses on the emergence of life as different as they seem? *Biology and Philosophy*, *10*, 389-417. https://doi.org/10.1007/BF00857591

Fullmer, W. D., & Hrenya, C. M. (2017). The clustering instability in rapid granular and gas-solid flows. *Annual Review of Fluid Mechanics*, *49*, 485-510. https://doi.org/10.1146/annurev-fluid-010816-060028

Furnes, H., Dilek, Y., & de Wit, M. (2015). Precambrian greenstone sequences represent different ophiolite types. *Gondwana Research*, *27*, 649-685. https://doi.org/10.1016/j.gr.2013.06.004

Gaudin, D., & Cimarelli, C. (2019). The electrification of volcanic jets and controlling parameters: A laboratory study. *Earth and Planetary Science Letters*, *513*, 69-80. https://doi.org/10.1016/j.epsl.2019.02.024

Goldblatt, C., Claire, M. W., Lenton, T. M., Matthews, A. J., Watson, A. J., & Zahnle, K. J. (2009). Nitrogen-enhanced greenhouse warming on early Earth. *Nature Geoscience*, *2*, 891-896. https://doi.org/10.1038/ngeo692

Goodwin, A. (1996). *Principles of Precambrian Geology*. Academic Press.

Gough, D. O. (1981). Solar interior structure and luminosity variations. In V. Domingo (Ed.), *Physics of solar variations* (pp. 21-34). Springer, Dordrecht. https://doi.org/10.1007/978-94-010-9633-1_4

Gradstein, F. M., Ogg, J. G., Smith, A. G., Bleeker, W., & Lourens, L. J. (2004). A new geologic time scale, with special reference to Precambrian and Neogene. *Episodes*, *27*, 83-100. https://doi.org/10.18814/epiiugs/2004/v27i2/002

Grapes, R., Sokol, E., Kokh, S., Kozmenko, O., & Fishman, I. (2013). Petrogenesis of Na-rich paralava formed by methane flares associated with mud volcanism, Altyn-Emel National Park, Kazakhstan. *Contributions to Mineralogy and Petrology*, *165*, 781-803. https://doi.org/10.1007/s00410-012-0835-4

Greeley, R., & Spudis, P. D. (1981). Volcanism on mars. *Reviews of Geophysics*, *19*, 13-41. https://doi.org/10.1029/RG019i001p00013

Green, D. H., Nicholls, I. A., Viljoen, M., & Viljoen, R. (1975). Experimental demonstration of the existence of peridotitic liquids in earliest Archean magmatism. *Geology*, *3*, 11-14. https://doi.org/10.1130/0091-7613(1975)3<11:EDOTEO>2.0.CO;2

Guo, M., & Korenaga, J. (2020). Argon constraints on the early growth of felsic continental crust. *Science Advances*, *6*, eaaz6234. https://doi.org/10.1126/sciadv.aaz6234

Gupta, S., Ochiai, E., & Ponnamperuma, C. (1981). Organic synthesis in the atmosphere of Titan. *Nature*, *293*, 725-727. https://doi.org/10.1038/293725a0

Gurnett, D. A., Zarka, P., Manning, R., Kurth, W. S., Hospodarsky, G. B., Averkamp, T. F., Kaiser, M. L., & Farrell, W. M. (2001). Non-detection at Venus of high-frequency radio signals characteristic of terrestrial lightning. *Nature*, *409*, 313-315. https://doi.org/10.1038/35053009

Haberle, R. M. (2015). SOLAR SYSTEM/SUN, ATMOSPHERES, EVOLUTION OF ATMOSPHERES | Planetary Atmospheres: Mars. In G. R. North, J. Pyle, & F. Zhang (Eds.), *Encyclopedia of Atmospheric Sciences (Second Edition)* (pp. 168-177). Academic Press. https://doi.org/10.1016/B978-0-12-382225-3.00312-1

Hackam, R. (1969). Total secondary ionization coefficients and breakdown potentials of hydrogen, methane, ethylene, carbon monoxide, nitrogen, oxygen and carbon dioxide between mild steel coaxial cylinders. *Journal of Physics B: Atomic and Molecular Physics*, *2*, 216-233. https://doi.org/10.1088/0022-3700/2/2/309

Haldane, J. B. S. (1929). The origin of life. *Rationalist Annual*, *148*, 3 - 10.

Harada, K., & Fox, S. W. (1964). Thermal synthesis of natural amino-acids from a postulated primitive terrestrial atmosphere. *Nature*, *201*, 335-336. https://doi.org/10.1038/201335a0

Hargie, K. A., Van Eaton, A. R., Mastin, L. G., Holzworth, R. H., Ewert, J. W., & Pavolonis, M. (2019). Globally detected volcanic lightning and umbrella dynamics during the 2014 eruption of Kelud, Indonesia. *Journal of Volcanology and Geothermal Research*, *382*, 81-91. https://doi.org/10.1016/j.jvolgeores.2018.10.016

Harrison, T. M., Schmitt, A. K., McCulloch, M. T., & Lovera, O. M. (2008). Early (≥ 4.5 Ga) formation of terrestrial crust: Lu–Hf, δ18O, and Ti thermometry results for Hadean zircons. *Earth and Planetary Science Letters*, *268*, 476-486. https://doi.org/10.1016/j.epsl.2008.02.011

Hawkesworth, C. J., Cawood, P. A., Dhuime, B., & Kemp, T. I. (2017). Earth's continental lithosphere through time. *Annual Review of Earth and Planetary Sciences*, *45*, 169-198. https://doi.org/10.1146/annurev-earth-063016-020525

Hay, W. W., Wold, C. N., Söding, E., & Floegel, S. (2001). Evolution of sediment fluxes and ocean salinity. In D. F. Merriam & J. C. Davis (Eds.), *Geologic modeling and simulation. Computer Applications in the Earth Sciences* (pp. 153-167). Springer. https://doi.org/10.1007/978-1-4615-1359-9_9

Hayashi, C., Nakazawa, K., & Mizuno, H. (1979). Earth's melting due to the blanketing effect of the primordial dense atmosphere. *Earth and Planetary Science Letters*, *43*, 22-28. https://doi.org/10.1016/0012-821X(79)90152-3

Hazen, R. M. (2012). Geochemical origins of life. In A. H. Knoll, D. E. Canfield, & K. O. Konhauser (Eds.), *Fundamentals of Geobiology* (pp. 315-332). Blackwell Publishing Ltd. https://doi.org/10.1002/9781118280874.ch17

Hazen, R. M., Filley, T. R., & Goodfriend, G. A. (2001). Selective adsorption of L-and D-amino acids on calcite: Implications for biochemical homochirality. *Proceedings of the National Academy of Sciences*, *98*, 5487-5490. https://doi.org/10.1073/pnas.101085998

Hazen, R. M., & Sverjensky, D. A. (2010). Mineral surfaces, geochemical complexities, and the origins of life. *Cold Spring Harbor Perspectives in Biology*, *2*, a002162. https://doi.org/10.1101/cshperspect.a002162

Helling, C., Jardine, M., Stark, C., & Diver, D. (2013). Ionization in atmospheres of brown dwarfs and extrasolar planets. III. Breakdown conditions for mineral clouds. *The Astrophysical Journal*, *767*, 136. https://doi.org/10.1088/0004-637x/767/2/136

Hessler, A. M., Lowe, D. R., Jones, R. L., & Bird, D. K. (2004). A lower limit for atmospheric carbon dioxide levels 3.2 billion years ago. *Nature*, *428*, 736-738. https://doi.org/10.1038/nature02471

Hickman-Lewis, K., Cavalazzi, B., Foucher, F., & Westall, F. (2018). Most ancient evidence for life in the Barberton greenstone belt: Microbial mats and biofabrics of the~ 3.47 Ga Middle Marker horizon. *Precambrian Research*, *312*, 45-67. https://doi.org/10.1016/j.precamres.2018.04.007

Hirose, Y., Ohmuro, K., Saigoh, M., Nakayama, T., & Yamagata, Y. (1990). Synthesis of biomolecules from N2, CO, and H2O by electric discharge. *Origins of Life and Evolution of the Biosphere*, *20*, 471-481. https://doi.org/10.1007/BF01808195

Holland, H. D. (1962). Model for the evolution of the Earth's atmosphere. In A. E. J. Engel, H. L. James, & B. F. Leonard (Eds.), *Petrologic Studies*. The Geological Society of America. https://doi.org/10.1130/Petrologic.1962.447

Holland, H. D. (1972). The geologic history of sea water—an attempt to solve the problem. *Geochimica et Cosmochimica Acta*, *36*, 637-651. https://doi.org/10.1016/0016-7037(72)90108-1

Holland, H. D. (1984). *Chemical Evolution of the Atmosphere and Oceans.* Princeton University Press.

Holland, H. D. (2006). The oxygenation of the atmosphere and oceans. *Philosophical Transactions of the Royal Society B: Biological Sciences*, *361*, 903-915. https://doi.org/10.1098/rstb.2006.1838

Honda, Y., Navarro-González, R., & Ponnamperuma, C. (1989). A quantitative assay of biologically important compounds in simulated primitive earth experiments. *Advances in Space Research*, *9*, 63-66. https://doi.org/10.1016/0273-1177(89)90209-3

Horvath, D. G., Moitra, P., Hamilton, C. W., Craddock, R. A., & Andrews-Hanna, J. C. (2021). Evidence for geologically recent explosive volcanism in Elysium Planitia, Mars. *Icarus*, *365*, 114499. https://doi.org/10.1016/j.icarus.2021.114499

Houghton, I. M. P., Aplin, K. L., & Nicoll, K. A. (2013). Triboelectric charging of volcanic ash from the 2011 Grímsvötn eruption. *Physical Review Letters*, *111*, 118501. https://doi.org/10.1103/physrevlett.111.118501

Hunter, J. D. (2007). Matplotlib: A 2D graphics environment. *Computing in Science & Engineering*, *9*, 90-95. https://doi.org/10.1109/MCSE.2007.55

Ikoma, M., & Genda, H. (2006). Constraints on the mass of a habitable planet with water of nebular origin. *The Astrophysical Journal*, *648*, 696. https://doi.org/10.1086/505780

James, M. R., Lane, S. J., & Gilbert, J. S. (2000). Volcanic plume electrification: Experimental investigation of a fracture-charging mechanism. *Journal of Geophysical Research: Solid Earth*, *105*, 16641-16649. https://doi.org/10.1029/2000JB900068

James, M. R., Wilson, L., Lane, S. J., Gilbert, J. S., Mather, T. A., Harrison, R. G., & Martin, R. S. (2008). Electrical charging of volcanic plumes. *Space Science Reviews*, *137*, 399-418. https://doi.org/10.1007/s11214-008-9362-z

Jessop, D. E., & Jellinek, A. M. (2014). Effects of particle mixtures and nozzle geometry on entrainment into volcanic jets. *Geophysical Research Letters*, *41*, 3858-3863. https://doi.org/10.1002/2014GL060059

Johnson, A. P., Cleaves, H. J., Dworkin, J. P., Glavin, D. P., Lazcano, A., & Bada, J. L. (2008). The Miller volcanic spark discharge experiment. *Science*, *322*, 404-404. https://doi.org/10.1126/science.1161527

Johnson, J. E., Gerpheide, A., Lamb, M. P., & Fischer, W. W. (2014). O2 constraints from Paleoproterozoic detrital pyrite and uraninite. *GSA Bulletin*, *126*, 813-830. https://doi.org/10.1130/B30949.1

Joyce, G. F. (1995). The RNA world: life before DNA and protein. In B. Zuckerman & M. H. Hart (Eds.), *Extraterrestrials: where are they?* (pp. 139-151). Cambridge University Press. https://doi.org/10.1017/CBO9780511564970.017

Joyce, G. F. (2002). The antiquity of RNA-based evolution. *Nature*, *418*, 214-221. https://doi.org/10.1038/418214a

Judd, A. (2005). Gas emissions from mud volcanoes. In G. Martinelli & B. Panahi (Eds.), *Mud volcanoes, geodynamics and seismicity* (pp. 147-157). Springer. https://doi.org/10.1007/1-4020-3204-8_13

Kahana, A., Schmitt-Kopplin, P., & Lancet, D. (2019). Enceladus: first observed primordial soup could arbitrate origin-of-life debate. *Astrobiology*, *19*, 1263-1278. https://doi.org/10.1089/ast.2019.2029

Kamber, B. S. (2015). The evolving nature of terrestrial crust from the Hadean, through the Archaean, into the Proterozoic. *Precambrian Research*, *258*, 48-82. https://doi.org/10.1016/j.precamres.2014.12.007

Kamber, B. S., Collerson, K. D., Moorbath, S., & Whitehouse, M. J. (2003). Inheritance of early Archaean Pb-isotope variability from long-lived Hadean protocrust. *Contributions to Mineralogy and Petrology*, *145*, 25-46. https://doi.org/10.1007/s00410-002-0429-7

Kamminga, H. (1988). Historical perspective: the problem of the origin of life in the context of developments in biology. *Origins of Life and Evolution of the Biosphere*, *18*, 1-11. https://doi.org/10.1007/BF01808777

Kasting, J. F. (1993). Earth's early atmosphere. *Science*, *259*, 920-926. https://doi.org/10.1126/science.11536547

Kasting, J. F. (2001). The rise of atmospheric oxygen. *Science*, *293*, 819-820. https://doi.org/10.1126/science.1063811

Kasting, J. F., & Siefert, J. L. (2002). Life and the evolution of Earth's atmosphere. *Science*, *296*, 1066-1068. https://doi.org/10.1126/science.1071184

Kempe, S., & Degens, E. T. (1985). An early soda ocean? *Chemical Geology*, *53*, 95-108. https://doi.org/10.1016/0009-2541(85)90023-3

Kempe, S., & Kazmierczak, J. (1994). The role of alkalinity in the evolution of ocean chemistry, organization of living systems, and biocalcification processes. In F. Doumenge (Ed.), *Past and present biomineralization processes. Considerations about the Carbonate Cycle; IUCN COE workshop, Monaco, 15 - 16 November 1993* (Vol. 13, pp. 61-117). Bulletin de l'Institut Océanographique.

Kikuchi, K., & Endoh, T. (1982). Atmospheric electrical properties of volcanic ash particles in the eruption of Mt. Usu volcano, 1977. *Journal of the Meteorological Society of Japan. Ser. II*, *60*, 548-561. https://doi.org/10.2151/jmsj1965.60.1_548

Kirschvink, J. L., & Weiss, B. P. (2002). Mars, panspermia, and the origin of life: where did it all begin. *Palaeontologia electronica*, *4*, 8-15. https://palaeo-electronica.org/2001_2/editor/mars.htm

Kitadai, N., & Maruyama, S. (2018). Origins of building blocks of life: A review. *Geoscience Frontiers*, *9*, 1117-1153. https://doi.org/10.1016/j.gsf.2017.07.007

Kloprogge, J. T., & Hartman, H. (2022). Clays and the origin of life: The experiments. *Life*, *12*, 259. https://doi.org/10.3390/life12020259

Knauth, L. P. (1998). Salinity history of the Earth's early ocean. *Nature*, *395*, 554-555. https://doi.org/10.1038/26879

Knauth, L. P. (2005). Temperature and salinity history of the Precambrian ocean: implications for the course of microbial evolution. In N. Noffke (Ed.), *Geobiology: Objectives, concepts, perspectives* (pp. 53-69). Elsevier. https://doi.org/10.1016/B978-0-444-52019-7.50007-3

Knauth, L. P., & Lowe, D. R. (2003). High Archean climatic temperature inferred from oxygen isotope geochemistry of cherts in the 3.5 Ga Swaziland Supergroup, South Africa. *GSA Bulletin*, *115*, 566-580. https://doi.org/10.1130/0016-7606(2003)115<0566:HACTIF>2.0.CO;2

Knoll, A. H., & Nowak, M. A. (2017). The timetable of evolution. *Science Advances*, *3*, e1603076. https://doi.org/10.1126/sciadv.1603076

Kokh, S. N., Sokol, E. V., Dekterev, A. A., Kokh, K. A., Rashidov, T. M., Tomilenko, A. A., Bul'Bak, T. A., Khasaeva, A., & Guseinov, A. (2017). The 2011 strong fire eruption of Shikhzarli mud volcano,

Azerbaijan: a case study with implications for methane flux estimation. *Environmental Earth Sciences*, *76*. https://doi.org/10.1007/s12665-017-7043-5

Kopf, A. J. (2003). Global methane emission through mud volcanoes and its past and present impact on the Earth's climate. *International Journal of Earth Sciences*, *92*, 806-816. https://doi.org/10.1007/s00531-003-0341-z

Korenaga, J. (2021). Was There Land on the Early Earth? *Life*, *11*, 1142. https://doi.org/10.3390/life11111142

Koshland Jr, D. E. (2002). The seven pillars of life. *Science*, *295*, 2215-2216. https://doi.org/10.1126/science.1068489

Krissansen-Totton, J., Arney, G. N., & Catling, D. C. (2018). Constraining the climate and ocean pH of the early Earth with a geological carbon cycle model. *Proceedings of the National Academy of Sciences*, *115*, 4105-4110. https://doi.org/10.1073/pnas.1721296115

Krissansen-Totton, J., Olson, S., & Catling, D. C. (2018). Disequilibrium biosignatures over Earth history and implications for detecting exoplanet life. *Science Advances*, *4*, eaao5747. https://doi.org/10.1126/sciadv.aao5747

Lacks, D. J., & Levandovsky, A. (2007). Effect of particle size distribution on the polarity of triboelectric charging in granular insulator systems. *Journal of Electrostatics*, *65*, 107-112. https://doi.org/10.1016/j.elstat.2006.07.010

Lacks, D. J., & Sankaran, R. M. (2011). Contact electrification of insulating materials. *Journal of Physics D: Applied Physics*, *44*, 453001. https://doi.org/10.1088/0022-3727/44/45/453001

Lambert, J.-F. (2008). Adsorption and polymerization of amino acids on mineral surfaces: a review. *Origins of Life and Evolution of Biospheres*, *38*, 211-242. https://doi.org/10.1007/s11084-008-9128-3

Lavrentiev, G. A., Strigunkova, T. F., & Egorov, I. A. (1984). Abiological synthesis of amino acids, purines and pyrimidines under conditions simulating the volcanic ash-gas cloud. *Origins of Life*, *14*, 205-212. https://doi.org/10.1007/BF00933659

Le Bas, M. J. (2000). IUGS reclassification of the high-Mg and picritic volcanic rocks. *Journal of Petrology*, *41*, 1467-1470. https://doi.org/10.1093/petrology/41.10.1467

Lee, V., Waitukaitis, S. R., Miskin, M. Z., & Jaeger, H. M. (2015). Direct observation of particle interactions and clustering in charged granular streams. *Nature Physics*, *11*, 733-737. https://doi.org/10.1038/nphys3396

Lorenz, R. D. (2018). Lightning detection on Venus: a critical review. *Progress in Earth and Planetary Science*, *5*, 1-25. https://doi.org/10.1186/s40645-018-0181-x

Lowe, D. R., & Byerly, G. R. (2003). Ironstone pods in the Archean Barberton greenstone belt, South Africa: Earth's oldest seafloor hydrothermal vents reinterpreted as Quaternary subaerial springs. *Geology*, *31*, 909-912. https://doi.org/10.1130/G19664.1

Luhr, J. F., & Simkin, T. (1993). *Parícutin: the volcano born in a Mexican cornfield*. US Geoscience Press.

Luo, G., Ono, S., Beukes, N. J., Wang, D. T., Xie, S., & Summons, R. E. (2016). Rapid oxygenation of Earth's atmosphere 2.33 billion years ago. *Science Advances*, *2*, e1600134. https://doi.org/10.1126/sciadv.1600134

Lyons, T. W., Reinhard, C. T., & Planavsky, N. J. (2014). The rise of oxygen in Earth's early ocean and atmosphere. *Nature*, *506*, 307-315. https://doi.org/10.1038/nature13068

Macklem, P. T., & Seely, A. (2010). Towards a definition of life. *Perspectives in Biology and Medicine*, *53*, 330-340. https://doi.org/10.1353/pbm.0.0167

Markhinin, E. K., & Podkletnov, N. E. (1977). The phenomenon of formation of prebiological compounds in volcanic processes. *Origins of Life*, *8*, 225-235. https://doi.org/10.1007/BF00930684

Martin, W., Baross, J., Kelley, D., & Russell, M. J. (2008). Hydrothermal vents and the origin of life. *Nature Reviews Microbiology*, *6*, 805-814. https://doi.org/10.1038/nrmicro1991

Martin, W., & Russell, M. J. (2007). On the origin of biochemistry at an alkaline hydrothermal vent. *Philosophical Transactions of the Royal Society B: Biological Sciences*, *362*, 1887-1926. https://doi.org/10.1098/rstb.2006.1881

Marty, B., Avice, G., Bekaert, D. V., & Broadley, M. W. (2018). Salinity of the Archaean oceans from analysis of fluid inclusions in quartz. *Comptes Rendus Geoscience*, *350*, 154-163. https://doi.org/10.1016/j.crte.2017.12.002

Marty, B., Zimmermann, L., Pujol, M., Burgess, R., & Philippot, P. (2013). Nitrogen isotopic composition and density of the Archean atmosphere. *Science*, *342*, 101-104. https://doi.org/10.1126/science.1240971

Mather, T. A., & Harrison, R. G. (2006). Electrification of volcanic plumes. *Surveys in Geophysics*, *27*, 387-432. https://doi.org/10.1007/s10712-006-9007-2

Mazzini, A., Akhmanov, G., Manga, M., Sciarra, A., Huseynova, A., Huseynov, A., & Guliyev, I. (2021). Explosive mud volcano eruptions and rafting of mud breccia blocks. *Earth and Planetary Science Letters*, *555*, 116699. https://doi.org/10.1016/j.epsl.2020.116699

Mazzini, A., & Etiope, G. (2017). Mud volcanism: An updated review. *Earth-Science Reviews*, *168*, 81-112. https://doi.org/10.1016/j.earscirev.2017.03.001

Mazzini, A., Svensen, H., Etiope, G., Onderdonk, N., & Banks, D. (2011). Fluid origin, gas fluxes and plumbing system in the sediment-hosted Salton Sea Geothermal System (California, USA). *Journal of Volcanology and Geothermal Research*, *205*, 67-83. https://doi.org/10.1016/j.jvolgeores.2011.05.008

McCauley, J. F., Carr, M. H., Cutts, J. A., Hartmann, W. K., Masursky, H., Milton, D. J., Sharp, R. P., & Wilhelms, D. E. (1972). Preliminary Mariner 9 report on the geology of Mars. *Icarus*, *17*, 289-327. https://doi.org/10.1016/0019-1035(72)90003-6

McCollom, T. M. (2013). Miller-Urey and beyond: what have we learned about prebiotic organic synthesis reactions in the past 60 years? *Annual Review of Earth and Planetary Sciences*, *41*, 207-229. https://doi.org/10.1146/annurev-earth-040610-133457

McDonald, G. D., Thompson, W. R., Heinrich, M., Khare, B. N., & Sagan, C. (1994). Chemical investigation of Titan and Triton tholins. *Icarus*, *108*, 137-145. https://doi.org/10.1006/icar.1994.1046

McKinney, W. (2010). Data structures for statistical computing in python. In S. Van der Walt & J. Millman (Eds.), *Proceedings of the 9th Python in Science Conference* (pp. 56-61). https://doi.org/10.25080/Majora-92bf1922-00a

McNutt, S. R., & Thomas, R. J. (2015). Chapter 62 - Volcanic Lightning. In H. Sigurdsson (Ed.), *The encyclopedia of volcanoes (Second Edition)* (pp. 1059-1067). Elsevier. https://doi.org/10.1016/B978-0-12-385938-9.00062-6

McNutt, S. R., & Williams, E. R. (2010). Volcanic lightning: global observations and constraints on source mechanisms. *Bulletin of Volcanology*, *72*, 1153-1167. https://doi.org/10.1007/s00445-010-0393-4

Melnik, O., & Parrot, M. (1998). Electrostatic discharge in Martian dust storms. *Journal of Geophysical Research: Space Physics*, *103*, 29107-29117. https://doi.org/10.1029/98JA01954

Méndez Harper, J., Cimarelli, C., Cigala, V., Kueppers, U., & Dufek, J. (2021). Charge injection into the atmosphere by explosive volcanic eruptions through triboelectrification and fragmentation charging. *Earth and Planetary Science Letters*, *574*, 117162. https://doi.org/10.1016/j.epsl.2021.117162

Méndez Harper, J., Courtland, L., Dufek, J., & McAdams, J. (2020). Microphysical effects of water content and temperature on the triboelectrification of volcanic ash on long time scales. *Journal of Geophysical Research: Atmospheres*, *125*, e2019JD031498. https://doi.org/10.1029/2019JD031498

Méndez Harper, J., & Dufek, J. (2016). The effects of dynamics on the triboelectrification of volcanic ash. *Journal of Geophysical Research: Atmospheres*, *121*, 8209-8228. https://doi.org/10.1002/2015JD024275

Michalski, J. R., & Bleacher, J. E. (2013). Supervolcanoes within an ancient volcanic province in Arabia Terra, Mars. *Nature*, *502*, 47-52. https://doi.org/10.1038/nature12482

Miller, S. L. (1953). A production of amino acids under possible primitive earth conditions. *Science*, *117*, 528-529. https://doi.org/10.1126/science.117.3046.528

Miller, S. L. (1955). Production of some organic compounds under possible primitive earth conditions. *Journal of the American Chemical Society*, *77*, 2351-2361. https://doi.org/10.1021/ja01614a001

Miller, S. L. (1957). The mechanism of synthesis of amino acids by electric discharges. *Biochimica et Biophysica Acta*, *23*, 480-489. https://doi.org/10.1016/0006-3002(57)90366-9

Miura, T., Koyaguchi, T., & Tanaka, Y. (2002). Measurements of electric charge distribution in volcanic plumes at Sakurajima Volcano, Japan. *Bulletin of Volcanology*, *64*, 75-93. https://doi.org/10.1007/s00445-001-0182-1

Mizuno, H., Nakazawa, K., & Hayashi, C. (1980). Dissolution of the primordial rare gases into the molten Earth's material. *Earth and Planetary Science Letters*, *50*, 202-210. https://doi.org/10.1016/0012-821X(80)90131-4

Mojzsis, S. J., Harrison, T. M., & Pidgeon, R. T. (2001). Oxygen-isotope evidence from ancient zircons for liquid water at the Earth's surface 4,300 Myr ago. *Nature*, *409*, 178-181. https://doi.org/10.1038/35051557

Molina-Cuberos, G. J., Schwingenschuh, K., López-Moreno, J. J., Rodrigo, R., Lara, L. M., & Anicich, V. (2002). Nitriles produced by ion chemistry in the lower ionosphere of Titan. *Journal of Geophysical Research: Planets*, *107*, 9-1-9-11. https://doi.org/10.1029/2000JE001480

Morse, J. W., & Mackenzie, F. T. (1998). Hadean ocean carbonate geochemistry. *Aquatic Geochemistry*, *4*, 301-319. https://doi.org/10.1023/A:1009632230875

Mueller, S. P., Helo, C., Keller, F., Taddeucci, J., & Castro, J. M. (2018). First experimental observations on melting and chemical modification of volcanic ash during lightning interaction. *Scientific Reports*, *8*, 1389. https://doi.org/10.1038/s41598-018-19608-3

Mulkidjanian, A. Y., Bychkov, A. Y., Dibrova, D. V., Galperin, M. Y., & Koonin, E. V. (2012a). Open questions on the origin of life at anoxic geothermal fields. *Origins of Life and Evolution of Biospheres*, *42*, 507-516. https://doi.org/10.1007/s11084-012-9315-0

Mulkidjanian, A. Y., Bychkov, A. Y., Dibrova, D. V., Galperin, M. Y., & Koonin, E. V. (2012b). Origin of first cells at terrestrial, anoxic geothermal fields. *Proceedings of the National Academy of Sciences*, *109*, E821-E830. https://doi.org/10.1073/pnas.1117774109

Navarro-Gonzalez, R., & Basiuk, V. A. (1998). Prebiotic synthesis by lightning in Martian volcanic plumes. In J. Chela-Flores & F. Raulin (Eds.), *Exobiology: Matter, Energy, and Information in the Origin and Evolution of Life in the Universe* (pp. 255-260). Springer. https://doi.org/10.1007/978-94-011-5056-9_36

Navarro-González, R., & Segura, A. (2004). The possible role of volcanic lightning in chemical evolution. In J. Seckbach (Ed.), *Origins. Cellular Origin, Life in Extreme Habitats and Astrobiology, vol 6.* (pp. 139-152). Springer, Dordrecht. https://doi.org/10.1007/1-4020-2522-X_9

Navarro-González, R., Molina, M. J., & Molina, L. T. (1998). Nitrogen fixation by volcanic lightning in the early Earth. *Geophysical Research Letters*, *25*, 3123-3126. https://doi.org/10.1029/98GL02423

Nicklas, R. W., Puchtel, I. S., & Ash, R. D. (2018). Redox state of the Archean mantle: Evidence from V partitioning in 3.5–2.4 Ga komatiites. *Geochimica et Cosmochimica Acta*, *222*, 447-466. https://doi.org/10.1016/j.gca.2017.11.002

Nicoll, K., Airey, M., Cimarelli, C., Bennett, A., Harrison, G., Gaudin, D., Aplin, K., Koh, K. L., Knuever, M., & Marlton, G. (2019). First in situ observations of gaseous volcanic plume electrification. *Geophysical Research Letters*, *46*, 3532-3539. https://doi.org/10.1029/2019GL082211

Nisbet, E. G. (1985). The geological setting of the earliest life forms. *Journal of Molecular Evolution*, *21*, 289-298. https://doi.org/10.1007/BF02102361

Nisbet, E. G., Cheadle, M. J., Arndt, N. T., & Bickle, M. J. (1993). Constraining the potential temperature of the Archaean mantle: a review of the evidence from komatiites. *Lithos*, *30*, 291-307. https://doi.org/10.1016/0024-4937(93)90042-B

O'Neil, J., Carlson, R. W., Francis, D., & Stevenson, R. K. (2008). Neodymium-142 evidence for Hadean mafic crust. *Science*, *321*, 1828-1831. https://doi.org/10.1126/science.1161925

O'Neill, C., & Debaille, V. (2014). The evolution of Hadean–Eoarchaean geodynamics. *Earth and Planetary Science Letters*, *406*, 49-58. https://doi.org/10.1016/j.epsl.2014.08.034

Ohmoto, H., Watanabe, Y., Ikemi, H., Poulson, S. R., & Taylor, B. E. (2006). Sulphur isotope evidence for an oxic Archaean atmosphere. *Nature*, *442*, 908-911. https://doi.org/10.1038/nature05044

Oparin, A. I. (1957). *The origin of life on the Earth*. Academic Press Inc.

Orgel, L. E. (1998). Polymerization on the rocks: theoretical introduction. *Origins of Life and Evolution of the Biosphere*, *28*, 227-234. https://doi.org/10.1023/A:1006595411403

Oró, J. (1961). Comets and the formation of biochemical compounds on the primitive Earth. *Nature*, *190*, 389-390. https://doi.org/10.1038/190389a0

Oró, J., Lazcano, A., & Ehrenfreund, P. (2006). Comets and the origin and evolution of life. In P. J. Thomas, R. D. Hicks, C. F. Chyba, & C. P. McKay (Eds.), *Comets and the Origin and Evolution of Life. Advances in Astrobiology and Biogeophysics.* (pp. 1-28). Springer. https://doi.org/10.1007/3-540-33088-7_1

Oró, J., Mills, T., & Lazcano, A. (1991). Comets and the formation of biochemical compounds on the primitive Earth–A review. *Origins of Life and Evolution of the Biosphere*, *21*, 267-277. https://doi.org/10.1007/BF01808302

Ortenzi, G., Noack, L., Sohl, F., Guimond, C. M., Grenfell, J. L., Dorn, C., Schmidt, J. M., Vulpius, S., Katyal, N., Kitzmann, D., & Rauer, H. (2020). Mantle redox state drives outgassing chemistry and atmospheric composition of rocky planets. *Scientific Reports*, *10*. https://doi.org/10.1038/s41598-020-67751-7

Owen, J. E., Shaikhislamov, I. F., Lammer, H., Fossati, L., & Khodachenko, M. L. (2020). Hydrogen Dominated Atmospheres on Terrestrial Mass Planets: Evidence, Origin and Evolution. *Space Science Reviews*, *216*, 129. https://doi.org/10.1007/s11214-020-00756-w

Owen, T., Biemann, K., Rushneck, D. R., Biller, J. E., Howarth, D. W., & Lafleur, A. L. (1977). The composition of the atmosphere at the surface of Mars. *Journal of Geophysical Research*, *82*, 4635-4639. https://doi.org/10.1029/JS082i028p04635

Pahlevan, K., Schaefer, L., & Hirschmann, M. M. (2019). Hydrogen isotopic evidence for early oxidation of silicate Earth. *Earth and Planetary Science Letters*, *526*, 115770. https://doi.org/10.1016/j.epsl.2019.115770

Paola, C., Straub, K., Mohrig, D., & Reinhardt, L. (2009). The “unreasonable effectiveness” of stratigraphic and geomorphic experiments. *Earth-Science Reviews*, *97*, 1-43. https://doi.org/10.1016/j.earscirev.2009.05.003

Piper, J. D. A. (2013). A planetary perspective on Earth evolution: lid tectonics before plate tectonics. *Tectonophysics*, *589*, 44-56. https://doi.org/10.1016/j.tecto.2012.12.042

Planck Collaboration, Aghanim, N., Akrami, Y., Ashdown, M., Aumont, J., Baccigalupi, C., Ballardini, M., Banday, A. J., Barreiro, R. B., Bartolo, N., Basak, S., Battye, R., Benabed, K., Bernard, J.-P., Bersanelli, M., Bielewicz, P., Bock, J. J., Bond, J. R., Borrill, J., . . . Zonca, A. (2020). Planck 2018 results - VI. Cosmological parameters. *Astronomy & Astrophysics*, *641*, A6. https://doi.org/10.1051/0004-6361/201833910

Planke, S., Svensen, H., Hovland, M., Banks, D. A., & Jamtveit, B. (2003). Mud and fluid migration in active mud volcanoes in Azerbaijan. *Geo-Marine Letters*, *23*, 258-268. https://doi.org/10.1007/s00367-003-0152-z

Plankensteiner, K., Reiner, H., Schranz, B., & Rode, B. M. (2004). Prebiotic formation of amino acids in a neutral atmosphere by electric discharge. *Angewandte Chemie International Edition*, *43*, 1886-1888. https://doi.org/10.1002/anie.200353135

Podkletnov, N. E., & Markhinin, E. K. (1981). New data on abiogenic synthesis of prebiological compounds in volcanic processes. *Origins of Life*, *11*, 303-315. https://doi.org/10.1007/BF00931484

Prata, A. T., Folch, A., Prata, A. J., Biondi, R., Brenot, H., Cimarelli, C., Corradini, S., Lapierre, J., & Costa, A. (2020). Anak Krakatau triggers volcanic freezer in the upper troposphere. *Scientific Reports*, *10*, 3584. https://doi.org/10.1038/s41598-020-60465-w

Pujol, M., Marty, B., Burgess, R., Turner, G., & Philippot, P. (2013). Argon isotopic composition of Archaean atmosphere probes early Earth geodynamics. *Nature*, *498*, 87-90. https://doi.org/10.1038/nature12152

Pyke, D. R., Naldrett, A. J., & Eckstrand, O. R. (1973). Archean ultramafic flows in Munro township, Ontario. *GSA Bulletin*, *84*, 955-978. https://doi.org/10.1130/0016-7606(1973)84<955:AUFIMT>2.0.CO;2

Rasmussen, B., & Buick, R. (1999). Redox state of the Archean atmosphere: evidence from detrital heavy minerals in ca. 3250–2750 Ma sandstones from the Pilbara Craton, Australia. *Geology*, *27*, 115-118. https://doi.org/10.1130/0091-7613(1999)027<0115:RSOTAA>2.3.CO;2

Rayborn, L., & Jellinek, A. M. (2022). Random Forest Predictions of Fine Ash Concentration and Charging Processes from Experimentally Generated Volcanic Discharges. *Journal of Geophysical Research: Solid Earth*, *127*, e2021JB023599. https://doi.org/10.1029/2021JB023599

Reback, J., jbrockmendel, McKinney, W., Van den Bossche, J., Augspurger, T., Roeschke, M., Hawkins, S., Cloud, P., gfyoung, Sinhrks, Hoefler, P., Klein, A., Petersen, T., Tratner, J., She, C., Ayd, W., Naveh, S., Darbyshire, J., Garcia, M., . . . Battiston, P. (2022). *pandas-dev/pandas: Pandas 1.4.2*. In (Version v1.4.2) Zenodo. https://doi.org/10.5281/zenodo.6408044

Renner, R., Nisbet, E. G., Cheadle, M. J., Arndt, N. T., Bickle, M. J., & Cameron, W. E. (1994). Komatiite flows from the reliance formation, Belingwe Belt, Zimbabwe: I. Petrography and mineralogy. *Journal of Petrology*, *35*, 361-400. https://doi.org/10.1093/petrology/35.2.361

Richter, F. M. (1985). Models for the Archean thermal regime. *Earth and Planetary Science Letters*, *73*, 350-360. https://doi.org/10.1016/0012-821X(85)90083-4

Ridd, M. F. (1970). Mud volcanoes in New Zealand. *AAPG Bulletin*, *54*, 601-616. https://doi.org/10.1306/5D25CA19-16C1-11D7-8645000102C1865D

Robert, F., & Chaussidon, M. (2006). A palaeotemperature curve for the Precambrian oceans based on silicon isotopes in cherts. *Nature*, *443*, 969-972. https://doi.org/10.1038/nature05239

Roche, O. (2012). Depositional processes and gas pore pressure in pyroclastic flows: an experimental perspective. *Bulletin of Volcanology*, *74*, 1807-1820. https://doi.org/10.1007/s00445-012-0639-4

Roche, O., & Carazzo, G. (2019). The contribution of experimental volcanology to the study of the physics of eruptive processes, and related scaling issues: A review. *Journal of Volcanology and Geothermal Research*, *384*, 103-150. https://doi.org/10.1016/j.jvolgeores.2019.07.011

Rode, B. M. (1999). Peptides and the origin of life. *Peptides*, *20*, 773-786. https://doi.org/10.1016/S0196-9781(99)00062-5

Rode, B. M., Son, H. L., Suwannachot, Y., & Bujdak, J. (1999). The combination of salt induced peptide formation reaction and clay catalysis: a way to higher peptides under primitive earth conditions. *Origins of Life and Evolution of the Biosphere*, *29*, 273-286. https://doi.org/10.1023/A:1006540101290

Rosas, J. C., & Korenaga, J. (2018). Rapid crustal growth and efficient crustal recycling in the early Earth: Implications for Hadean and Archean geodynamics. *Earth and Planetary Science Letters*, *494*, 42-49. https://doi.org/10.1016/j.epsl.2018.04.051

Rubey, W. W. (1955). Development of the hydrosphere and atmosphere, with special reference to probable composition of the early atmosphere. In A. Poldervaart (Ed.), *Crust of the Earth: A Symposium* (pp. 631-650). The Geological Society of America. https://doi.org/10.1130/SPE62-p631

Ruiz-Mirazo, K., Peretó, J., & Moreno, A. (2010). Defining life or bringing biology to life. *Origins of Life and Evolution of Biospheres*, *40*, 203-213. https://doi.org/10.1007/s11084-010-9201-6

Russell, C. T. (1991). Venus lightning. *Space Science Reviews*, *55*, 317-356. https://doi.org/10.1007/BF00177140

Russell, C. T. (1993). Planetary lightning. *Annual Review of Earth and Planetary Sciences*, *21*, 43-87. https://doi.org/10.1146/annurev.ea.21.050193.000355

Russell, C. T., Von Dornum, M., & Scarf, F. L. (1988). Planetographic clustering of low-altitude impulsive electric signals in the night ionosphere of Venus. *Nature*, *331*, 591-594. https://doi.org/10.1038/331591a0

Russell, M. J., Daniel, R. M., Hall, A. J., & Sherringham, J. A. (1994). A hydrothermally precipitated catalytic iron sulphide membrane as a first step toward life. *Journal of Molecular Evolution*, *39*, 231-243. https://doi.org/10.1007/BF00160147

Russell, M. J., Hall, A. J., Boyce, A. J., & Fallick, A. E. (2005). 100th Anniversary Special Paper:> On Hydrothermal Convection Systems and the Emergence of Life. *Economic Geology*, *100*, 419-438. https://doi.org/10.2113/gsecongeo.100.3.419

Russell, M. J., Hall, A. J., & Martin, W. (2010). Serpentinization as a source of energy at the origin of life. *Geobiology*, *8*, 355-371. https://doi.org/10.1111/j.1472-4669.2010.00249.x

Rye, R., & Holland, H. D. (1998). Paleosols and the evolution of atmospheric oxygen: a critical review. *American Journal of Science*, *298*, 621-672. https://doi.org/10.2475/ajs.298.8.621

Sagan, C. (2010). 23 • Definitions of life. In M. A. Bedau & C. E. Cleland (Eds.), *The Nature of Life: Classical and Contemporary Perspectives from Philosophy and Science* (pp. 303-306). Cambride University Press.

Sagan, C., & Chyba, C. (1997). The early faint sun paradox: Organic shielding of ultraviolet-labile greenhouse gases. *Science*, *276*, 1217-1221. https://doi.org/10.1126/science.276.5316.1217

Sagan, C., & Mullen, G. (1972). Earth and Mars: Evolution of atmospheres and surface temperatures. *Science*, *177*, 52-56. https://doi.org/10.1126/science.177.4043.52

Sanchez, R. A., Ferris, J. P., & Orgel, L. E. (1966). Cyanoacetylene in prebiotic synthesis. *Science*, *154*, 784-785. https://doi.org/10.1126/science.154.3750.784

Saverikko, M. (1985). The pyroclastic komatiite complex at Sattasvaara in northern Finland. *Bulletin of the Geological Society of Finland*, *57*, 55-87. https://doi.org/10.17741/bgsf/57.1-2.005

Scarf, F. L., & Russell, C. T. (1983). Lightning measurements from the Pioneer Venus orbiter. *Geophysical Research Letters*, *10*, 1192-1195. https://doi.org/10.1029/GL010i012p01192

Schaefer, S. J., & Morton, P. (1991). Two komatiitic pyroclastic units, Superior Province, northwestern Ontario: their geology, petrography, and correlation. *Canadian Journal of Earth Sciences*, *28*, 1455-1470. https://doi.org/10.1139/e91-128

Scheu, B., & Dingwell, D. B. (2022). Magma fragmentation. *Reviews in Mineralogy and Geochemistry*, *87*, 767-800. https://doi.org/10.2138/rmg.2021.87.16

Schoonen, M., Smirnov, A., & Cohn, C. (2004). A perspective on the role of minerals in prebiotic synthesis. *AMBIO: A Journal of the Human Environment*, *33*, 539-551. https://doi.org/10.1579/0044-7447-33.8.539

Schulze-Makuch, D., Fairén, A. G., & Davila, A. F. (2008). The case for life on Mars. *International Journal of Astrobiology*, *7*, 117-141. https://doi.org/10.1017/S1473550408004175

Sharp, Z. D., McCubbin, F. M., & Shearer, C. K. (2013). A hydrogen-based oxidation mechanism relevant to planetary formation. *Earth and Planetary Science Letters*, *380*, 88-97. https://doi.org/10.1016/j.epsl.2013.08.015

Sheldon, N. D. (2006). Precambrian paleosols and atmospheric CO2 levels. *Precambrian Research*, *147*, 148-155. https://doi.org/10.1016/j.precamres.2006.02.004

Shock, E. L., & Schulte, M. D. (1998). Organic synthesis during fluid mixing in hydrothermal systems. *Journal of Geophysical Research: Planets*, *103*, 28513-28527. https://doi.org/10.1029/98JE02142

Skinner Jr, J. A., & Mazzini, A. (2009). Martian mud volcanism: Terrestrial analogs and implications for formational scenarios. *Marine and Petroleum Geology*, *26*, 1866-1878. https://doi.org/10.1016/j.marpetgeo.2009.02.006

Sleep, N. H. (2010). The Hadean-Archaean environment. *Cold Spring Harbor Perspectives in Biology*, *2*, a002527. https://doi.org/10.1101/cshperspect.a002527

Sleep, N. H., Zahnle, K., & Neuhoff, P. S. (2001). Initiation of clement surface conditions on the earliest Earth. *Proceedings of the National Academy of Sciences*, *98*, 3666-3672. https://doi.org/10.1073/pnas.071045698

Sleep, N. H., Zahnle, K. J., & Lupu, R. E. (2014). Terrestrial aftermath of the Moon-forming impact. *Philosophical Transactions of the Royal Society A: Mathematical, Physical and Engineering Sciences*, *372*, 20130172. https://doi.org/10.1098/rsta.2013.0172

Smith, C. M., Gaudin, D., Van Eaton, A. R., Behnke, S. A., Reader, S., Thomas, R. J., Edens, H., McNutt, S. R., & Cimarelli, C. (2021). Impulsive volcanic plumes generate volcanic lightning and vent discharges: A statistical analysis of Sakurajima volcano in 2015. *Geophysical Research Letters*, *48*, e2020GL092323. https://doi.org/10.1029/2020GL092323

Smith, C. M., Van Eaton, A. R., Charbonnier, S., McNutt, S. R., Behnke, S. A., Thomas, R. J., Edens, H. E., & Thompson, G. (2018). Correlating the electrification of volcanic plumes with ashfall textures at Sakurajima Volcano, Japan. *Earth and Planetary Science Letters*, *492*, 47-58. https://doi.org/10.1016/j.epsl.2018.03.052

Smithies, R. H., Champion, D. C., Van Kranendonk, M. J., Howard, H. M., & Hickman, A. H. (2005). Modern-style subduction processes in the Mesoarchaean: geochemical evidence from the 3.12 Ga Whundo intra-oceanic arc. *Earth and Planetary Science Letters*, *231*, 221-237. https://doi.org/10.1016/j.epsl.2004.12.026

Smithies, R. H., Ivanic, T. J., Lowrey, J. R., Morris, P. A., Barnes, S. J., Wyche, S., & Lu, Y.-J. (2018). Two distinct origins for Archean greenstone belts. *Earth and Planetary Science Letters*, *487*, 106-116. https://doi.org/10.1016/j.epsl.2018.01.034

Snead, R. E. (1964). Active mud volcanoes of Baluchistan, West Pakistan. *Geographical Review*, *54*, 546-560. https://doi.org/10.2307/212981

Sokol, E. V., Novikov, I. S., Zateeva, S. N., Sharygin, V. V., & Vapnik, Y. (2008). Pyrometamorphic rocks of the spurrite-merwinite facies as indicators of hydrocarbon discharge zones (the Hatrurim Formation, Israel). *Doklady Earth Sciences*, *420*, 608-614. https://doi.org/10.1134/S1028334X08040181

Som, S. M., Buick, R., Hagadorn, J. W., Blake, T. S., Perreault, J. M., Harnmeijer, J. P., & Catling, D. C. (2016). Earth's air pressure 2.7 billion years ago constrained to less than half of modern levels. *Nature Geoscience*, *9*, 448-451. https://doi.org/10.1038/ngeo2713

Som, S. M., Catling, D. C., Harnmeijer, J. P., Polivka, P. M., & Buick, R. (2012). Air density 2.7 billion years ago limited to less than twice modern levels by fossil raindrop imprints. *Nature*, *484*, 359-362. https://doi.org/10.1038/nature10890

Springsklee, C., Manga, M., Scheu, B., Cimarelli, C., & Dingwell, D. B. (2022a). Electric discharge in erupting mud. *Geophysical Research Letters*, *49*, e2022GL100852. https://doi.org/10.1029/2022GL100852

Springsklee, C., Manga, M., Scheu, B., Cimarelli, C., & Dingwell, D. B. (2022b). *Experimental insights on electric discharges as a potential mechanism for self-ignition of mud volcanoes.* GFZ Data Services. https://doi.org/10.5880/fidgeo.2022.026

Springsklee, C., Scheu, B., Manga, M., Cigala, V., Cimarelli, C., & Dingwell, D. B. (2022b). *Experimental dataset for the influence of grain size distribution on experimental volcanic lightning.* GFZ Data Services. https://doi.org/10.5880/fidgeo.2022.009

Springsklee, C., Scheu, B., Manga, M., Cigala, V., Cimarelli, C., & Dingwell, D. B. (2022a). The Influence of Grain Size Distribution on Laboratory-Generated Volcanic Lightning. *Journal of Geophysical Research: Solid Earth*, *127*, e2022JB024390. https://doi.org/10.1029/2022JB024390

Stanley, S. (2021). Is Venus volcanically active? New approach could provide an answer. *Eos 102*. https://doi.org/10.1029/2021EO163155

Stern, R. J., Gerya, T., & Tackley, P. J. (2018). Stagnant lid tectonics: Perspectives from silicate planets, dwarf planets, large moons, and large asteroids. *Geoscience Frontiers*, *9*, 103-119. https://doi.org/10.1016/j.gsf.2017.06.004

Stern, S., Cimarelli, C., Gaudin, D., Scheu, B., & Dingwell, D. B. (2019). Electrification of experimental volcanic jets with varying water content and temperature. *Geophysical Research Letters*, *46*, 11136-11145. https://doi.org/10.1029/2019GL084678

Stow, C. D. (1969). Dust and sand storm electrification. *Weather*, *24*, 134-144. https://doi.org/10.1002/j.1477-8696.1969.tb03165.x

Stribling, R., & Miller, S. L. (1987). Energy yields for hydrogen cyanide and formaldehyde syntheses: the HCN and amino acid concentrations in the primitive ocean. *Origins of Life and Evolution of the Biosphere*, *17*, 261-273. https://doi.org/10.1007/BF02386466

Stüeken, E. E. (2016). Nitrogen in ancient mud: a biosignature? *Astrobiology*, *16*, 730-735. https://doi.org/10.1089/ast.2016.1478

Stüeken, E. E., Anderson, R. E., Bowman, J. S., Brazelton, W. J., Colangelo-Lillis, J., Goldman, A. D., Som, S. M., & Baross, J. A. (2013). Did life originate from a global chemical reactor? *Geobiology*, *11*, 101-126. https://doi.org/10.1111/gbi.12025

Sundaram, S., & Collins, L. R. (1997). Collision statistics in an isotropic particle-laden turbulent suspension. Part 1. Direct numerical simulations. *Journal of Fluid Mechanics*, *335*, 75-109. https://doi.org/10.1017/S0022112096004454

Svensen, H., Hammer, Ø., Mazzini, A., Onderdonk, N., Polteau, S., Planke, S., & Podladchikov, Y. Y. (2009). Dynamics of hydrothermal seeps from the Salton Sea geothermal system (California, USA) constrained by temperature monitoring and time series analysis. *Journal of Geophysical Research: Solid Earth*, *114*. https://doi.org/10.1029/2008JB006247

Teffeteller, H., Filiberto, J., McCanta, M. C., Treiman, A. H., Keller, L., Cherniak, D., Rutherford, M., & Cooper, R. F. (2022). An experimental study of the alteration of basalt on the surface of Venus. *Icarus*, *384*, 115085. https://doi.org/10.1016/j.icarus.2022.115085

Tehei, M., Franzetti, B., Maurel, M.-C., Vergne, J., Hountondji, C., & Zaccai, G. (2002). The search for traces of life: the protective effect of salt on biological macromolecules. *Extremophiles*, *6*, 427-430. https://doi.org/10.1007/s00792-002-0275-6

Thomas, R. J., Krehbiel, P. R., Rison, W., Edens, H. E., Aulich, G. D., Winn, W. P., McNutt, S. R., Tytgat, G., & Clark, E. (2007). Electrical activity during the 2006 Mount St. Augustine volcanic eruptions. *Science*, *315*, 1097-1097. https://doi.org/10.1126/science.1136091

Thomas, R. J., McNutt, S. R., Krehbiel, P. R., Rison, W., Aulich, G., Edens, H. E., Tytgat, G., & Clark, E. (2010). Lightning and electrical activity during the 2006 eruption of Augustine Volcano, chapter 25. In J. A. Power, M. L. Coombs, & J. T. Freymueller (Eds.), *The 2006 Eruption of Augustine Volcano, Alaska* (Vol. 1769, pp. 579-608). US Geological Survey Professional Paper. [https://pubs.usgs.gov/pp/1769/chapters/p1769_chapter25.pdf]

Thompson, W. R., Henry, T. J., Schwartz, J. M., Khare, B. N., & Sagan, C. (1991). Plasma discharge in N2+ CH4 at low pressures: experimental results and applications to Titan. *Icarus*, *90*, 57-73. https://doi.org/10.1016/0019-1035(91)90068-5

Tomlinson, K. Y., & Condie, K. C. (2001). Archean mantle plumes: evidence from greenstone belt geochemistry. In R. E. Ernst & K. L. Buchan (Eds.), *Mantle plumes: their identification through time* (Vol. 352, pp. 341-358). The Geological Society of America. https://doi.org/10.1130/0-8137-2352-3.341

Tonks, W. B., & Melosh, H. J. (1993). Magma ocean formation due to giant impacts. *Journal of Geophysical Research: Planets*, *98*, 5319-5333. https://doi.org/10.1029/92JE02726

Toupance, G., Raulin, F., & Buvet, R. (1975). Formation of prebiochemical compounds in models of the primitive Earth's atmosphere. *Origins of Life*, *6*, 83-90. https://doi.org/10.1007/BF01372392

Trail, D., Watson, E. B., & Tailby, N. D. (2011). The oxidation state of Hadean magmas and implications for early Earth's atmosphere. *Nature*, *480*, 79-82. https://doi.org/10.1038/nature10655

Tran, A., Rudolph, M. L., & Manga, M. (2015). Bubble mobility in mud and magmatic volcanoes. *Journal of Volcanology and Geothermal Research*, *294*, 11-24. https://doi.org/10.1016/j.jvolgeores.2015.02.004

Tsokolov, S. A. (2009). Why is the definition of life so elusive? Epistemological considerations. *Astrobiology*, *9*, 401-412. https://doi.org/10.1089/ast.2007.0201

Valley, J. W., Peck, W. H., King, E. M., & Wilde, S. A. (2002). A cool early Earth. *Geology*, *30*, 351-354. https://doi.org/10.1130/0091-7613(2002)030<0351:ACEE>2.0.CO;2

Van Eaton, A. R., Amigo, Á., Bertin, D., Mastin, L. G., Giacosa, R. E., González, J., Valderrama, O., Fontijn, K., & Behnke, S. A. (2016). Volcanic lightning and plume behavior reveal evolving hazards during the April 2015 eruption of Calbuco volcano, Chile. *Geophysical Research Letters*, *43*, 3563-3571. https://doi.org/10.1002/2016GL068076

Van Eaton, A. R., Schneider, D. J., Smith, C. M., Haney, M. M., Lyons, J. J., Said, R., Fee, D., Holzworth, R. H., & Mastin, L. G. (2020). Did ice-charging generate volcanic lightning during the 2016–2017 eruption of Bogoslof volcano, Alaska? *Bulletin of Volcanology*, *82*. https://doi.org/10.1007/s00445-019-1350-5

Van Kranendonk, M. J., & Pirajno, F. (2004). Geochemistry of metabasalts and hydrothermal alteration zones associated with c. 3.45 Ga chert and barite deposits: implications for the geological setting of the Warrawoona Group, Pilbara Craton, Australia. *Geochemistry: Exploration, Environment, Analysis*, *4*, 253-278. https://doi.org/10.1144/1467-7873/04-205

Viljoen, M. J., & Viljoen, R. P. (1969). The geology and geochemistry of the lower ultramafic unit of the Onverwacht Group and a proposed new class of igneous rocks. *Geological Society of South Africa Special Publication*, *2*, 55-86.

Viljoen, R., & Viljoen, M. (2019). Discovery and significance of komatiite: 50th Anniversary. *South African Journal of Science*, *115*. https://doi.org/10.17159/sajs.2019/7531

Viljoen, R. P., & Viljoen, M. J. (1969). The geological and geochemical significance of the upper formations of the Onverwacht Group. *Geological Society of South Africa Special Publication*, *2*, 113-151.

Villafañe-Barajas, S. A., & Colín-García, M. (2021). Submarine hydrothermal vent systems: the relevance of dynamic systems in chemical evolution and prebiotic chemistry experiments. *International Journal of Astrobiology*, *20*, 427-434. https://doi.org/10.1017/S1473550421000331

Vossen, C. E. J., Cimarelli, C., Bennett, A. J., Geisler, A., Gaudin, D., Miki, D., Iguchi, M., & Dingwell, D. B. (2021). Long-term observation of electrical discharges during persistent Vulcanian activity. *Earth and Planetary Science Letters*, *570*, 117084. https://doi.org/10.1016/j.epsl.2021.117084

Vossen, C. E. J., Cimarelli, C., Bennett, A. J., Schmid, M., Kueppers, U., Ricci, T., & Taddeucci, J. (2022). The electrical signature of mafic explosive eruptions at Stromboli volcano, Italy. *Scientific Reports*, *12*, 9049. https://doi.org/10.1038/s41598-022-12906-x

Wächtershäuser, G. (1988). Pyrite formation, the first energy source for life: a hypothesis. *Systematic and Applied Microbiology*, *10*, 207-210. https://doi.org/10.1016/S0723-2020(88)80001-8

Wang, L.-P., Wexler, A. S., & Zhou, Y. (2000). Statistical mechanical description and modelling of turbulent collision of inertial particles. *Journal of Fluid Mechanics*, *415*, 117-153. https://doi.org/10.1017/S0022112000008661

Weit, A., Roche, O., Dubois, T., & Manga, M. (2018). Experimental measurement of the solid particle concentration in geophysical turbulent gas-particle mixtures. *Journal of Geophysical Research: Solid Earth*, *123*, 3747-3761. https://doi.org/10.1029/2018JB015530

Weit, A., Roche, O., Dubois, T., & Manga, M. (2019). Maximum solid phase concentration in geophysical turbulent gas-particle flows: Insights from laboratory experiments. *Geophysical Research Letters*, *46*, 6388-6396. https://doi.org/10.1029/2019GL082658

Westall, F., De Ronde, C. E., Southam, G., Grassineau, N., Colas, M., Cockell, C., & Lammer, H. (2006). Implications of a 3.472–3.333 Gyr-old subaerial microbial mat from the Barberton greenstone belt, South Africa for the UV environmental conditions on the early Earth.

Philosophical Transactions of the Royal Society B: Biological Sciences, *361*, 1857-1876. https://doi.org/10.1098/rstb.2006.1896

Westall, F., Hickman-Lewis, K., Hinman, N., Gautret, P., Campbell, K., Bréhéret, J.-G., Foucher, F., Hubert, A., Sorieul, S., & Dass, A. V. (2018). A hydrothermal-sedimentary context for the origin of life. *Astrobiology*, *18*, 259-293. https://doi.org/10.1089/ast.2017.1680

Wilde, S. A., Valley, J. W., Peck, W. H., & Graham, C. M. (2001). Evidence from detrital zircons for the existence of continental crust and oceans on the Earth 4.4 Gyr ago. *Nature*, *409*, 175-178. https://doi.org/10.1038/35051550

Williams, E. R., & McNutt, S. R. (2005). Total water contents in volcanic eruption clouds and implications for electrification and lightning. In C. Pontikis (Ed.), *Recent progress in lightning physics* (pp. 81-93). Research Signpost Publishing.

Wilson, L., & Mouginis-Mark, P. J. (2003). Phreato-magmatic dike–cryosphere interactions as the origin of small ridges north of Olympus Mons, Mars. *Icarus*, *165*, 242-252. https://doi.org/10.1016/S0019-1035(03)00197-0

Wordsworth, R. D. (2016). Atmospheric nitrogen evolution on Earth and Venus. *Earth and Planetary Science Letters*, *447*, 103-111. https://doi.org/10.1016/j.epsl.2016.04.002

Wurm, G., Schmidt, L., Steinpilz, T., Boden, L., & Teiser, J. (2019). A challenge for martian lightning: Limits of collisional charging at low pressure. *Icarus*, *331*, 103-109. https://doi.org/10.1016/j.icarus.2019.05.004

Yair, Y., Fischer, G., Simões, F., Renno, N., & Zarka, P. (2008). Updated review of planetary atmospheric electricity. In F. Leblanc, K. L. Aplin, Y. Yair, R. G. Harrison, J. P. Lebreton, & M. Blanc (Eds.), *Planetary Atmospheric Electricity. Space Sciences Series of ISSI* (Vol. 30, pp. 29-49). Springer. https://doi.org/10.1007/978-0-387-87664-1_4

Yuen, D. A., Scruggs, M. A., Spera, F. J., Zheng, Y., Hu, H., McNutt, S. R., Thompson, G., Mandli, K., Keller, B. R., Wei, S. S., Peng, Z., Zhou, Z., Mulargia, F., & Tanioka, Y. (2022). Under the surface: Pressure-induced planetary-scale waves, volcanic lightning, and gaseous clouds caused by the submarine eruption of Hunga Tonga-Hunga Ha'apai volcano. *Earthquake Research Advances*, *2*, 100134. https://doi.org/10.1016/j.eqrea.2022.100134

Zahnle, K., Arndt, N., Cockell, C., Halliday, A., Nisbet, E., Selsis, F., & Sleep, N. H. (2007). Emergence of a habitable planet. *Space Science Reviews*, *129*, 35-78. https://doi.org/10.1007/s11214-007-9225-z

Zhou, Y., Wexler, A. S., & Wang, L.-P. (1998). On the collision rate of small particles in isotropic turbulence. II. Finite inertia case. *Physics of Fluids*, *10*, 1206-1216. https://doi.org/10.1063/1.869644

Appendix

Appendix A

Table A-1. Summary of the samples analyzed for potential organics formed during the experiments. The composition 'air' indicates that the tank was closed with the air present in the lab. As the gas compositions were not analyzed, the contamination with air is unknown. The numbers represent the vol% that was pumped into the tank (contamination unknown). Before filling the particle collector tank with the given gas composition, the tank was flushed once with nitrogen and two times with CO_2.

Number	EXP	Type	Material	Gas composition [vol%]		
				Air	CO_2	CO
1	290	Filter	TB	100	-	-
2	291	Filter	TB	100	-	-
3	292	Filter	TB	-	100	-
4	293	Filter	TB	-	100	-
5	290	Ash	TB	100	-	-
6	291	Ash	TB	100	-	-
7	292	Ash	TB	-	100	-
8	293	Ash	TB	-	100	-
9	297	Ash	TB	-	98	2
10	298	Ash	TB	-	95	5
11	299	Ash	TB	-	92	8
12	300	Ash	TB	-	92	8

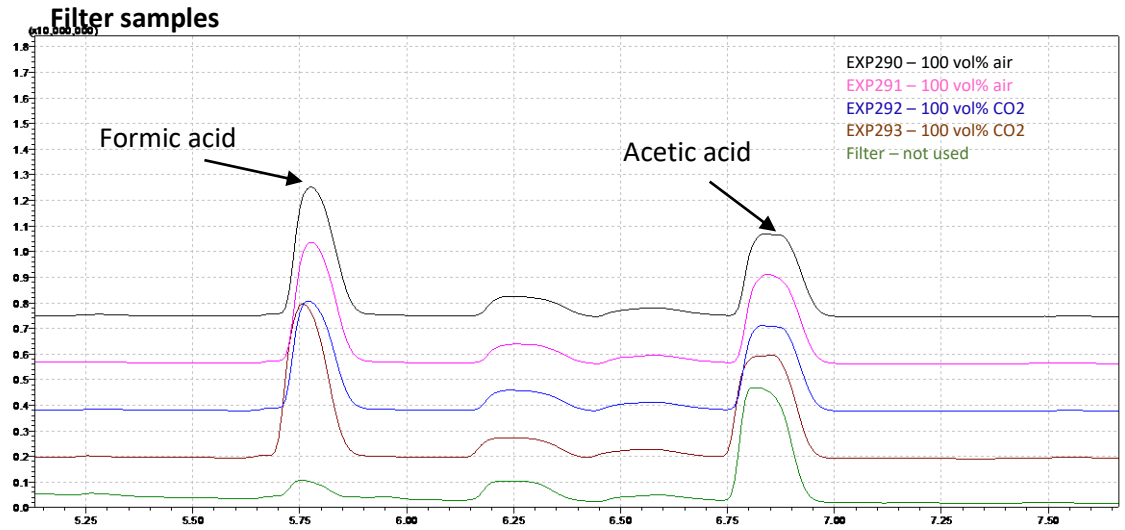

Figure A-1. Chromatogram obtained from the samples of the filter for formic acid and acetic acid. In green, the spectrum of only a plain filter as a reference is given. The filter samples were extracted (24h at room temperature) in 1 ml MeOH and blown dry with N_2. The samples were derivatized in 50 µl ACN and MTBSTFA (N-tert-butyldimethylsilyl-N-methyltrifluoroacetamide) for 30 min at 70 °C. The analysis was conducted as a GC/MS analysis (GC-2010 coupled with MS-QP2010 Ultra (Shimadzu GmbH, D-Duisburg) with a 30 m × 0.25 mm × 0.25 µm fused silica capillary column (Equity TM5, Supelco, Bellefonte, PA, USA) and AOC-20i auto injector). At a retention time of 5.79 formic acid and at 6.85 acetic acid were detected. Although it seems like the filters used in the experiments contain a higher concentration of formic acid compared to the plain, unused filter, this signal was evaluated as contamination based on the fact, that there is no difference between the filter used with air as atmosphere (EXP290 and EXP291) and CO_2 as atmosphere (EXP292 and EXP 293). Analysis and interpretation were done by Thomas Geisler (TU Munich). Information about analysis were provided by Thomas Geisler.

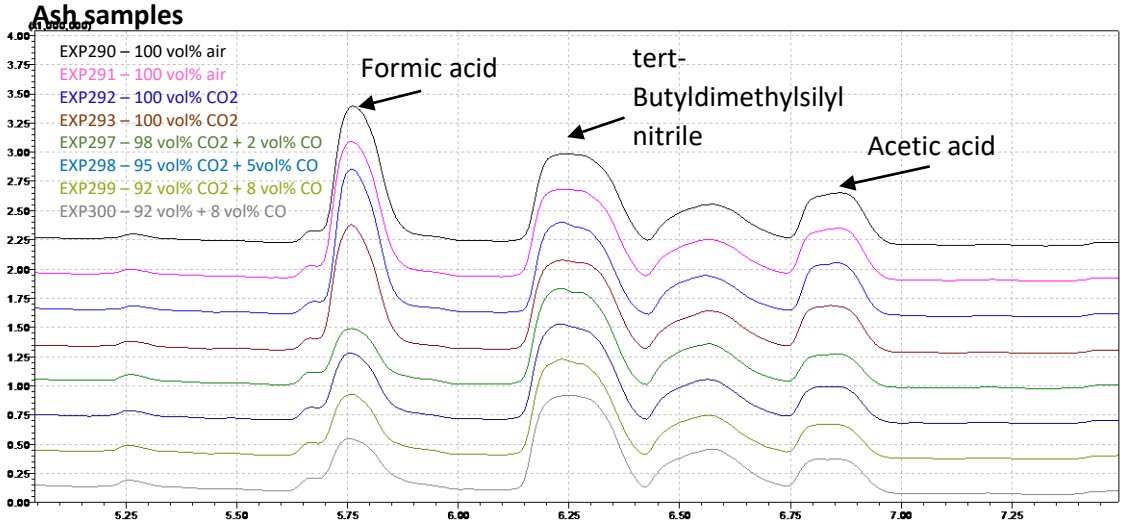

Figure A-2. Chromatogram obtained from the samples of the ash for formic acid, tert-Butyldimethylsilyl nitrile and acetic acid. The ash samples were extracted (24h at room temperature) in 1 ml MeOH and blown dry with N_2. The samples were derivatized in 50 µl ACN and MTBSTFA (N-tert-butyldimethylsilyl-N-methyltrifluoroacetamide) for 30 min at 70 °C. The analysis was conducted as a GC/MS analysis (GC-2010 coupled with MS-QP2010 Ultra (Shimadzu GmbH, D-Duisburg) with a 30 m × 0.25 mm × 0.25 µm fused silica capillary column (Equity TM5, Supelco, Bellefonte, PA, USA) and AOC-20i auto injector). At a retention time of 5.79 formic acid, at 6.25 tert-Butyldimethylsilyl nitrile (originating from the silage medium) and at 6.85 acetic acid were detected. Acetic acid was detected in in experiments conducted in air as well as conducted in CO_2, therefore not considered as products of the experiments but contamination. Analysis and interpretation were done by Thomas Geisler (TU Munich). Information about analysis were provided by Thomas Geisler.

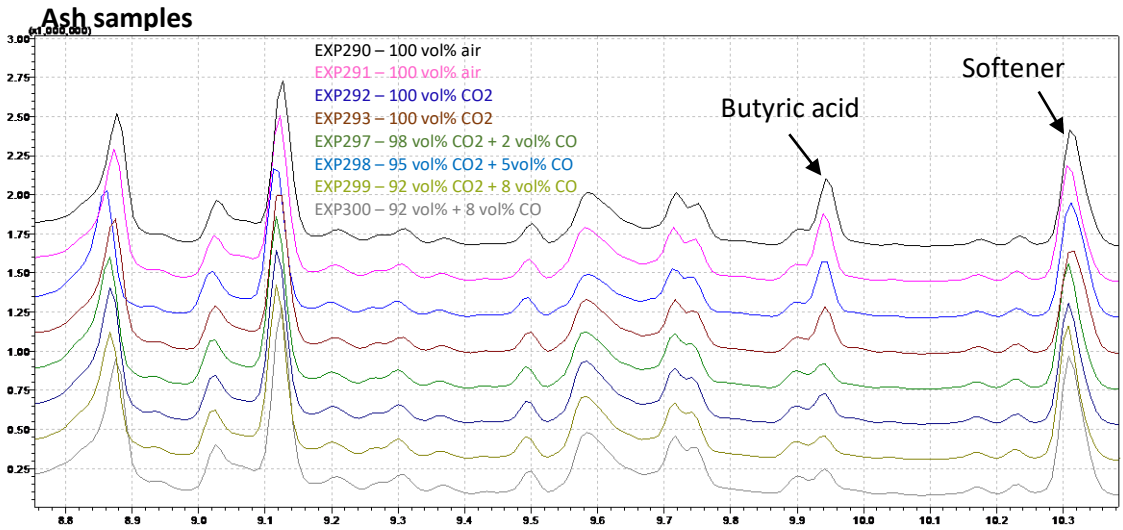

Figure A-3. Chromatogram obtained from the samples of the ash for butyric acid and softeners. The ash samples were extracted (24h at room temperature) in 1 ml MeOH and blown dry with N_2. They were derivatized in 50 µl ACN and MTBSTFA (N-tert-butyldimethylsilyl-N-methyltrifluoroacetamide) for 30 min at 70 °C. The analysis was conducted as a GC/MS analysis (GC-2010 coupled with MS-QP2010 Ultra (Shimadzu GmbH, D-Duisburg) with a 30 m × 0.25 mm × 0.25 µm fused silica capillary column (Equity TM5, Supelco, Bellefonte, PA, USA) and AOC-20i auto injector). At a retention time of 9.95 butyric acid and at 10.3 a softener was detected. Because butyric acid was more represented in the samples for experiments conducted in air, butyric acid was evaluated as a contamination. Analysis and interpretation were done by Thomas Geisler (TU Munich). Information about analysis were provided by Thomas Geisler.

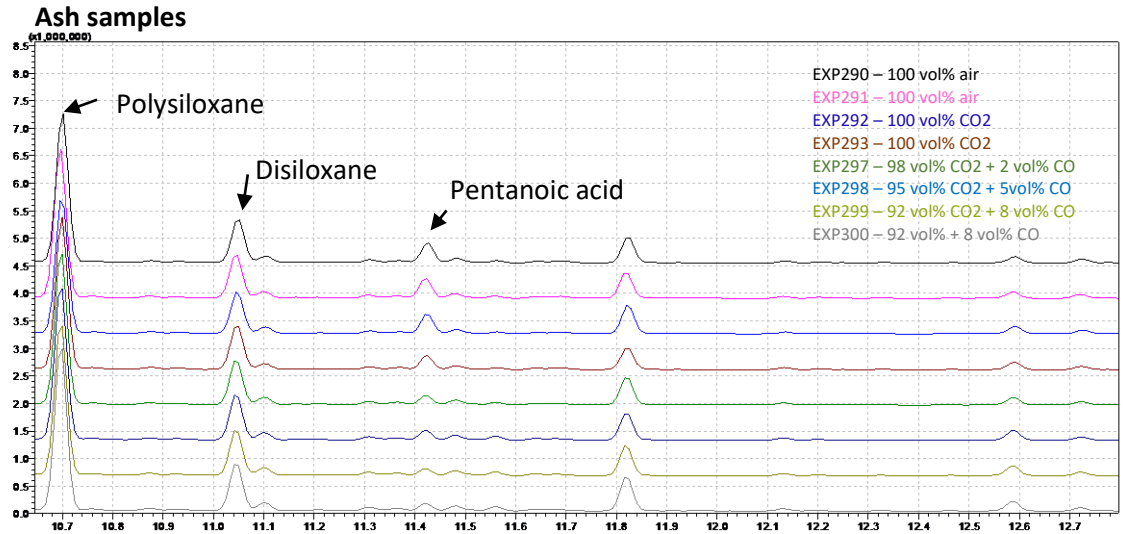

Figure A-4. Chromatogram obtained from the samples of the ash for polysiloxane, disiloxane and pentanoic acid. The ash samples were extracted (24h at room temperature) in 1 ml MeOH and blown dry with N_2. They were derivatized in 50 µl ACN and MTBSTFA (N-tert-butyldimethylsilyl-N-methyltrifluoroacetamide) for 30 min at 70 °C. The analysis was conducted as a GC/MS analysis (GC-2010 coupled with MS-QP2010 Ultra (Shimadzu GmbH, D-Duisburg) with a 30 m × 0.25 mm × 0.25 µm fused silica capillary column (Equity TM5, Supelco, Bellefonte, PA, USA) and AOC-20i auto injector). At a retention time of 10.71 polysiloxane (From the GC column), at 11.06 disiloxane and at 11.44 pentanoic acid were detected. Again, the pentanoic acid was more abundant in the experiments conducted in air and therefore evaluated as contamination. The addition of CO did not cause any significant change in products measured from the ash samples by GC/MS analysis. Analysis and interpretation were done by Thomas Geisler (TU Munich). Information about analysis were provided by Thomas Geisler.

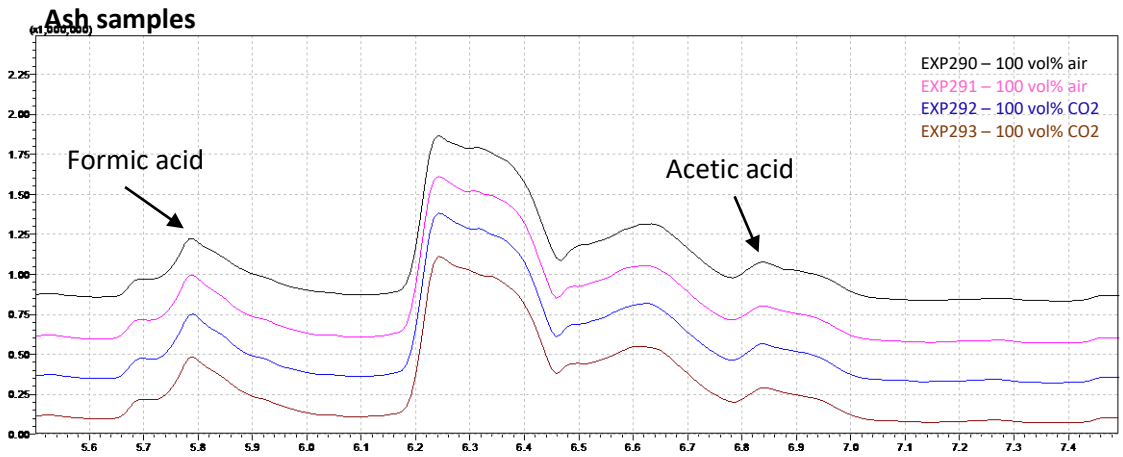

Figure A-5. Chromatogram obtained from the ash samples for formic acid and acetic acid. The filter samples were extracted (24h at room temperature) in 1 ml MeOH and blown dry with N_2. They were derivatized in 50 µl ACN and MTBSTFA (N-tert-butyldimethylsilyl-N-methyltrifluoroacetamide) for 30 min at 70 °C. The analysis was conducted as a GC/MS analysis (GC-2010 coupled with MS-QP2010 Ultra (Shimadzu GmbH, D-Duisburg) with a 30 m × 0.25 mm × 0.25 µm fused silica capillary column (Equity TM5, Supelco, Bellefonte, PA, USA) and AOC-20i auto injector). At a retention time of 5.79 formic acid and at 6.85 acetic acid were detected Analysis and interpretation were done by Thomas Steiner (TU Munich). Information about analysis were provided by Thomas Geisler.

Table A-2. Results for NO_2 and NO_3 by IC measurement. No concentration of NO_2 and NO_3 was detected at all. The gas of the particle collector tank with experiments conducted in air was purge by 100 ml of distilled water.

Number	Dilution factor	NO_2 [mg/l]	NO_3 [mg/l]	Note
EXP43	10	n.a.	n.a.	-
EXP43	100	n.a.	n.a.	-
EXP47	10	n.a.	n.a.	-
EXP47	100	n.a.	n.a.	-
EXP48	10	n.a.	n.a.	-
EXP48	100	n.a.	n.a.	-
EXP43	1	n.a.	n.a.	Repetition
EXP47	1	n.a.	n.a.	Repetition
EXP48	1	n.a.	n.a.	Repetition

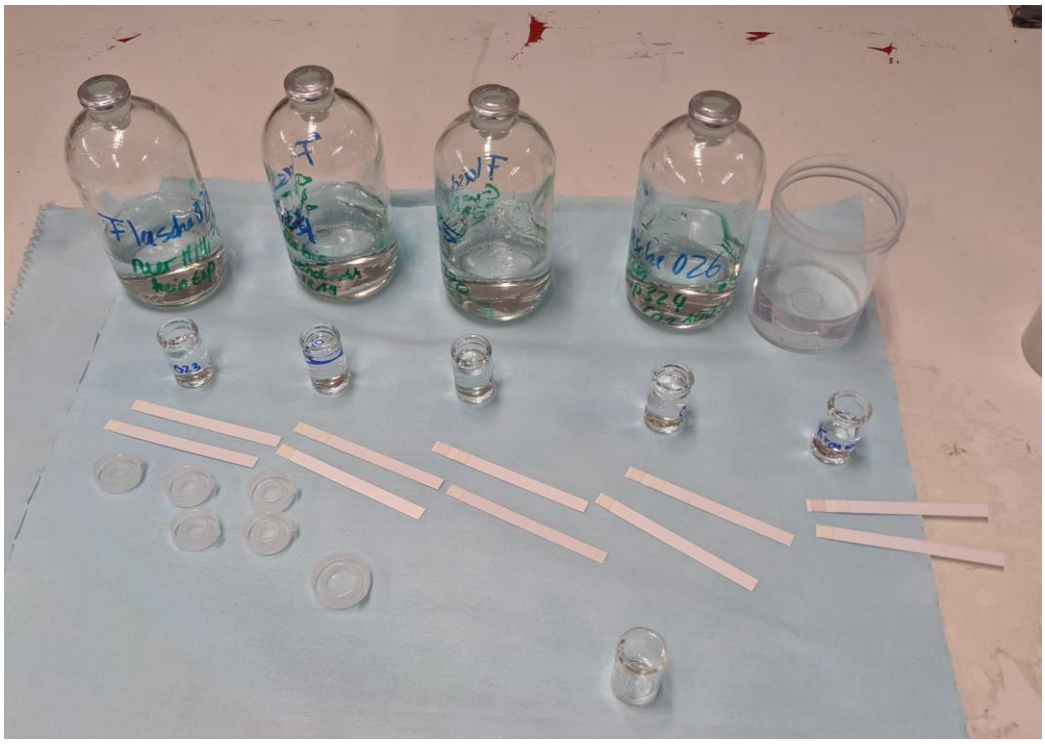

Figure A-6. Results for the detection of NO_2 and NO_3 within water which was used to purge the air after conducting experiments from the particle collector tank. Bottle 23 (no experiment, reference), 24 (after experiment 323 in air), 25 (after experiment 323 in air), 26 (after Exp 324 100 % CO_2) were used during experiments, whereas the plastic cup with water next to them just contains tab water. To determine the amount of NO_2 and NO_3 in water, colorimetric test strips by MQuant® (10 – 500 mg/l NO_3 and 2 – 80 mg/l NO_2) were used.

Appendix B

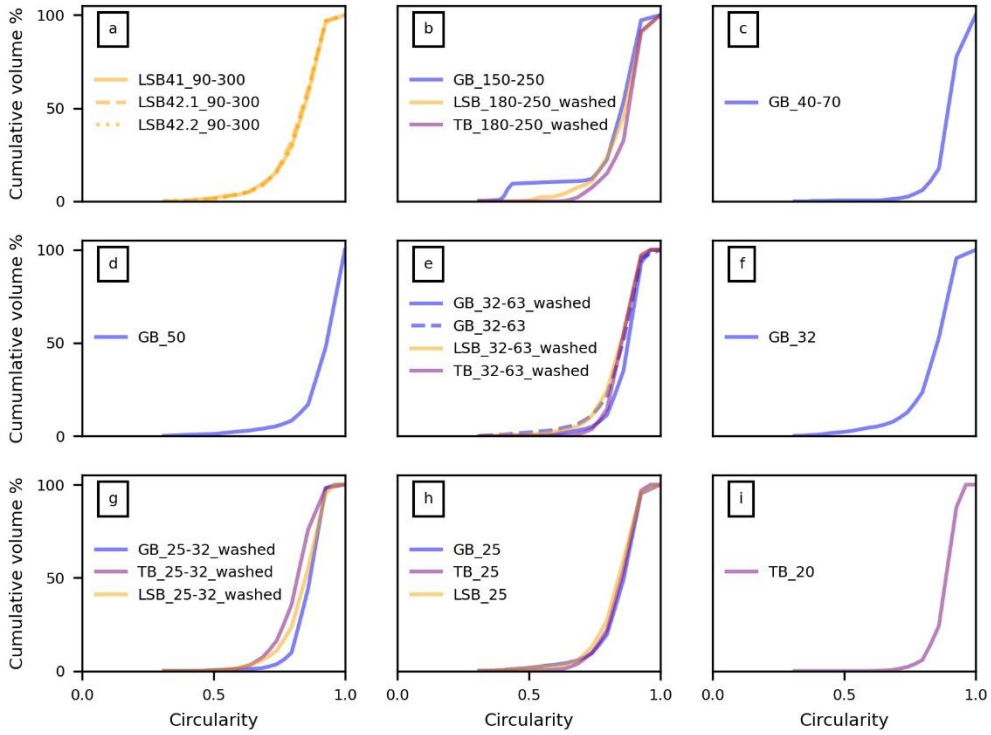

Figure A-7. Summary of the circularity of all grain size fractions used in the study as cumulative volume %. The circularity describes the degree of similarity of the particle (or its projected area) with a circle, considering the smoothness of its perimeter. The circularity is influenced by shape, symmetry, and surface roughness. A limitation of this metric is that different shapes can have the same circularity.

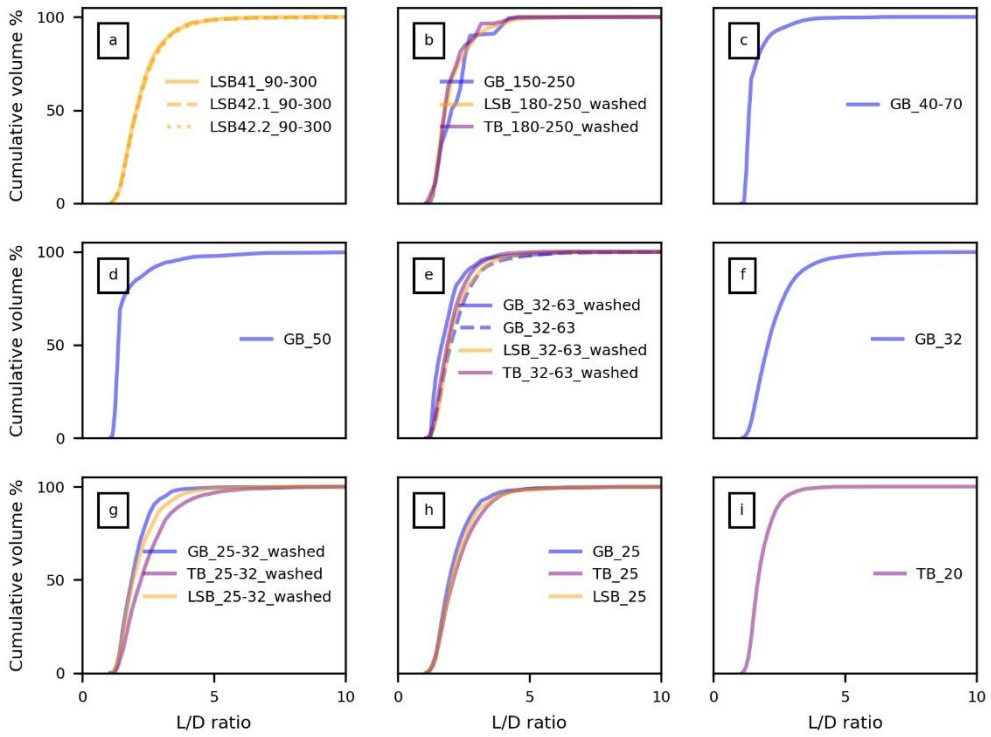

Figure A-8. Summary of the aspect ratio (L/D ratio) of all grain size fractions used in this study as cumulative volume %. The L/D ratio describes the ratio of the particle dimensions where D describes the minimal diameter of the particle and L is the length perpendicular to this minimal diameter D.

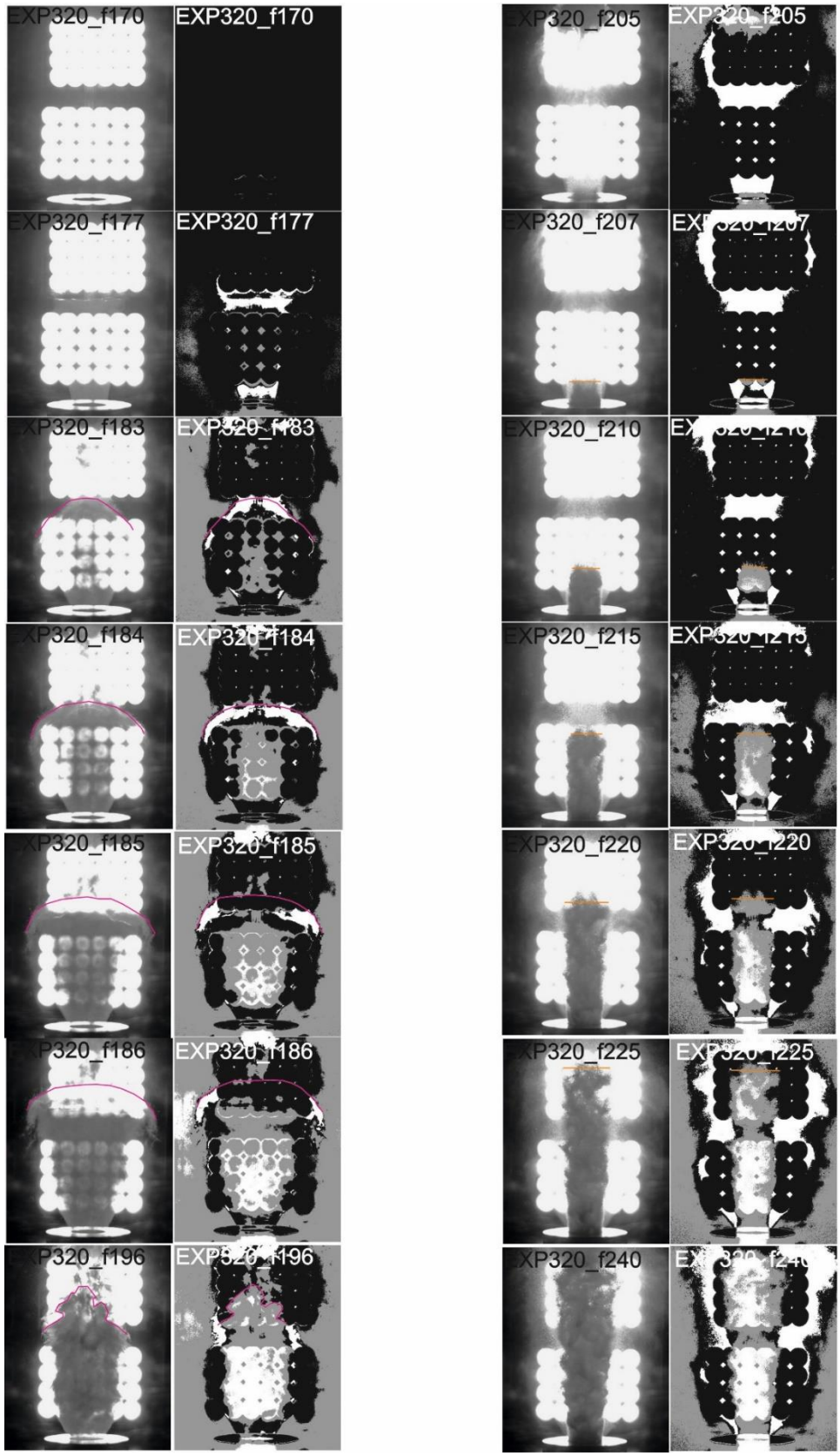

Figure A-9. Comparison of images from the high-speed recording of experiment 320 with the image subtracted counterpart. The gas-exit front is indicated with a purple outline, the gas-particle exit front is highlighted by an orange line. The individual frame numbers are indicated as the heading of each individual image. The python library used for the image subtraction is OpenCV (Bradski, 2000).

Appendix C

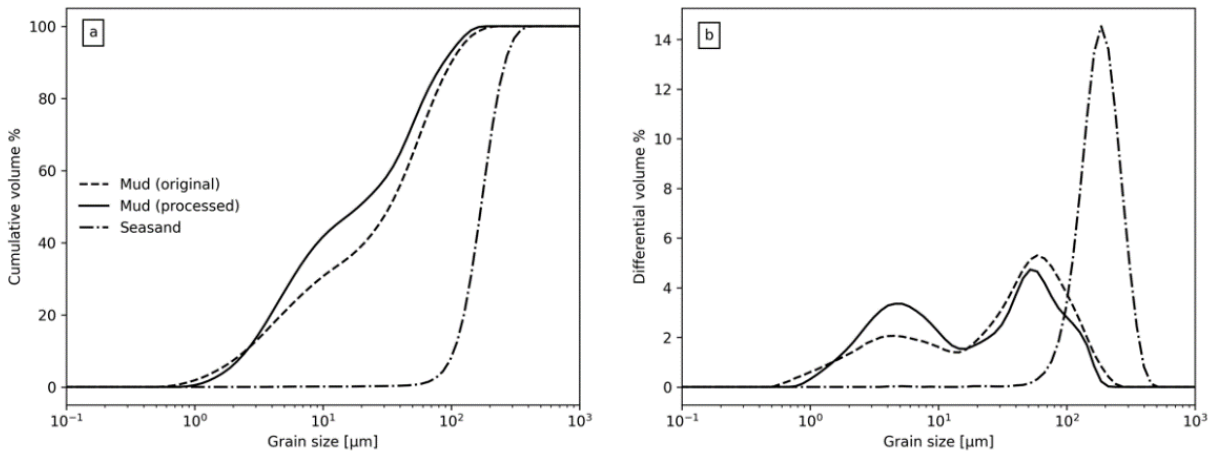

Figure A-10. Grain size distribution of samples measured with a Bettersizer S3 Plus: mud erupted at the Davis-Schrimpf vents as sampled (dashed line), dried and ground (solid line), and quartz sand that was added to mud samples in three experiments (dashed line with points).

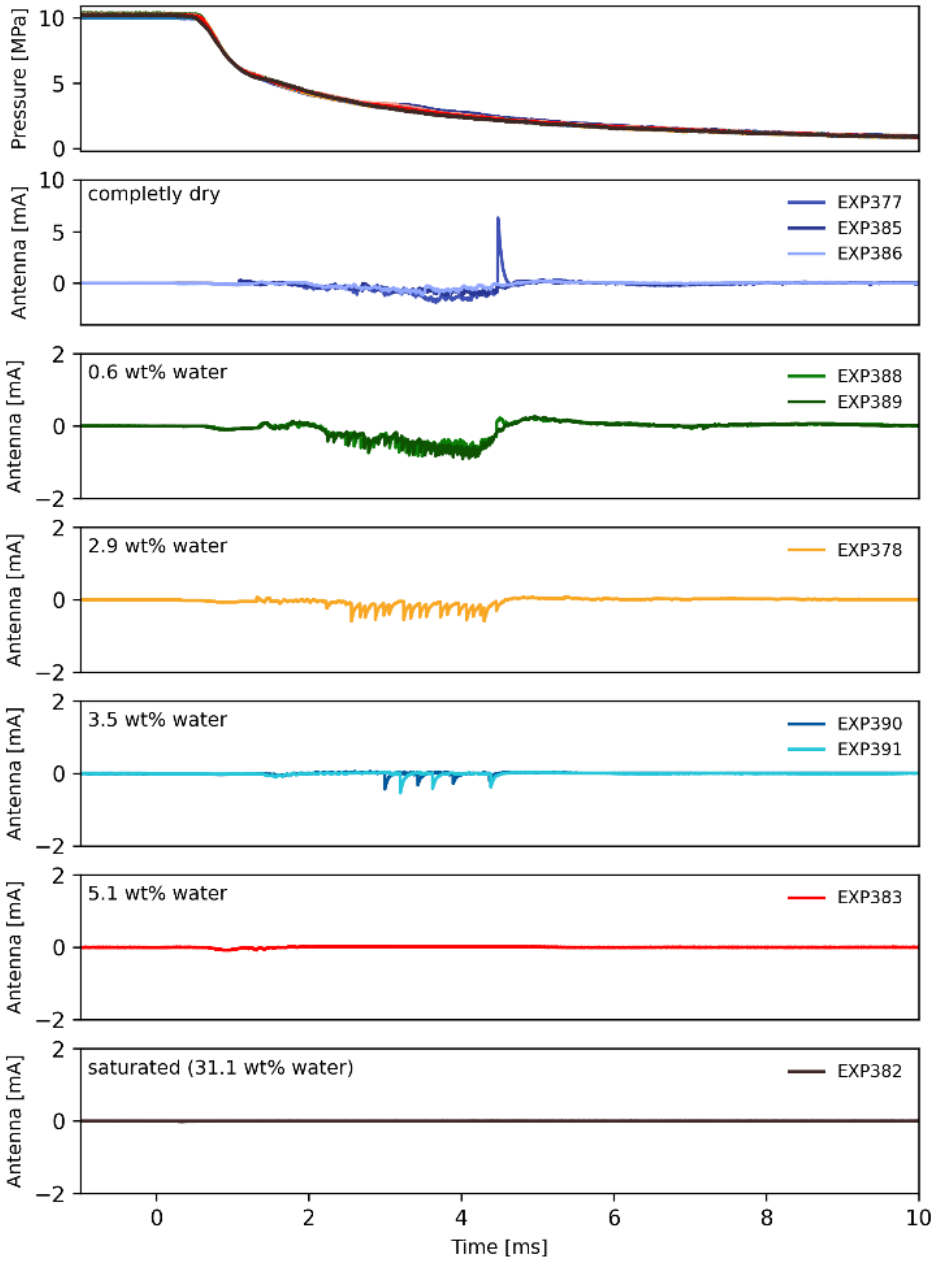

Figure A-11. Time series of recorded current for all experiments without sand, ranked in order of increasing water content. The top panel shows pressure evolution for all experiments.

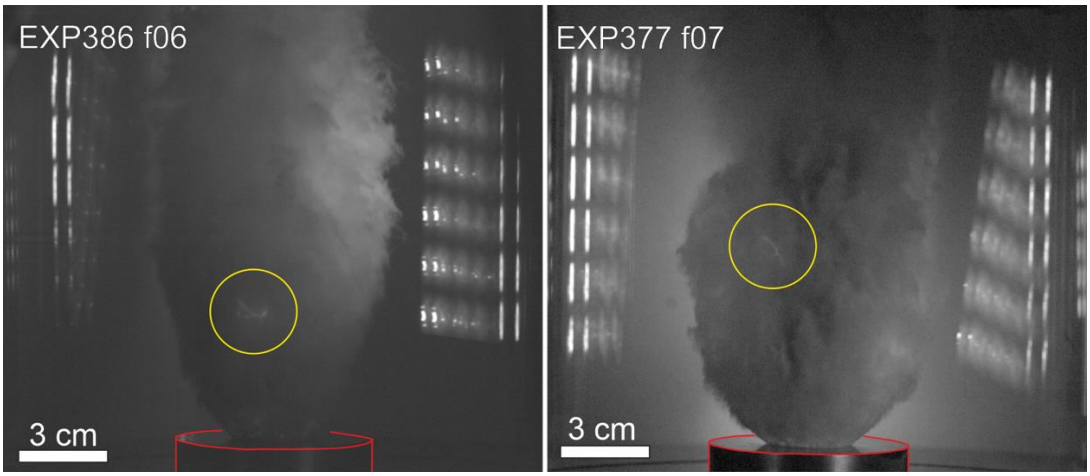

Figure A-12. Photographs from the high-speed videos showing discharges within the jet that do not connect to the Faraday cage. Such intracloud discharges do not change the total charge within the Faraday cage and therefore are not detected in this experimental setup, but nonetheless may take place during the experiments.

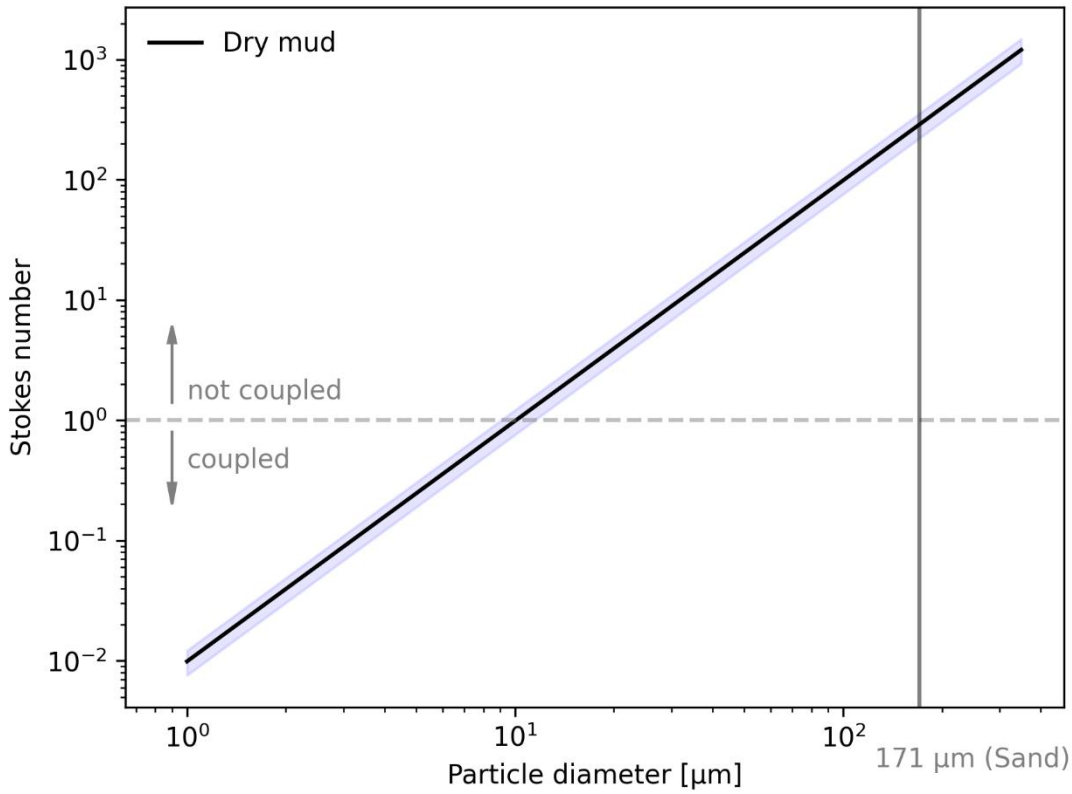

Figure A-13. Particle diameter and its corresponding Stokes number of the particles used in the experiments. The shaded region shows the range of St for $u_0 = 262 \pm 61$m/s. For St > 1 the particles are expected to be collimated as they exit the vent, whereas for St < 1 the particles are better coupled to the turbulent gas motions. The average diameter of the sand is indicated by the vertical line.

Acknowledgments

First of all, I would like to thank my supervisor, who supported me through all the years of my PhD, thank you very much Betty. You were not only a patient supervisor concerning all the scientific question we encountered during our project, but I also enjoyed talking to you about everything else in life. You have a golden heart, thank you very much. I am happy that I had the opportunity to learn so much from you, but I also had the freedom to develop my own scientific interests.

I am very grateful to all the wonderful people I met at the University of Munich. Thank you very much Don, thank you for showing me how to melt a rock. Nothing is as fascinating as to produce your own lava. Thank you very much Corrado, for your help on investigating volcanic lightning and your support. I met so many kind people and I want to thank all of them, it is very important to work in a nice and friendly working environment. I would like to thank Iphi, Steffi and Michi (the Mensa group who always went to Mensa), Joana, Zeynep, Daniel (the emergence of life team), Jérémie, Luiz, Marize, Siemon, Omar, Natascha, Anthony, Eleonora (you guys always cheered me up with a beer), Francisco, Markus (my former office colleagues), Caron (thank you for your beautiful and kind character), Mathieu (despacito!), Vale (not scalable!), Ana (most Bavarian girl I ever met), Baha, Mandana (Geophysics rules!), Adriana and Antonia (thank you for always helping us patiently in the lab), Andre (coolest IT-expert ever), Kai-Uwe (talking with you is always inspiring), Werner (beinhart!), Dirk (thank you for helping us patiently), Margot, Rieke (master over the chaos we produced), Rosa (thank you very much for all your help), Nataliya, Ira, Thomas (thank you very much), Melanie, Malte (you made the museum so cool! And thank you for the coffee), Markus, Günther and all the other lovely people from the workshop, Max, and all the other unforgettable people in Munich I forgot to mention!

I want to thank Michael, who somehow was something like a third supervisor to me. Thank you for reading all my writing so carefully and helping me so patiently with the scaling. Thank you for letting me work with you on your mud samples, I hope I can see once in real-life a mud explosion. Thank you for all the discussions. Without your help, I would have been lost :D.

I want to thank all the lovely people from the University of Münster, where I got fascinated by Earth Sciences. Thank you, Carmen, you are a very inspiring person, I really appreciate all your support. Thank you, Marion, for all your lovely help. Thank you very much Herr Strauß that I could do such a cool Bachelor thesis with you. During my PhD, finally I had the chance to visit Iceland and thank you for reading my thesis. Many thanks to the CRC Emergence of life, I learned so much and enjoyed so much working on this fascinating but enigmatic topic, thank you very much for this opportunity. I really enjoyed being in such a big team. I am very grateful for the support of the DFG for the period of my PhD. I want to thank the Mentoring Program from the LMU, for all the nice meetings and the support. Also, many thanks to all the wonderful people from the University of Düsseldorf, being a Mekuwi means lots to me: what is science without science fiction?

Ganz besonders möchte ich natürlich meiner Familie und meinen Freunden (allen Assiköppen auf der Welt) danken. Vielen lieben Dank an all meine Freunde, die mich während all der Jahre unterstützt haben. Lora, du bist die Beste, danke dass du dir diesen ganzen Textwust durchgelesen hast und so aufmerksam durchgearbeitet hast. Danke, Mama und Papa, dass ihr mich immer unterstützt habt und mich immer dafür respektiert habt, dass ich so dickköpfig bin, wie ich bin, und meinen eigenen Weg gegangen bin. Danke, dass ihr mir diese Freiheit ermöglicht habt. Ich bin sehr dankbar für meine liebe Schwester Daniela, danke, dass du meine Schwester bist. Ich möchte meinen Großeltern danken, die immer ein Vorbild für mich waren, ich vermisse euch sehr und werde euch immer vermissen. Vielen lieben Dank Onkel Eckart und Tante Cornelia. Und mir am wichtigsten: vielen lieben Dank Jarno, du bist mein bester Freund.

Declaration

München, 18 January 2023

I hereby confirm that my thesis entitled *'Experimental volcanic lightning under early Earth conditions: Implications for prebiotic synthesis and the origin of life'* is the result of my own original work. Furthermore, I certify that this work contains no material that has been accepted for the award of any other degree or diploma in my name, in any university and, to the best of my knowledge and belief, contains no material previously published or written by another person, except where due reference has been made in the text. In addition, I certify that no part of this work will be used in a submission in my name in the future, for any other degree or diploma in any university or other tertiary institution without the prior approval of the Ludwig-Maximilians-Universität München.

Christina Springsklee